UNIVERSITAT POMPEU FABRA

TESIS DOCTORAL UPF 2015

Prognosis and risk models of depression are built from analytical components of the rs-fMRI activity in patients

**Cristian Tornador Antolin**

Department of Experimental and Healh Science

Computational Neuroscience Group

*Thesis Director*

Prof. Dr. Phil. Dr. Rer. Nat. Habil. Gustavo Deco

Barcelona, 2015

*A mi familia*
*y en memoria a Teresa Moretó*

*"It's a dangerous business, Frodo, going out your door. You step onto the road, and if you don't keep your feet, there's no knowing where you might be swept off to."*
*— J.R.R. Tolkien, The Lord of the Rings*

*ACKNOWLEDGEMENTS*

Entiendo el documento de tesis como un punto importante en la vida, en donde intentas compactar brevemente todo el esfuerzo de un trabajo de investigación realizado en los últimos años. Sin embargo, es un duro trabajo que en muchas ocasiones es necesario la aportación de otra gente tanto a nivel profesional como a nivel personal. Y mi experiencia personal, me indica que es necesario un equilibrio entre ambas si se quiere llegar a obtener los resultados deseados.

La experiencia es un factor importante en la vida y no cambiaría nada de lo vivido puesto que no hubiera aprendido lo que he aprendido y no hubiera conocido a la gente que he conocido. Las circunstancias se crean a partir de las motivaciones e ilusiones que llevas contigo y de las que te hacen llegar otras personas. Eso si incorporas errores para ser más eficiente en futuros trabajos.

En este sentido he tenido la suerte de conocer una serie de personas durante estos años, que son de valor incuestionable para la consecución de mi proyecto de tesis.

En primer lugar y sobretodo agradecer de forma especial a prof. Dr. Gustavo Deco, puesto que ha depositado en mí su confianza y la posibilidad de realizar mi proyecto de tesis. No sólo le tengo en alta estima como profesional, que lo considero unas de las mentes más brillantes que hay en la actualidad en la neurociencia computacional, sino que me ha acompañado de forma personal durante los diferentes años de mi tesis, en especial en los últimos meses, en donde, me ha sido realmente duro, sobre todo en lo mental. Él ha estado ahí apoyándome y creyendo que podría hacer un buen trabajo pese a mis circunstancias. Este último apoyo a veces es lo que representa para una persona poder lograr resultados o no. Esto quiere decir mucho de una persona que pese a estar en el nivel intelectual y profesional que se encuentra, puede bajar y guiar a una persona en momentos difíciles. En mi modesta opinión, todo director tanto de tesis o de proyectos debería tener este tipo de atributos, por lo que me estoy muy agradecido y he sé que he tenido mucha suerte poder ser alumno suyo durante mi etapa de doctorado.

En segundo lugar un agradecimiento personal a la Dr. Nuria Nabau, y futura socia de la fundación de lucha contra el cáncer y enfermedades mentales. Que durante los últimos años ha representado en lo personal un apoyo incondicional. "¡Ya lo sabes!, que te voy a contar", pero me gustaría dejar aquí y ahora constancia de ello. Puesto que el documento de tesis representa algo importante en la vida de una persona. En general mis agradecimientos a la familia Nabau Moretó y es por ello que les dedico esta tesis: a

la memoria de Teresa Moretó. Sin el apoyo de la familia Nabau y en especial de Nuria tengo claro que me hubiera sido muy difícil finalizar este trabajo de forma satisfactoria. Un estado animo estable es tan importante o más que unas buenas facultades y motivaciones personales.

En tercer lugar un agradecimiento a mi familia, en concreto a mi madre Teresa Antolin y a mi padre Juan Tornador, y a mi hermano Juan Carlos Tornador, ¡obviamente!. Pese a que no entendían mi motivación para dejar de lado mi carrera profesional anterior,- para ellos "bien remunerado"-, y que me embarcase en algo que a priori para ellos iba aportarme una "insatisfacción económica" y "con lo que está cayendo", siempre me han apoyado en mi decisión. Solo decirles: "todo saldrá bien, ¡tranquilos! yo sé porque lo hago, porque es lo que quiero hacer". Espero que se entienda en estas palabras que hay momentos en la vida donde cada uno tiene que hacer lo que tiene que hacer, y siempre hay otros momentos para realizar satisfacciones secundarias, todo llega. En todo caso sé que estáis orgullosos de mí y siempre lo estaréis y espero que algún día veáis que he decido lo correcto.

En cuarto lugar dar las gracias a nivel profesional al Dr. Aldo Córdova y a la Dr. Lourdes Fagañas. Gracias a ellos, y a su aportación tanto en conocimiento como en las muestras han hecho posible la realización de mi tesis. Ya desde el primer momento, Lourdes me sorprendió gratamente por su manera tan simple de explicar problemas complejos, y la capacidad por escucharme y dirigir las ideas hacia hechos concretos, y de esta forma poder cerrar proyectos para mí en un tiempo record. Además tanto Aldo como Lourdes siempre me han tratado de una forma que me han hecho sentir como en casa y esto es de agradecer. Espero poder seguir aprendiendo mucho, tanto al prof. Dr. Deco como a la Dr. Lourdes, dos personas que he tenido la suerte de conocer durante este periodo y que han supuesto un baluarte y una guía impagable en la formación en el campo de la neurociencia y neurociencia computacional. Espero poder llegar algún dia como ellos.

Para mí, estas son las 7 personas que han representado un peso muy específico durante este tiempo de tesis, y quería agradecerlo de forma especial.

Sin embargo hay otras personas que han sido importantes durante este periodo de tesis. Destacaría las buenas palabras y voluntad del Dr. Carles Soriano, MD. Dr. Narcis Cardoner, que han aportado las muestras para poder realizar una parte de mi tesis, y en especial a Dr. Carles que siempre ha estado ayudando y aportando en lo que podía. En este sentido también me gustaría agradecer a la Dr. Vesna Prčkovska y a Dr.

Carles Falcon por la ayuda en el procesamiento de datos de neuroimagen.

Por un lado, a nivel profesional del departamento Computational Neuroscience de la UPF al futuro Dr. Murat Demirtaş, Dr. Etienne Hugues- por lo que ha tenido que sufrir conmigo en el análisis de los datos ECOG-, Dra. Joana cabral- en mis inicios- y a Dr. Tristan T. Nakagawa.

Por otro lado, a nivel profesional en mi estancia en el CRG al Dr. Xavier Estivill, en donde me dió la oportunidad de formarme en la genética y como bioinformático durante casi 4 años, y a la Dra. Laia Bassaganyas, "espero que te vaya muy bien por estados unidos, ya me contras", pero en especial a la Dr. Georgia Escaramis una muy buena profesional, en donde he aprendido mucho con ella tanto en la parte de variantes estructurales como en estadística: "¿va a haber un tercero? o ¿ya con dos os plantáis?, en todo caso ¡felicidades!" y finalmente al Dr. Jose Manuel C. Tubio, que por lo que veo le está yendo muy bien por Sanger Institute (Cambridge). Evidentemente, no puedo olvidarme del Dr. Daniel Trujillano durante mi estancia en el CRG, un gran apoyo y "¡espero verte pronto!" y agradecerle sus palabras durante su defensa de tesis.

Otras personas que quisiera agradecer en mi estancia en el PRBB, en donde he estado durante más de 6 años, en primer lugar a Dr. Jordi Villà i Freixa (actual director de la politécnica de UVIC), y que ya en la actualidad, gracias a sus consejos y las diferentes charlas mantenidas, ya le considero un amigo y persona fiable para comenzar proyectos nuevos. Una persona que en mi opinión te puede dar una mano en momentos de decisión difíciles y hay aprovechar muy bien sus palabras, ya que tiene una visión de la vida y una habilidad para analizar a las personas que muy pocos pueden. De él siempre conseguirás recibir apoyo y buenas palabras, pero palabras sinceras. Otras personas que me gustaría agradecer en mi estancia en el IMIM son la Dr. Nuria Lopez, Dr. Manuel Pastor, y Dr. Nuria Centeno "¡Nos queda un café pendiente!".

Y finalmente al Dr. Oscar Gonzalez a las órdenes de Dr. Roderic Guigó, un profesional como ninguno y experto en Clusters y administración. Las veces que he bajado a pedirle cosas y las veces que he tirado los clusters abajo es digno de ver. Vaya paciencia! Gracias!. "Seguimos en contacto, vía skype, y nos vemos en las Navidades".

También a compañeros y amigos en la actualidad como la Dr. Alba Jene, Dr. Eva Noboa, Laia Codo y Dr. Meritxell. También agradecer a Laura Duhé por su ayuda inestimable en la traducción en las últimas fechas de la tesis.

Finalmente, y no por eso menos importante, me gustaría dar las gracias a Dr. Miguel Molina co-chair de la ETOP y director de laboratorio de Quiro-Dexeus-Pangaea.

En este punto me gustaría parar un segundo. Darle muchísimas gracias no sólo por el impulso y confianza a nivel profesional sino por haberme dado la posibilidad de ir como P.I en un proyecto de cáncer a nivel internacional en un H2020 y en donde acabamos a unas décimas de conseguirlo en última vuelta,- y por lo que me cuentas volvemos a intentarlo este año próximo-, sino por la ayuda incondicional que mostrasteis para el tratamiento de Joan. Joan e Isabel y yo siempre estaremos agradecidos por desatascar el problema en un tiempo record de forma que en la actualidad Joan este feliz y con ganas de vivir y pueda disfrutar de sus próximas navidades. En este aspecto me gustaría también agradecer al Dr. Villanueva del ICO por su interés y al MD. Maria Gonzalez Cao por su seguimiento y al Dr. MD. Manzano del Hospital la Vall d'Hebron. Sin dejarme claro a la MD. Dra. Dana Morales. Pero en especial, al MD. Dr. Rafael Rosell, que fue el encargado de coordinar evaluar y dirigir el tratamiento de Joan para su tratamiento, y en lo profesional nos apoyó para ir al H2020. He podido constatar que Dr. Rosell se desvive por sus pacientes.

Por lo que estas últimas palabras son para Joan e Isabel: "gracias por ser felices en momento difíciles", el veros bien supone una gran fuerza para mí.

La depresión es el tipo de trastorno emocional más común en la población mundial. Se caracteriza por sentimientos de culpa o negativos, baja autoestima, pérdida de interés, alto nivel de reflexión y en general una disminución de las funciones psíquicas del individuo. Las nuevas técnicas de neuroimagen no invasivas han incrementado la habilidad para estudiar posibles variaciones de la actividad cerebral en pacientes. En concreto, las imágenes por resonancia funcional magnética (fRMI) se han convertido en las dos últimas décadas el método más importante, no-invasivo sin riesgo para la salud humana, para el estudio de las funciones cerebrales humanas. Biswal y otros en 1995, y posteriormente Lowe y compañía en 1998, demostraron la existencia de actividad espontanea continua en la actividad cerebral en estado de reposo. Estas fluctuaciones también han sido confirmadas en otras especies como en macacos (Vincent JL y compañía, 2007). El estudio mediante técnicas de neuroimagen sobre la actividad cerebral en reposo (rs-fMRI) se ha convertido en una potente herramienta para el estudio de enfermedades, puesto que, por un lado, se ha demostrado tener una mejor relación señal-ruido respecto a enfoques basados en tareas, y por otro lado, ciertos pacientes podrían tener dificultades para realizar algún tipo de tareas cognitivas, de lenguaje o motoras.

Sin embargo, parece ser que debido a ciertas inconsistencias encontradas entre estudios, las técnicas de rs-fMRI no estarían llegando a un uso clínico-práctico para el seguimiento, pronóstico o pre-diagnostico personalizado en individuos con depresión. En línea a esto, aunque Grecius MD en 2008 expuso los beneficios de la técnica rs-fMRI también comentó que para poder ser utilizada en la rutina clínica aún se debería mejorar la relación señal-ruido. Propuso alargar los tiempos de las series temporales en estado de reposo y mejorar los procedimientos de análisis.

En esta tesis se trabaja para dilucidar si existen ciertos factores o componentes en la señal funcional en estado de reposo que pudieran ser utilizados para su uso en la salud clínica. Por ello, utilizamos datos de rs-fMRI sobre dos conjunto de muestras. En el primer conjunto, 27 pacientes con depresión mayor (MDD) y 27 individuos como control, diseñamos descriptores que describan aspectos estáticos y dinámicos de la señal de reposo para la construcción de modelos de prónostico. En cambio, con el segundo tipo de muestras, 48 gemelos, analizamos la relación de posibles factores genéticos y de entorno que pudieran explicar ciertos componentes depresivos en la actividad en estado de reposo.

Por un lado, los resultados muestran que la depresión pudiera estar afectando diferentes redes cerebrales al mismo tiempo localizadas en la parte prefrontal-limbica, en la red DMN, y entre los lóbulos frontoparietales. Además, parece ser que las alteraciones sobre estas redes pudieran ser explicadas tanto por aspectos estáticos y dinámicos existentes en la señal de reposo. Finalmente, conseguimos crear modelos que explicarían parcialmente ciertos fenómenos clínicos presentes en los pacientes depresivos, mediante descriptores globales de estas redes. Estos descriptores de red pudieran ser utilizados para el seguimiento personalizado en pacientes con depresión mayor.

Por otro, utilizando la muestra de gemelos, conseguimos construir un modelo de riesgo a partir de la actividad amigdalar que evalúa el riesgo o propensión de un individuo a partir de componentes analíticas en la actividad de reposo. También sobre esta muestra, se analizó el cerebelo encontrando que el entorno pudiera estar modificando la actividad en estas regiones.

Depression is the most common type of emotional disorder among the world's population. It is characterized by negative sentiments, the feeling of guilt, low self-esteem, a loss of interest, a high-level process of reflection, and in general by a decrease of the individual's psychic functions. The new non-invasive neuroimaging techniques have increased the ability of studying possible variations in patients' brain activity. In concrete, functional magnetic resonance imaging (fMRI) has become the most important method to study human brain functions in the past two decades, being non-invasive and with no risk for human health. Biswal and others in 1995, and later Lowe and his colleagues in 1998, showed the existence of continous spontaneous activity in the brain's activity at rest. These fluctuations have also been verified in other species like macaques (Vicent JL et l, 2007). Studying the brain's activity at rest (rs-fMRI) by means of neuroimaging techniques has become a powerful tool for the investigation of diseases, since it has demonstrated a better signal to noise ratio concerning task-based approaches on one hand, and since certain patients could have difficulties to perform cognitive, language or motor tasks on the other hand.

However, it seems that because of certain inconsistencies found among studies, rs-fMRI techniques would not reach a practical clinical use of a personalised monitoring, prognosis or pre-diagnosis in individuals with depression. In this respect, even if Grecius MD exposed in 2008 the benefits of rs-fMRI techniques, he also commented that the signal to noise ratio remains to be improved to be used in a clinical routine. Grecius suggested to lenghthen the time of the temporal series at rest, and to improve analysis procedures.

The aim of this thesis is to elucidate if the existence of certain factors or components in the functional signal at rest could be used at the clinical health level. In order to achieve this, we use rs-fMRI data on two sets of samples. In the first set of samples, composed by 27 patients with major depression (MDD) and 27 individuals as controls, we design descriptors that describe both static and dynamic aspects of the resting-state signal for the construction of prediction models. Conversely, with the second type of samples (48 twins), we analyse the relation between possible genetic and environmental factors which could explain certain depressive components in the activity in resting condition.

On the one hand, the results show that depression could simultaneously affect different brain networks located in the prefrontal-limbic area, in the DMN, and between

the frontoparietal lobes. Besides, it seems that the alterations in these networks could be explained by both static and dynamic aspects existing in the rest signal. Finally, we achieve the creation of models that would partially explain certain clinical phenomenons present in depressive patients by means of global descriptors in these networks. These network descriptors could be used for personalised monitoring in patients with major depression.

On the other hand, using the twin sample, we achieve the construction of a risk model from the amygdalar activity which evaluates the risk or predisposition of an individual from analytical components in the activity at rest. The cerebellum of this sample was also analysed, and the environment was found to be possibly modifying the activity in these regions.

Even though the clinical phenomenons of depressions are well known, the pathophysiological mechanisms remain unclear. At the moment a high percentage of patients do not respond adequately to the first and second treatment, provoking a high rate of suicides. The depression is considered as a severe emotional disorder, complex to treat and affecting several biological dimensions. In the two last decades the emergence of new techniques of non-invasive neuroimages without risking for the human health have allowed the scientific community to advance in the knowledge of human functions. Concretely, it was observed that the brain activities in resting state could be utilized to detect alterations in the brain of patients with mental disorders. Furthermore, it might be closely related to an underlying anatomical connectivity, which could contains aspects of cerebral organization. Nevertheless, the resting-state functional magnetic resonance (rs-fMRI) is mainly used for research and seems not to be part of the clinical routine for patients with depressions, despite the potential benefits. In order to achieve this objective is necessary the standardization of procedures together with the design of new methods which allow to build a series of models useful to assess the disorder.

In the following studies, prognosis and risk models of the disease are provided for the scientific community which could be of great benefit in the clinical routine. In chapter 1 and 2 dynamic and static components of the resting-state signal are analyzed, however in chapter 3 and 4 descriptors are designed on analytic components of the signal which could contain genetic and environmental factors.

In the first and second chapter a sample size of 27 patients with major depression and 27 controls has been used. However, in chapter three and four a sample size of 48 twins was used (24 monozygotic pairs) informative for depressive psychopathology (6 concordant, 8 discordant and 10 healthy control pairs).

On the one hand, in chapter 1 in the results section, both general aspects that remain constant over time (static) and those time varyng factors (dynamic) of the resting-state singal are analyzed in patients with major depression. In chapter 2 those factors are evaluated together in order to provide an biological explanation and create prognosis modules by use global descriptors of different networks.

Conversely, in chapter 3 we study the genetic and environment factors of depression in the amygdalar resting-state connectivity for your relation with the SERT and serotonin pathway. However, In chapter 4 those factors are analyzed in the regions

of cerebellum, stating that they have a regulating function over the rest of our cerebral areas.

Finally in the last part of this thesis, new lines, in order to advance in methods which could help to explain the depression, are considered. Deco et al. (2014) defines a procedure, which makes it possible to recalibrate the weight of probability of the anatomic structure, constructed through techniques of Neuroimage (DTI), through resting state activity creating a new and improved structure, called enhanced SC (EC). According to this network it seems that certain tracts could be reconstructed respect to the anatomical network where the DTI techniques present limitations. In view of the obtained results in other studies such as bipolar and obsessive compulsives, we think that is possible to use this method in the sample of twins in order to see whether the enhanced SC could help to understand better the etiology of the disorder.

# CONTENTS

## 1. The BOLD signal - functional MRI

In the last decades, magnetic resonance imaging (MRI) and functional MRI (fMRI) have been playing an important role in studies about brain structure, function and the development of pathologies in the brain (Stephen et al. 2004). In particular, fMRI has increased the ability to study possible variations in the brain activity of human beings through non-invasive techniques. Within a short period of time, fMRI has evolved to become the most important method for investigating human brain functions (Nikos K. Logothetis and Brian A. Wandell 2003).

On the one hand, the cerebral blood flow contains water molecules. On the other hand, the Magnetic Resonance (MR) uses radio frequency electromagnetic waves to measure changes of energy states in real time that occur in the hydrogen nuclei of these dipoles in water. Consequently, in fMRI studies, the blood-oxygen-level-dependent (BOLD) signals reflect changes in the cerebral blood volume, cerebral blood flow and oxygen consumption (Nikos K. Logothetis and Brian A. Wandell 2003). However, the BOLD signal depends on the attenuation grade of the local image intensity produced by the introduction of deoxyhemoglobin (dHb) in veins and tissues inasmuch as it is responsible for the extraction of oxygen for the aerobic metabolism. An increment of tissue perfusion rate triggers a dissolution of venous dHb, reducing the tendency of the blood in this region. Consequently, it produces an attenuation of the magnetic resonance signal (Ogawa S et al. 1992). An increase in the signal intensity is detected in the images of fMRI brain mapping. However, nowadays the causality of the neuronal activity with the aerobic metabolism and the extraction of oxygen is still being discussed.

Even though the BOLD signal seems to be related to various factors including cell types, the kind of circuitry driven during activation and the processes of energy demand in the brain, the causes do not seem to correlate with neuronal action potential. So that, a direct comparison between the single-unit physiology and BOLD signal seems to be complicated (Richard D. Hoge et al. 1999).

Although the exact mechanisms that underlie neurovascular coupling are not completely understood, there is empirical evidence that these mechanisms might be altered in the ageing and disease. Besides on the one hand, fMRI can measure brain activity in a noninvasive way and with no significant health risk. And on the other hand, the fMRI method provides a higher spatio-temporal resolution than other methods

available for human research, such as EEG (*scalp potentials*), MEG (*magnetoencephalography*) and PET (*positron emission tomography*). These alternative methods for human brain research suffer from lack of spatial resolution. Despite that the PET stands as an exception of this, the repeated testing on the same brain do not seem recommendable because of the introduction of radioactive substances. So that, as technique could be impractical depending on the case.

## 2. Resting-state fMRI (rs-fMRI)

Resting-state functional magnetic resonance (rs-fMRI) has been converted into a powerful tool for studying the brain function. For human beings, resting-state is defined as the absence of an active state in terms of condition and instructions given from a subject. (B. Wicker et al. 2003).

During the absence of cognitive or sensory stimulation, a significant ongoing spontaneous activity was demonstrated using diverse kinds of techniques. Consistent (Beckmann et al. 2005; Damoiseaux et al. 2006; De Luca et al. 2006; Fox and Raichle 2007; Smith et al, 2009) and large-scale patterns of spontaneous fluctuations in the BOLD signal were identified from fMRI (Biswal et al. 1995; Lowe et al. 1998) and PET data (Shulman et al. 1997; Raichle et al. 2001) in the human brain at rest .

Biswal et al. (1995), and then Lowe et al. (1998) demonstrated for the first time that these fluctuations typically exhibit their highest intervoxel coherence at low temporal frequencies (*<0.1 Hz*). This significant ongoing spontaneous activity in the brain was also found during state of alertness (Fox MD et al. 2006; Rissman J. et al. 2004), sleep (Horovitz et al. 2009; Larson-Prior LJ et al. 2009), light sedation (Grecius MD et al. 2008) and general anesthesia (Martuzzi R et al. 2010; Peltier SJ et al. 2005). Consequently, this type of experiment has begun to be used on animals in the last years (Pawela CP et al. 2008; Majeed W et al. 2009). In recent studies with macaques, it has been observed that those fluctuations have very similar characteristics to the ones found in human beings. This means, that the ongoing fluctuations might unmask the brain intrinsic functional architecture, reflecting an evolutionarily conserved aspect of brain organization which transcends levels of consciousness (Vincent JL et al. 2007).

Even though rs-fMRI can be used for various experiments, this method is at present widely employed among studies about mental diseases or disorders for what it offers. One the one hand, a better noise ratio is achieved with this technique than

conventional task-based approaches (Michael D. Fox and Michael Greicius 2010) demonstrated that during a standard fMRI task session, over 80% of the BOLD modulation may be discarded as noise. A large number of trials would thus be needed, as well as a much more extensive averaging session in order to obtain a good signal to noise ratio (SNR). On the other hand, certain patients could have difficulties to perform any cognitive, language or motor tasks.

Despite of this, rs-fMRI studies do not seem to be part of the clinical routine in most cases. It is due to certain inconsistencies among studies about mental health disorders on the one hand (Jonathan S. Abramowitz and Ryan J. Jacoby severe criticism in the annual review, 2015), and to a certain skepticism about the way functional connectivity- from fMRI data- estimates neural connectivity on the other hand (Maldjian 2001).

A functional connectivity matrix is usually obtained from rs-fMRI data which represents an individual brain. It can be built from the correlation or partial correlation of the average BOLD signal in Regions Of Interest (ROI) or from the BOLD signals by voxels. It has been observed that in this matrix of connectivity, not only correlations between areas with structural connectivity exist (Michael D. Grecius et al. 2009), but also correlations among regions without structural connectivity. It can be due to false positives, being as the matrix represents just probabilities of connectivity, or because of they are showing indirect correlations, by the synchronization of information among third regions which might be cooperating in the implementation of a task (Jessica S. Damoiseaux and Michale D. Grecius 2009). Besides, they can also contain certain level of noise hemodynamic or vascular artifacts, which would be increasing levels of correlation among certain areas (Honey et al. 2009; Cordes et al. 2001).

Despite of all this, nowadays rs-fMRI technique is being used in pre-surgical planning for patients with brain tumors (combining various protocols of neuroimaging, like diffusion-weighted MRI in multivariate analysis) or epilepsy, as well as for patients which could undergo available methods in order to localize lesions or identify diseases, especially Alzheimer (M. H. Lee et al. 2013).

## 3. Resting-State Networks (RSN)

Analyses about the rs-fMRI data have proved the existence of temporal correlations or intrinsic functional connectivity among widely separated brain regions (Biswal et al. 1995; Cordes et al. 2001). In some studies, it has also been demonstrated that this functional connectivity can be found in a coherent way in networks that might be specialized in codifying brain functions such as vision, hearing language and saliency detection (Michael D. Greicius et al. 2009: Hampson et al. 2002; Beckman et al. 2005; Seeley et al. 2007). Greicius et al (2003), Beckman et al. (2005) and De Luca et al. (2006) among others hypothesized that these intrinsic connectivity networks, also known as resting-state networks (RSN), are an amplification of the neuronal activity triggered by intrinsic energy demands of a neuronal population that fire synchronically with a common purpose (David M. Cole et al. 2010: Saini et al., 2004; Lewis et al., 2009). Besides, these coactivating functional systems have been replicated in several studies and over different groups of individuals (Beckmann et al. 2005; Damoiseaux et al. 2006; De Luca et al. 2006; Fox and Raichle, 2007; Smith et al. 2009) and in other species (Vincent et al. 2007). Therefore, this might reflect an evolutionarily conserved aspect of cerebral organization and it might be closely related to an underlying anatomical connectivity (review Gustavo Deco, Viktor K. Jirsa and Anthony R. Mcintosh 2011).

Perhaps the most known RSN is the Default Mode Network (DMN). Greicius et al. (2003) suggested two large opposing systems in the brain that were confirmed afterwards (review M. H. Lee et al. 2012): one in which the DMN could be included, and another one in which the attentional or task-based systems such as somatosensory, visual or attention networks, commonly known as task-positive and task-negative networks, would be incorporated.

In recent years, other RSNs have been shown thanks to methods of analysis such as seed-based correlation analysis (SCA) or independent component analysis (ICA) (Marieke L. Schölvinck et al. 2009). These networks seem to be specially related somehow in the codification of possible brain functions- attentional network (Fox MD et al. 2006), visual (Bianciardi et al. 2009; Eckert MA et al. 2008), auditory (Cordes D. et al. 2000), somatomotor (Biswal et al. 1995; Xiong J. 1999) and others including the thalamus (Zhang et al. 2008), cerebellum (O'Reilly JX et al. 2010) and basal ganglia (Di Martino A. et al. 2008)-. In this sense, Smith et al. (2009) and Laird et al. (2010), using

the BrainMap database that would be involving large number of human subjects, carried out a study using ICA on resting-state data and dividing the brain into several RSNs. On the one hand, Smith et al. concluded that these networks are continuously and dynamically active when the brain is in resting-state. On the other hand, Laird associated them, through meta-analysis, to functions and possible brain disorders. In particular, they basically showed 10 main large-scale networks- there are two frontoparietal networks: one was located on the left hemisphere, and another one on the right one; three visual networks were located on the occipital, parieto-occipital and cerebellar-vermis areas; other was located on prefrontal network; another one on the somatomotor region; and finally the DMN was detected-.

However, the DMN has specially raised a great interest due to its possible relation with the function codification about self-referential nature and its alterations found in mental disorders. This alterations seem to be particularly in patients with Major Depression Disorder-MDD-(Yvette I. Sheline et al. 2009). Besides, the activity in DMN regions appears to be reduced during non-self-referential goal-directed task in healthy individuals (Yvette I. Sheline et al. 2009). Buckner R et al. (2008). This might be related with the evaluation of potentially survival-salient information such as perspective taking of the desires, beliefs and intentions of others and in remembering the past and planning of the future (Raichle M et al. 2001, 2007; Buckner R et al. 2007).

## 4. Diffusion Tensor Imaging (DTI)

During the last years, Diffusion Tensor Imaging (DTI) along with diffusion-weighted MRI (DW), has become one of the neuroimaging techniques most used which is related not only to brain research but also to clinical practice. The increment of the use of DTI in the last decade seems to be sustained (Yaniv Assaf and Ofer Pasternak 2008).

The base of this success is due to the fact that DTI enables the visualization and characterization of the White Matter (WM) in both two and three dimensions in a noninvasive way and without any risk for the health of study subjects, and to its capability to observe micro abnormalities in fibers, or tracts, which connect different regions of the brain.

This technique was first used in 1994, and since then, it has been employed to

characterize brains affected by different diseases such as; multiple sclerosis, stroke, aging, dementia, schizophrenia and so on (Yaniv Assaf and Ofer Pasternak 2008). This technique is based on a statistical basis in order to capture the displacements of water molecules present within regions of the brain with less than mm3 voxels (Denis Le Bihan et al. 2001). The intra-inter matter displacement of molecules enables the conformation of the structure and geometric organization of the matter. More precisely, MR imaging can be sensitized to the random and thermally driven motions (diffusion) of water molecules in the direction of the field gradient (Brian et al. 2004).

Consequently, the diffusion is directionally dependent (anisotropic), on one of the deficiencies of the technique and its virtues, resulting in the general coincidence of WM fiber tract orientation (where the direction of the water molecules does not ensure parallelism in axonal membranes and myelin sheaths of the fiber tracts) with the direction of maximum diffusivity (Brian et al. 2004: Moseley ME et al. 1990). This information is captured thanks to the MRI method and saved inside a three-dimensional space matrix called tensor. Then, this matrix can be analyzed to estimate the degree of diffusivity in any direction or determine the direction of maximum diffusivity, in other words, the more probable direction of fiber tracts. Consequently, the tensor matrix can be mapped in the space, and thus analyzing the WM. Its potential use for clinical practice was suggested earlier by Le Bihan D et al. (1986) who took the first practical application to ischemia in 1992 (Warach S et al. 1992).

However, due to the anisotropic dependency, the DTI technique currently presents a series of problems which must be resolved in order to detect correctly those tracts in regions where a high density of anatomical connections exists. This could limit the characterization of diseases, because of alterations could be on tracts of regions. For instance, the ventral striatum has not shown connection with the cingulate cortex in different DTI studies, when it has been observed in primates (Kunishio and Haber 1994; Haber et al. 2006). Besides, DTI fiber tract reconstruction in specific areas is another troublesome example. It is a rather complex process due to the fiber directions present in frontal lobe or among interhemispheric regions. (A. Di Martino et al. 2008). According to Michael D. Greicius et al. (2009), it was impossible to analyze certain fiber tracts which should be present among certain posterior and posterior regions of DMN by using DTI techniques. This group (Greicius et al. 2003) showed that bilateral angular regions are key to the DMN, however, they were not able to examine tracts going laterally to and from the angular gyrus, revealing a problem that should be

resolved (Mori and Zheng 2006; Peled et al. 2006). And even though it is more than likely that exist some connectivity among angular regions and the posterior cingulate cortex (and maybe with the medial temporal and medial prefrontal cortex), neither of them could be traced. All this can produce a series of inconsistencies among DTI studies.

## 5. Enhanced structural Connectivity matrix (EC)

On one hand, the anatomical structure of a subject's brain can be deduced from DTI data, and on the other hand, activity changes can be observed in real time in the individual through fMRI. Both techniques have become two precious resources in the study of the human brain and the characterization of mental disorders in the individuals. On one side, the structural connectivity matrix (SC), extracted from DTI data, enables to detect structural defects in fiber tracts of the WM. On the other side, the functional connectivity matrix (FC), extracted from fMRI data about the Grey Matter (GM), enables to detect not only potential alterations in brain activity in patients implementing actions (task-evoked), but also abnormalities in ongoing spontaneous activity that could help to deduce intrinsic functional connectivity via rs-fMRI. Both techniques show complementarity since the SC matrix describes potential anatomical and structural changes in the patient, and the FC matrix reports potential abnormalities in different RSNs which encode various brain functions. The incorporation of these neuroimaging techniques, which are non-invasive and spatio-temporal high-resolution procedures without risk to health, has increased significantly in recent years, as far as brain research is concerned. Nonetheless, important lacks exist, and they claim for being solved to avoid inconsistency. In fact, results from different studies have created skepticism or problem when creating models or bases in order to constitute effective profiles that help the clinician associate them with potential treatments of different mental disorders or illnesses. On the one hand, fMRI data often pose a problem of replicability because of issues in signal-to-noise ratio (SNR) processing, produced by hemodynamic noise or cerebral vascular artifacts and by connecting the signal to third regions of the system. On the other hand, the issue with DTI is mainly due to anisotropy dependence, which makes a good tract reconstruction impossible in brain regions where many tracts converge in different directions.

It has been demonstrated that the functional connectivity from the ongoing

activity is closely related to the underlying anatomical connectivity (Honey et al. 2009). This relationship becomes more apparent in studies on the RSN (Deco et al. 2014: Biswal et al. 1995; Damoiseaux et al. 2006; Fox and Raichle 2007; Mantini et al. 2007; Brookes et al. 2011). A possible explanation is that the RSNs might be fluctuating close to a critical point of instability (Ghosh et al. 2008). When global dynamics of a system arrives to this point, the interaction of the underlying SC matrix with local dynamics is amplified (Gustavo et al. 2014). In this moment, the FC matrix concerning rs-fMRI can be simulated (Deco and Jirsa, 2012).

Deco et al. (2014) defined an interactive procedure, in which the weights of structural connectivity are reformulated from the empirical FC matrix at resting-state, thus getting an enhanced structure (EC). From this EC, the simulated BOLD signal can be extracted thanks to the Balloon-Windkessel model, and its results show to be close to the empirical signal (Buxton and Frank, 1997; Mandeville et al., 1999). This process reduces the tolerance between SC and FC matrix connections until the fitting at bifurcation is maximal, producing the final enhanced SC matrix -EC-. The procedure uses a dynamic mean field neural model (DMF) reduction of the detailed spiking/synaptic model (Deco and Jirsa, 2012) developed in the Virtual Brain Platform project (Ritter et al. 2013, Sanz Leon et al. 2013) to fit the empirical SC matrix with the FC one. The DMF, basically, is a mathematical model which integrates fire neurons with excitatory (NMDA) and inhibitory (GABA-A) synaptic receptors (Brunel and Wang, 2001). This matrix, via reducing distances between FC and SC links, should be able to reconstruct DTI connections in regions where DTI technique shows shortcomings.

In sum, we assume that the resulting EC matrix could finally help in analyzing and finding out potential structural abnormalities in regions where the behavior of the SC matrix shows inconsistency.

## 6. RSN estimation using group-ICA strategy from rs-fMRI data

In the analysis of the resting state using preprocessed rs-fMRI data, Independent Component Analysis (ICA) has become an useful method to discover regions that may work collaboratively as coding regions in the brain. These self-organized networks are of particular interest because of they allow to study the association between functional anomalies and behavioral changes. Unlike univariate statistical methods, such as linear regression, does not seem to exist currently a standard method to infer differences between groups. In a regression one can apply common characteristics from group of individuals, whereas in ICA, each subject has unequal temporal. Even though there are methods in the literature (Beckmann and Smith 2005; Calhoun et al. 2001,2002,2004; Esposito et al 2005; Lukic et al. 2002; Schmithorst and Holland 2004; Svensen et al 2002) for the analysis of multiple individuals some that pay special attention into organizing data, others reporting averaged values whereas others on how an individual contributes into the group. All these differences in the method increase the complexity of results.

When ICA is applied, the first step is to choose the adequate analysis design for the hypothesis. Two possible designs are single-subject ICA and group-ICA. In single-subject ICA, temporal and spatial individual characteristics are properly defined, but noisy series may arise and overlap with useful IC. In the other design, group-ICA, it is possible to define common regions for each group but we assume similar temporal series.

One parameter that one has to be taken into account when working with the design group-ICA is the concatenation protocol, that is, if it is spatial or temporal. When working with a temporal protocol, a single time series is obtained, assuming a common mapping for the group. On the other hand, a single mapping is obtained when the spatial approximation is used, assuming the assumption that there are common time series in certain regions. Schmithorst and Holland (2004) proved that when are working with fMRI data, temporal concatenations would give better results due to the fact that, probably, the fMRI signal variations in temporal series are bigger than the spatial ones.

However, the critical point in this strategy is a priori number of components that one wants to obtain. Depending on the number, the algorithm could break a single RSN into different ICs. For obtaining the optimal number of components a possibility is to

apply the Minimum Description Length (MDL) algorithm (Rissanen J. et al).

Once the number of optimal components are estimated a group-ICA approach works basically in three steps: 1) data reduction in order to reduce complexity and retain most of the variance; 2) ICA analysis; 3) and additionally, a back reconstruction to map the components and the individuals. In the first phase of data reduction, the complexity of each individual's matrix is reduced by means of PCA and is temporarily concatenated by groups. These groups suffer another reduction in the number of components initially estimated, and are concatenated again to obtain a data matrix with that number of components. After the phase of back-reconstruction, one obtain the maps of common components for all individuals of that group.

## 6.1. Theory of the Group ICA strategy

Usually, a PCA for each individual is used to reduce the complexity of the data due to computational requirements. So that, we obtain a matrix $X_i = F_i^{-1} Y_i$ with dimensions $LxV$ for each of subjects $i$, where Y is $KxV$ matrix that contains the preprocessed and the normalized spatial data, $F_i^{-1}$ is the matrix determined by the PCA, V is the voxel number , K is the number of time points and L is the size of the dimension of the temporal matrix after the reduction. Then, all the reduced matrices for each individual are concatenated into a new matrix that is again reduced with PCA until reaching N dimensions, which will correspond to the number of components initially estimated. As a consequence, we obtain the reduced matrix of $LMxV$ , where M is the number of individuals:

$$X = G^{-1} \begin{bmatrix} F_1^{-1} Y_1 \\ \vdots \\ F_M^{-1} Y_M \end{bmatrix}$$

And where $G^{-1}$ is a $NxLM$ matrix obtained from the decomposition by PCA that is being multiplied on the right by the reduced matrix of $LMxV$ . In the decomposition of ICA, we can write X = AS, where A is a matrix $N \ x \ N$ and S is the map of components $N \ x \ V$. If X is substituted and matrix G is decomposed for each individual, we have:

$$
\begin{bmatrix} G_1 \\ \vdots \\ G_M \end{bmatrix} AS = \begin{bmatrix} F_1^{-1} Y_1 \\ \vdots \\ F_M^{-1} Y_M \end{bmatrix}
$$

One can rewrite then the partitioned matrices equation for each individual as $G_i AS_i = F_i^{-1} Y_i$ , where the matrix $S_i$ contains the map of an individual i and is calculated from $S_i = (G_i A)^{-1} F_i^{-1} Y_i$ . At this step, multiplying at both sides by $F_i$ , and solving for $Y_i$ we obtain: $Y_i \approx F_i G_i AS_i$ where $Y_i$ would contain the result of ICA of an individual i. The matrix $S_i$ with dimensions $N \; x \; V$ contains the N maps and the $F_i G_i A$ $(K \; x \; N)$ matrix contains for each component N the temporal series per individual.

## 7. Bases of Network Construction using graph theory from rs-fMRI data

A network is defined as a group of nodes linked together through edges creating a connection graph. Nodes show the different brain areas which were divided in the preprocessing step by using an atlas. So a graph represents the statistics interdependence between signals in two different areas.

### 7.1. Edge Definition

Usually, each ROI comes from the average temporary course of all spatio-temporal signals that are found in every voxel. Typically, the interdependence between two areas is extracted by the partial correlation coefficient between the average temporary courses in two different brain regions (obtaining the FC). As this shows only a probability of connection between areas. So that, we should have a special consideration with the low probability connections due to might introduce nonexistent connections creating noise in the post analysis. When using regression techniques (for the correction of movement or to cancel the global signal of the system), the average of the system could be displaced. It could explain much of the negative values, being only low correlation values, so in other words, most of them artifacts with random values. So in some studies the connections are analyzed excluding the negative values on FC matrices.

## 7.2. Network metrics from graph theory

Metrics or descriptors are used to quantify the infrastructure and organization of the complex networks that form the brain. Two different kinds of metrics are usually deduced: global, in which the whole network is summarized by an unique value, and local, in which the function of the node in its network is retained.

Nowadays, several topological studies have shown that brain networks tend to have high levels of clustering together with a high global efficiency creating community structures that also be creating efficient interconnected hubs.

It is possible to characterize a brain network if we can describe different points of view: the degree of connection or its infrastructure, the efficiency level when it carries information among connected nodes, or in other words how these nodes are integrated, and the segregation level, to know if they are creating groups or not. On the one hand, the segregation allows a network to specialize in the coding of different functions and tasks, but on the other hand, a high global efficiency allows a network to have the ability to process the information in an efficient way. So, global or local metrics can be characterized by 1) its infrastructure (strength, average strength, degree and average degree), 2) its own capacity to carry information on different channels in a parallel form (global efficiency), 3) its own capacity to create groups (local efficiency, nodal efficiency). The definition of these metrics together with the explanation and rules are described by Rubinov and Sporns (2010). In addition, it should also be taken into consideration that the brain is really sensitive to energetic shortage, and most of the energy is obtained by the glucose metabolism, in other words the brain is sensitive to the oxidative stress.

So that, in disorders, it is reasonable to find an increment of costs among nodes which might be sensitively important to codify affected functions. There are proofs that the metabolic cost of a node is proportional in one way or another to its own degree and/or centrality (degree, strength nodal) and the physical distance that it has regarding to other nodes (efficiency). In sum, in brain disorders it would expect some kind of defects in networks with costs abnormalities or changes in the connection density such as long interconnection hubs. For assessing these features in a network, a cost estimator is typically used for correcting them by total of connections.

**The Depression**

Major Depression Disorder (MDD) is the most common type of mood disorder among the global population. The World Health Organization (WHO) in 2001 ranked MDD as the main cause of years of life lived with disability (Wayne C.Drevets, et al. 2008). In 2004, it was considered as the third main cause of the global burden of disease (Gabriel S.Dichter, et al. 2014), and in 2010, it was already considered to be the main cause of disability (Ferrari, et al. 2013). This disease, that affects more than 150 million people worldwide (WHO, 2008), it has a 16% lifetime prevalence rate that affects the 7% of the EU population each year (Wittchen, et al. 2011). Besides, the disorder brings not just a personal suffering but also socioeconomic consequences for a country. Moreover, 10% of suicides are caused by untreated or misdiagnosed depression (APA, 2000). So that, an early diagnosis and a personalized treatment during the different sub-phases of the disease- which are remission, monitoring, relapse and maintenance- are crucial for a long-term complete recovery of the patient (Ellen Frank, Kupfer et al. 1991).

Depression is characterized by ruminations, self-blame and an increased association of their self with negative emotions (Gruenbaum et al., 2005; Ingram, 1990; Northoff, 2007; Rimes and Watkins, 2005; Treynor, 2003). Clinically, patients show a medical history of an abnormal focus in self-attribution of the negative emotions. Even though the clinical phenomenons are well known, the underlying neural networks and pathophysiological mechanisms remain unclear (Simone Grimm, 2009). Nowadays, the therapeutic response still present a low ratio of success during the first and second treatment which causes a high suicide rate (Ronald S. Duman, et al. 2012).

The theories of behaviorism from Plato to Freud, already emphasized repeatedly the relationship between the emotion and the reasoning. This relationship could be attributed in the present days to relationships that coexist among brain systems which are regulated by neurophysiological pathways. The definition of anatomical networks, that would hold the emotional behavior (as seen from studies on animals), and the ones developed by neuroimaging technologies- which are allowing a deep characterization of the anatomy, physiology and neurochemistry in humans in relation to the mood disorders- have made important progress in the pathophysiology of the depression (Joseph L Price, Wayne C. Drevets, 2009).

Broca (1879) in his study 'Grand lobe limbique' and James W. (1884) related the emotions with visceral functions. Later on, in the studies of Gaskell, Langley, Cannon et al. around the 90's indicated, moreover, that many of this visceral functions were controlled by the 'autonomic nervous system' where the hypothalamus ('head ganglion of the autonomic nervous system') was the one in charge of the self-control and coordination. Afterwards, Kluver and Bucy (1939) thanks to his studies carried out from the injuries in monkeys, together with MacLean (1949) and the model of Papez (1937) suggested 'the Limbic System', in which were included the hippocampal formation, cingulate gyrus and thalamus, medial and lateral temporal structures and their relationship with the hypothalamus and the amygdala- as the main responsible of emotions and emotional expression's production-. It was only in 1991 when Zola-Morgan et al. proved that the hippocampus might be more involved in memory processing and that the amygdala might have a more important role when it comes to its relationship with emotions and anxiety.

Around 1960 and 1970 the known relationships of the limbic system were expanded defining an interconnected circuit in which Nauta in 1962 (on monkeys), Cowan et al. In 1965 showed projections of the amygdala towards the hypothalamus and the relation among the medial thalamus, orbital cortex, striatum and hypothalamus and the amygdala. Likewise, Krettek and Price (1977, 1978), from their studies on rats, defined projections from the basal and lateral amygdala to the orbital and medial prefrontal, insular, and temporal cortical areas, the mediodorsal thalamic nucleus, and the medial and lateral hypothalamus at a neurophsyology level in the transportation of 3H-leucine. In 1987, Russchen et al. observed GABAergic axons from ventral and rostral pallidum to mediodorsal thalamic nucleus. And more recently, Buckwalter et al. (2008) identified amygdala projections towards the posterior cingulate cortex.

During 1990, after some studies on monkeys, the existing relationship between the 'Limbic System' and the amygdala towards the cortical sub-circuitry of the medial prefrontal area were identified along with a structure limbic-cortical, connected via mediodorsal thalamic, that could be implied in mood disorders. Later, this interconnected structure would be known as cortical-striato-pallido-thalamic circuitry, which is characterized by a bidirectional reciprocal overlap. Subsequently, in different studies carried out after the 90's and early 21st century, it was shown that this circuitry might be modulated or compensated via neurophysiologic by a substructure of connections, that might be also involved in mood disorders and in emotions control: the

Orbital and Medial Prefrontal Cortex (OMPC) circuit, identified by Carmichael and Price (1994, 1995, Kondo et al. 2005; Joseph L Price, Wayne C.Drevets, 2009).

Later, in 1999, Garcia R. et al. observed that the amygdala would condition the neuronal activity of one of the parts in the prefrontal medial area (mPF), during episodes of anxiety. However, in other studies, the existence of a possible control by the prefrontal cortex regions (PFC) over the amygdala was also argued (by inhibition control via dopamine: Armaral and Price 1984 – 1992; Likhtik E. et al. 2005; by excitation via glutamatergic: Bacon et al., 1996; Jackson and Moghaddam, 2001). Moreover, Ray and Price (1993) and Petrides and Pandya (1999) indicated that another set of cortical-cortical connection structures (Dorsal Lateral Prefrontal Cortex, DLPFC) would be also strongly linked to OMPFC circuit.

From the 70's and 80's, the development of new technologies in non-invasive neuroimaging (with really low aggressiveness and lack of radiation exposure), have allowed the characterization and the identification in vivo of structural alterations in the brain and neurophysiological changes in the MDD with and without treatment during the different phases of the disorder. At the beginning of this century, it was observed in different studies important alterations of the GM volume in patients with MDD, specially in the Anterior Cingulate Cortex (ACC) and in the subgenual PFC areas (Botteron et al. 2002, Drevets et al. 1997). The GM volume showed a reduction in patients with major depression in OrbitoPreFrontal Cortex (OPFC), ventrolateral PFC, frontal polar/dorsal anterior-lateral PFC, parahippocampal gyrus and temporal-polar cortex (Drevets and Price, 2005). Nonetheless, discrepancies in the volume have also presented in different studies about the disorder remission after the treatment of regions like ACC and hippocampus (Joseph L. Price and Wayne C Drevets, 2009).

Moreover, in connection with the limbic system, Caspi et al. (2003; David SP et al. 2005) identified that the serotonin transporter promoter region (5-HTT)- affecting to 5-HT1A receptor binding (used as a target in depression and anxiety treatments)- might be associated to genetic factors increasing the risk of developing depression in a stressful environment. And it seems that this could be phenotypically related to a decrease of volume in the ACC (Pezawas et al. 2005). Besides in line with the structural studies of neuroimaging, alterations in the metabolic activity of serotonin-1A receptor in regions such as the amygdala, anterior cingulate cortex, insula, hippocampus, dorsal raphe nuclei and the area of the mPFC (Jonathan Savitz et al. 2009, Wayne C. Drevets et al. 2009) were found in patients in with anxiety disorders or depression under stress

(Parsey RV et al. 2006). Moreover, regions such as the ACC, prefrontal cortex and amygdala show decrease of the serotonin metabolic activity (Joseph L. Price and Wayne C. Drevets, 2009).

However, in other studies, the existence of dopaminergic abnormalities has been described in patients with MDD, and has been connected to a set of structures that would form 'Reward System' (RS) where the nucleus accumbens might have a relevant role. (Adinoff 2004, de la Fuente-Fernandez et al. 2002). Violetta Klimek (2002) found dopaminergic abnormalities in the amygdaloid nuclei of patients with major depression in a post-mortem analysis. And later, a dopamine transporter affinity in the basal ganglia (putamen and caudate nucleus) area has been presented in comparative studies between depressive group and controls, suggesting that the dopamine function could also be altered in this disease (David J. Brunswick et al. 2003). On the basis of this, Lescia K. Tremblay (2005) suggested in his model that the dopamine-related neuroanatomical substrates could be involved in alterations of reward processing, anhedonia, lack of motivation and inattention in the depression and that these structures could also be used as putative therapeutic targets (like it already happened with serotonin-1A receptors). In the same line, Eric J. Nestler and Thomas E. Schlaepfer (2006), hold alterations in the mesolimbic dopamine system responsible for anhedonia in MDD, in which the nucleus accumbens (ventral striatum) and the dopaminic inputs of the ventral tegmental area would be implied. They also presented these structures as possible markers of the antidepressant medication.

But also, the concentrations of the glutamatergic neuroreceptors and, in particular, the inhibit neurotransmisor γ-Aminobutyric Acid (GABA), have also shown alterations in patients with depression, these being potential targets in antidepressant treatments. A deficit of GABA may produce anxiety disorders, on the contrary, an excess of glutamate seem to be toxic for neurons and it may produce brain damages. However the glutamate pathways, meanwhile, spread across all the nervous system, uniting most of the neurotransmitter pathways. Because of it vastness, it is involved a great amount of different physiological tasks and its dysfunctions can produce damages and disorders. Specifically, it has been observed that the glutamate-induced excitotoxicity in the hippocampus leads to a decrease of the neuronal regeneration and plasticity that produce a loss of spatial learning (Cortese and Luan Phan, 2005).

Furthermore, a capture of glutamate deficit is related to the problems in the RS (Bechtholt-Gompf et al. 2010). This suggests that the glutamatergic system can be an

important regulator of other via and it should be object of new therapeutic targets (Swanson et al. 2005). Nevertheless, the complexity of glutamate regulation and its large presence in the brain explains why just three prescription medications have been developed for the glutamate receivers (memantine, ketamine, and D-cylcoserine). It has been indeed noticed that the side effects of these medications are extremely high. However, more than 20 types of glutamate receptors have currently been identified, so that it could be possible to develop new specific biomarkers for each receptors group.

Dorothee P. Auer (2000) suggested that the alterations in glutamatergic neurotransmission inside the ACC can have an important role in the depression pathogenesis. Recently, Beata Karolewicz (2010) showed reduced levels of glutamic acid decarboxylase-67 KDa, and a reduction of GABA levels in the PFC in patients with depression treated with antidepressants. It has observed that concentrations of GABAergic neurons seem to be specially altered in the PFC, DLPFC and OPFC (Rajkowska G et al. 1999, 2005; Cotter D et al. 2002, 2005).

So that, from the symptomatology of the depression and thanks to the studies that were carried out initially in animals and also to the new analysis on non-invasive techniques of neuroimaging, it has been able to established strong connections between depressive traits and alterations found in different brain substructures in the disorder.

The problem is that depression seem to be complex disorder which is characterized by a heterogeneity along several psycho biological dimensions, therefore, allegedly different brain systems could be affected at the same time such as: the cortical-limbic system which is really related to the expression of the emotions and stress- which might be involved the serotonin pathway-; RS, related to the motivation or anhedonia and it is rather associated to alterations in the dopamine activity; and glutamatergic and gabaergic system, which, this last one, could be associated to anxiety problems and it is shown more altered in cortical regions such as PFC and LPFC in the MDD.

Moreover, it has been proven that certain alterations could be located on shared regions by different systems in the MDD, as Dorsal Nexus (DN). This might explain a part of this clinical heterogeneity, because although the different neuroreceptors (inhibitory and excitatory) have associated its own neurotransmissors, an induced excitotoxity located in a certain kind of neurons could indeed imply a number of alterations in different systems. Moreover, systems like the cortico-limbic show overlapping bidirectional connections among areas. Certain alterations in these

interconnected and bidirectional structures may cause an imbalance process by self-inducing alterations or damages.

Following with this, Northoff et al. (2011) argued that depression should be considered as a system disease and that a depressive model only based on the limbic system or a single region might explain rarely the clinical heterogeneity of this disorder. Furthermore, Georg Northoff et al. hypothesized that the abnormal levels of activity during resting-state in patients with depression might be enabling stimulus-induced neural activity for alterations in self-representation and behavior changes. In concrete they explained that alterations found among DMN regions in resting-state might be enabling stimulus-induced activity in sensory and limbic/paralimbic regions (Northoff et al. 2010).

Mayberg et al. (2005) showed that the increase of activity found in DMN regions in patients with depression correlated with the length of the current depressive episode. This kind of relation could be used for the prognosis of the different disorder stages and a personal monitoring of the patient to improve the ratio of success during the first and second treatment and therefore decrease the suicide rate of the disorder.

Anand et al. (2005) observed through his studies (with certain limitations) that after six weeks of treatment with setraline in depressive patients, connectivity changes during the resting state were produced between the dorsal ACC and medial thalamic regions. Recently, Ciara McCabe and Zevic Mishor (2011), in a resting-state study, showed that the application of antidepressant medications in volunteers decreased the FC among areas connected with the RS and emotional processing (amygdala and ventral mPF in the citalopram group, and striatal-orbitofrontal cortex connectivity in the reboxetine group).

Although Michael Greicius (2008) exhibited the benefits of rs-fMRI respect to the task-activation fMRI, Greicius also explained that the main limitation for its clinical application is the poor relation signal-to-noise (SNR) and proposed to improve both the techniques of analysis on the BOLD signal and the length of the time series.

Recently, Qiyong Gong and Yong He (2015) considered that certain discrepancies in some neuroimaging studies on patients with depression could be caused by factors such as age, depressive episodes, previous medication to the study, length of the time series, previous medication and cardiorespiratory and motions artifacts.

In this sense, it has observed a decrease of volume in the hippocampus (Vythilingam et al. 2002; Sheline et al. 2003) depending on the gender, contradictory

results in the amygdala volume (Drevets, 2004, Savitz et al. 2009) and also contradictory changes in the metabolic activities, either increase or decrease, in ACC region (Josep L Price and Wayne C Drevets, 2009) have been shown in the depression. Moreover, it has been also observed certain variability in the DLPFC (Paul B. Fitzgerald et al. 2005).

On the one hand, in order to increase the statistic power of the analysis, the whole brain can be divided in different RSNs by using ICA. Besides, the ICA allows to identify intrinsic brain networks by their unique neural signatures (J. Paul Hamilton et al. 2012) such as movement, vision, audition, language, memory, executive functions, salience (Cordes D et al. 2000, Hampson M et al. 2002, Beckmann CF et al. 2005, Seeley WW et al. 2007).

In this line, Greicius et al. (2007) found alterations between the thalamus and ventral ACC within the DMN. Although DMN is more studied in neuroimaging studies in depressive due to its activation associated to rumination, self-relational processing in MDD, other possible RSN seem to be altered in this disorder (J. Paul Hamilton et al. 2012), such as executive network, DLPFC (Bench et al. 1992, Mayberg et al. 2005, Pizzagalli et al. 2009, Strigo et al. 2008) and the salience network (O'Reardon et al. 2007, Gross, Nakumura, Pascual-Leone and Fregni, 2007).

On the other hand, the use of new strategies on the resting-state signal might unmask alterations in depression which might have a clinical purpose. This suggests analyzing the different analytic components of the BOLD signal in resting-state.

In light of the concepts reviewed in the previous introductory chapter, the general objective of this work is to elucidate how the ongoing fluctuation existing in the human brain activity in resting state can be analyzed to detect underlying anomalies in patients with depression. Different methodologies and mathematical procedures that may improve the relation signal-to-noise (SNR), might be applied on the BOLD signal at rest. In doing so, the main is to unmask those depressive specific features which could be used like putative markers in prognosis models, prevention, monitoring or personalized clinical treatments in patients with depression.

To achieve this goal, we will first design static (from averaged measures during all resting-state sessions) and dynamic (from time-varying measures) descriptors in the chapters 1 and 2 to assess possible depressive patterns on the BOLD signal a rest. It can be completed by means of a comparative analysis between the rs-fMRI data of a group of 27 patients with major depression disorder (MDD) and the rs-fMRI data of a control group of 27 subjects. Next, we will try to build prognosis models of depression using both these descriptors and the clinical variables of the patients.

However, in a second part (chapters 3 and 4), we want to evaluate the putative relationship between the genetic and environment factors that might exist in depression in regions which seem to play, a priori, an important role in the depressive disorder. For this purpose, we will use a sample of 48 twins (24 monozygotic pairs) informative for depressive psychopathology (6 concordant, 8 discordant and 10 healthy control pairs). We will assess different analytical components of the brain activity in resting-state to determine those which might be related with genetic or environment factors. Finally, these analytic components could also be used to build risk models which might be used to identify those individuals with a high predisposition to develop this disorder.

**CHAPTER I**

# Dynamic Functional Connectivity Reveals Altered Variability in Functional Connectivity Among Patients with Major Depressive Disorder

Murat Demirtaş[1*], Cristian Tornador[1], Carles Falcón[4], Marina López-Solà[5,6], Rosa Hernández-Ribas[7,8], Jesús Pujol[6,7], José M. Menchón[7,8,9], Petra Ritter[11,12], Narcis Cardoner[3], Carles Soriano Mas[7,8,10], Gustavo Deco[1,2*]

*Under review in Hum Brain Mapp*

[1]Center for Brain and Cognition, Department of Information and Communication Technologies, Universitat Pompeu Fabra, 08018 Barcelona, Spain; [2]Institució Catalana de Recerca i Estudis Avançats, 08010 Barcelona, Spain; [3]Depression and Anxiety Program, Mental Health Department, Parc Taulí Sabadell; Hospital Universitari Department of Psychiatry and Legal Medicine, Universitat Autònoma de Barcelona, Spain; [4]BarcelonaBeta Brain Research Center, Pasqual Maragall Foundation, Barcelona Spain; CIBER-BBN, Barcelona, Spain; [5]Department of Psychology and Neuroscience, University of Colorado, Boulder CO, USA; [6]MRI Research Unit, CRC Mar, Hospital del Mar, Barcelona, Spain; [7]Carlos III Health Institute, Centro de Investigación Biomédica en Red de Salud Mental (CIBERSAM), Spain; [8]Psychiatry Department, Bellvitge University Hospital, Bellvitge Biomedical Research Institute (IDIBELL), Barcelona, Spain; [9]Department of Clinical Sciences, University of Barcelona, Spain; [10]Department of Psychobiology and Methodology of Health Sciences, Universitat Autònoma de Barcelona, Spain. [11]Max-Planck Institute for Cognitive and Brain Sciences, Leipzig, Germany. [12]Department of Neurology, Charité, Charitéplatz 1, 10117 Berlin

Address correspondence to Email: murat.demirtas@upf.edu

**Short title**: Dynamic Functional Connectivity in Major Depression

**Key words**: mood disorders, major depressive disorder, dynamic functional connectivity, resting state, fMRI.

**Word count**: abstract: 204; text: 3890; references: 33; tables: 2; figures: 4

*Advisor report on the contribution of the Ph.D. candidate to the article.*

Prof. Dr. Gustavo Deco associate professor at the Universitat Pompeu Fabra of Barcelona, and supervisor of the present doctoral thesis by Cristian Tornador Antolin, hereby certifies that the participation of the Ph.D. candidate in the article "Dynamic Functional Connectivity Reveals Altered Variability in Functional Connectivity Among Patients with Major Depressive Disorder" included the following tasks:

- Participation in study design
- MRI data pre- and post- processing.
- Statistical analysis in the RSN parts.
- Critical revision

Prof. Dr. Phil. Dr. Rer. Nat. Habil. Gustavo Deco

Barcelona, 2015

Demirtaş M, Tornador C, Falcón C, López-Solà M, Hernández-Ribas R, Pujol J, Menchón JM, Ritter P, Cardoner N, Soriano-Mas C, Deco G. Dynamic functional connectivity reveals altered variability in functional connectivity among patients with major depressive disorder. Hum Brain Mapp. 2016 Apr 28. doi: 10.1002/hbm.23215.

**CHAPTER II**

# Altered resting state networks in Major Depression are explained by both static and dynamic aspects of the BOLD signal at rest

Cristian Tornador[1*], Murat Demirtaş[1*], Dafnis Batalle, Carles Falcón[4], Marina López-Solà[5,6], Rosa Hernández-Ribas[7,8], Jesús Pujol[6,7], José M. Menchón[7,8,9], Petra Ritter[11,12], Narcis Cardoner[3], Carles Soriano Mas[7,8,10], Gustavo Deco[1,2*]

[1]Center for Brain and Cognition, Department of Information and Communication Technologies, Universitat Pompeu Fabra, 08018 Barcelona, Spain; [2]Institució Catalana de Recerca i Estudis Avançats, 08010 Barcelona, Spain; [3]Depression and Anxiety Program, Mental Health Department, Parc Taulí Sabadell; Hospital Universitari Department of Psychiatry and Legal Medicine, Universitat Autònoma de Barcelona, Spain; [4]BarcelonaBeta Brain Research Center, Pasqual Maragall Foundation, Barcelona Spain; CIBER-BBN, Barcelona, Spain; [5]Department of Psychology and Neuroscience, University of Colorado, Boulder CO, USA; [6]MRI Research Unit, CRC Mar, Hospital del Mar, Barcelona, Spain; [7]Carlos III Health Institute, Centro de Investigación Biomédica en Red de Salud Mental (CIBERSAM), Spain; [8]Psychiatry Department, Bellvitge University Hospital, Bellvitge Biomedical Research Institute (IDIBELL), Barcelona, Spain; [9]Department of Clinical Sciences, University of Barcelona, Spain; [10]Department of Psychobiology and Methodology of Health Sciences, Universitat Autònoma de Barcelona, Spain. [11]Max-Planck Institute for Cognitive and Brain Sciences, Leipzig, Germany. [12]Department of Neurology, Charité, Charitéplatz 1, 10117 Berlin

Address correspondence to Email: cristian.tornador@upf.edu

**Short title**: Altered RSNs in depression

**Key words:** Dorsal Nexus, DMN, frontoparietal, prefrontal, limbic, resting-state fMRI, RSN, ICA, depression, signal processing, graph theory, NBS, dynamic descriptors, partial correlation, marker, vary-time, regression. HDRS, episodes of depression, autobiographical memory, episodic, stress, rumination, hyperconnectivity, hypogyrification, phase-coupling, decision tree.

*Advisor report on the contribution of the Ph.D. candidate to the article.*

Prof. Dr. Gustavo Deco associate professor at the Universitat Pompeu Fabra of Barcelona, and supervisor of the present doctoral thesis by Cristian Tornador Antolin, hereby certifies that the participation of the Ph.D. candidate in the article "Altered resting state networks in Major Depression are explained by both static and dynamic aspects of the BOLD signal at rest" included the following tasks:

- Participation in study design
- MRI data pre- and post- processing.
- Statistical analysis
- Writing of the manuscript
- Critical revision

Prof. Dr. Phil. Dr. Rer. Nat. Habil. Gustavo Deco

Barcelona, 2015

## ABSTRACT

Different findings indicate that major depression (MDD) is a complex disorder that involves several psychobiological dimensions implying several brain systems. Furthermore, different mathematical representations of resting-state fMRI data show that BOLD signal patterns are able to embed distinct kinds of information which may be relevant in the codifying of brain functions. However, the relative contribution of static and dynamic aspects of brain activity affected by depression remain unexplored.

The present study assesses the contribution of static and dynamic factors to activity in Resting State Networks (RSNs), in relation to clinical depression symptoms. In order to do so, a graph theoretical framework was employed to design static and dynamic measures (descriptors) which globally depict the defined RSNs.

Results show that both static and dynamic descriptors unmask anomalies in the Default Mode Network (DMN), specially in its posterior part, -PreFrontal-Limbic network (PFL) and FrontoParietal network (FPN)- in patients with MDD. In concrete terms, results indicate that the severity level of depression (HDRS) is strongly associated to both global problems of efficiency on dynamic aspects in the posterior DMN area, and local deficiencies in functional connectivity among areas of the PFL such as the Orbitofrontal Cortex (OFC), Dorsolateral Prefrontal Cortex (DLPFC) and Anterior Cingulate Cortex (ACC) regions. These deficiencies could be probably caused by a hyperconnectivity and loss of flexibility on phase-coupling in these networks. We also observe that both the length and total number of episodes of depression in patients seem to be related with alterations in functional connectivity between FP areas. Moreover, results show a general loss of variability on phase-coupling in connectivity among regions of these RSNs.

All this suggests that both phase-coupling problems in the BOLD signal and underlying structural alterations coexist within these RSNs in patient with MDD triggering depressive traits such as: maladaptive, high level of rumination, brooding, overgeneral autobiographical or episodic memories, negative emotional judgments and anxiety problems. However, additional studies should be realized to clarify the level of relationship. Finally, we hypothesize that this phase-coupling inflexibility found in these RSNs could be connected somehow with the idea of a gradual process of hypogyrification, which might be directly proportional to the length of depression or the severity level.

**INTRODUCTION**

Major Depression Disorder (MDD) is the most common type of mood disorder among the global population. The World Health Organization (WHO) in 2001 ranked MDD as the main cause of years of life lived with disability (Wayne C.Drevets, et al. 2008) and in 2010, it was already considered to be the main cause of disability (Ferrari, et al. 2013).

Depression is characterized by ruminations, self-blame and an increased association of their self with negative emotions (Gruenbaum et al., 2005; Ingram, 1990; Northoff, 2007; Rimes and Watkins, 2005; Treynor, 2003). Clinically, patients show a medical history of an abnormal focus in self-attribution of the negative emotions. Even though the clinical phenomenon is well known, the underlying neural networks and the pathophysiological mechanisms remain unclear (Simone Grimm, 2009).

Georg Northoff et al. (2011) argued that MDD should be seen as a disease of the brain system, because a depressive model only based in a single region could rarely explain the heterogeneity across several psychobiological dimensions. On the one hand, during the last two decades, different studies have shown that MDD could present several affected systems or networks. On the other hand, the brain has shown to be a dynamic complex system where brain functions involve overlapping regions, circuitry and pathways. So clinical phenomenons of MDD could thus be more adequately explained by closer approaches to brain functions.

Resting state functional magnetic resonance (rs-fMRI) has been converted into a powerful tool for studying the brain function. Resting state is defined as a lack of no perceptual input from the world (B. Wicker et al. 2003). During the absence of cognitive or sensory stimulation, a significant ongoing spontaneous activity was demonstrated by diverse techniques. Consistent (Beckmann et al. 2005; Damoiseaux et al. 2006; De Luca et al. 2006; review: Fox and Raichle 2007; Smith et al, 2009) and large-scale patterns of spontaneous fluctuations in the BOLD signal were identified in the human brain at rest from fMRI (Biswal et al. 1995; Lowe et al. 1998) and PET (Shulman et al. 1997; Raichle et al. 2001). Biswal et al. (1995), -and later Lowe et al. (1998)-, demonstrated for the first time, that these fluctuations typically occur at low temporal frequencies (<0.1 Hz). In recent studies with macaques, it was observed that those fluctuations had very similar characteristics to the ones found in humans. This fact could be due to the

ongoing fluctuations that could be unmasking an intrinsic functional architecture, reflecting an evolutionary conserved traits of brain systems (Vincent JL et al. 2007).

Besides, the rs-fMRI analysis has demonstrated the existence of intrinsic functional connectivity in widely separated brain regions (Biswal et al. 1995; Cordes et al. 2001). In some studies, it has also been proved as well that this functional connectivity can be found in a coherent way in networks that could be specialized in codifying brain functions (Michael D. Grecius et al. 2009: Hampson et al. 2002; Beckman et al. 2005; Seeley et al. 2007). Grecius et al. (2003), Beckman et al. (2005) and De Luca et al. (2006) among others, hypothesized that these intrinsic connectivity networks, also known as resting state networks (RSN; Smith et al. 2009 and Laird et al. 2010), are an amplification of the neuronal activity. This one would be produced by intrinsic energy demands of neuron population that would fire in a synchronized way with a common aim via the synaptic plasticity (David M. Cole et al. 2010: Saini et al., 2004; Lewis et al., 2009). Besides this, one of the features of these coactivating functional systems have been replicated in several studies and over different groups of individuals (Beckmann et al. 2005; Damoiseaux et al. 2006; De Luca et al. 2006; Fox and Raichle, 2007; Smith et al. 2009). Therefore, it might associated somehow to an underlying anatomical connectivity (review Gustavo Deco, Viktor K. Jirsa and Anthony R. Mcintosh 2011).

In this sense, the Default Mode Network (DMN) and Dorsal Nexus (DN) have raised a great interest, because of its possible relation with the codification of the functions of a self-referential nature and its alterations found in mental disorders, in particular when it comes to MDD (Yvette I. Sheline et al. 2009, 2010). Respect to this, J. Paul Hamilton et al. (2011) argued that the functional alterations in resting-state, that were found in the task-positive network (TPN) and the DMN, could be connected with an adaptive and maladaptive, depressive rumination in MDD.

Nonetheless to date, still few studies have studied depression-related changes of activity at rest in the DMN. Besides, there are certain discrepancies about anomalies in the functional connectivity (FC) among them, specially with the posterior part of this network. Grecius et al. (2007) and Marc G. Berman et al. (2011) reported an increment of FC in the DMN at rest associated with permanent rumination in patients with MDD. However, Xueling Zhu et al. (2012) found evidences of a dissociation pattern in resting-state concerning the FC between the anterior and the posterior part of the DMN, where the frontal part showed an increment of connectivity that correlated with high levels of

rumination and a decrement of connectivity in the posterior part which correlated with over general autobiographical memory (AM).

Moreover, other RSNs have also been shown to be involved in the disease (J. Paul Hamilton et al. 2013): the executive network, DLPFC (Bench et al. 1992; Mayberg et al. 2005; Pizzagalli et al. 2009; Strigo et al. 2008) and salience network (O'Reardon et al. 2007; Gross, Nakumura, Pascual-Leone and Fregni, 2007).

Specially, Simone Grimm et al. (2008) already dealt with the imbalance between the left and right sides of DLPFC in MDD, arguing as they could trigger a negative emotional judgment. Besides, Changjian Qiu et al. (2011) suggested more particularly that the alterations in right DLPFC and right inferior parietal gyrus activity, within the central executive network, could be a reflex of cognitive control deficit in social anxiety disorder. On the other hand, Sylvester et al. (2012, 2013) showed that the dysfunctions in anxiety might come from alterations in the ventral attention network, specially abnormalities between the Frontal and Parietal (FrontoParietal, FP) lobules. Meanwhile, Aneta Brzezicka (2013) argued that the dysfunctions found in the FP network in the MDD come from deficient transmission of information between PFC and parietal areas and to an disequilibrium between the FP network and DMN producing possibly persistent rumination and cognition problems in the patients. However, Northoff et al. (2011) explained that the depression may be affecting various functional networks in resting state and where alterations in the DMN could be enabling stimulus-induced activity in sensory and limbic / paralimbic regions.

All this suggest the need to integrate both local assessments or descriptors, with which the signal alteration among regions could be analyzed, and global or network descriptors, which show the activity changes at network level. Then we might observe whether different signal alterations among regions could be modulating the changes at network level.

Nevertheless, we consider that classical descriptors from rs-fMRI might be discovering only those changes persistent over time because they are built by using averaged metrics on functional connectivity among regions in all resting state session (static functional connectivity, sFC). However, there are certain brain functions affected by depression which could better be explained under a dynamic point of view. These functions should be defined from the time-varying functional connectivity measures between brain regions (dynamic functional connectivity, vFC). Those might be located specifically on networks where stands a high ratio of synchronization due to intensive

demands of exchange of information among areas. All those functions with high processing load should then be analyzed in a complementary way. This dynamical approach might unmask anomalies in space-time connectivity between regions by means of descriptors.

In this sense, several studies have shown the involvement of parietal areas and right DLPFC (Stephen M. Rao et al. 2001: Damen and Brunia 1994, Mohl and Pfurtscheller 1991) in task automatic timing. So, researchers have speculated that there must be some type of 'internal clock' between the sensorimotor, parietal and prefrontal regions. Specifically, Jones Catherine et al (2004) demonstrated that the right dorsolateral side showed a special selectivity in the phase, and which could be involved memory processes. Moreover, Catie Chang and Gary H. Glover (2010) also demonstrated that the resting state functional connectivity in DMN is not static and other metrics of variability should be taken into account when characterizing RSN.

In short, based on the working hypothesis that major depression is a complex disorder of systems that involves several psychobiological dimensions, where structural changes precede spatiotemporal disruptions to specific brain functions. So, we suggest the integration of both static and dynamic descriptors by networks in the same study. The aim is to assess if there are some specific brain functions that show dynamic functional pattern alterations in MDD and whether they can help to explain clinical variables together with static descriptors. Additionally, we analyze putative local markers together with these global descriptors to check their clinical relevance. All this may help in clarify some pathophysiological mechanisms of MDD.

A comparative analysis was done between the depressive group (27 subjects) and healthy group (27 subjects) from rs-fMRI data. In order to perform it, we previously divided the whole brain (WB) in different RSN using the independent components (IC) found by Smith et al. (2009), and doing an independent component analysis (ICA) approach of the healthy group. On one hand, the ICA allows to identify intrinsic brain networks by their unique neural signatures (J. Paul Hamilton et al. 2012) which are: movement, vision, audition, language, memory, executive functions, salience (Cordes D et al. 2001, Hampson M et al. 2002, Beckmann CF et al. 2005, Seeley WW et al. 2007). On the other hand, the resting-state BOLD signal obtained for each individual was analyzed and finally both sFC and vFC matrices were obtained (*Figure 1*).

Then, graph theory is applied to the different approximations in order to obtain global and local descriptors that will help us describe brain changes and we can

integrate them in a single framework. Local descriptors provide us with information about connectivity alterations or changes, connection losses or overcoupling among regions, and global descriptors show efficiency problems, segregation changes or deficiencies in the integration of a network. The application of graph theory on the rs-fMRI data, described by Rubinov M Sporns O (2010), has proved to be a powerful mathematical framework (review Qiyong Gong and Yong He) in the characterization and identification of the changes among groups in a study. These descriptors can be used as a potential clinical marker if they are correlated with clinical variables, prediction or disease classification. We have to keep in mind that the descriptors which depict the efficiency of a specific area or a network from sFC and vFC matrices can be the more adequate in the detection or prediction of changes states and disease monitoring.

Finally, two methods are applied by an approach from descriptors: a classification tree is made from the nodal descriptors in order to find those regions which would be maximizing the differences between groups, and general regression models are used to fitting the global variables of networks (RSN) with different clinical variables that describe the state of depression by patient.

**RESULTS**

## 1. Spatio-Temporal Alterations found using Network Based Statistics approach.

We used Network Based Statistics (NBS) and a False Discovery Rate (FDR) approaches to study the core networks that might characterize MDD by means of vFC (Variance/Mean - Index of Dispersion of Phase-coupling of a pair, IDP) and sFC (positive temporal relationship between two Region Of Interest (ROI) over time, pos-FC). An analysis through approximated NBS was realized at a global level (WB) as well as for each of the RSN (*Figure 2A-2B*), in order to identify altered networks for depressive disorders using a non-parametric test with 5000 permutations on vFC and sFC matrices (*see methods*). We calculated the sFC matrices using positive partial correlations, between each ROI, and the vFC was quantified using IDP for each pair.

At a global level no significant difference was found in the networks between depressive and controls groups. The vFC discovers changes in the networks located on the DMN, FP, PreFrontal-Limbic (PFL) networks. The differences in matrices of sFC approach were basically focused on the DMN and left FP network. However the altered circuitry found on IDP matrices were focus on basically DMN, PF and bilateral FP networks (*Figure 3A-3B; Table 3A-3B*).

Specifically regarding the DMN network, the NBS approach on the IDP matrix shows mainly an altered network in the right hemisphere and however on the pos-FC matrices it detects an altered circuitry on its left side for this component (*Figure 3A*).

In particular, the DMN (RSN_S2) contains an altered network on pos-FC matrices in the patients respect control group. It presents a significant increment of functional connectivity in the patients with a corrected pvalue *P* of network p=0.0258 (10 connections with t>1.93; df=53; so all connections in the network with one-tailed p<0.0295 no-corrected). The biggest connectivity increment within the altered circuitry is found between the connections with the core *CUN.R-MTG.L* (red *Figure 3A.A & table 3A*). Moreover it has an increment of pos-FC between the OrbitoPreFrontal (OPFC), superior medial PF and ACC regions with posterior part of the DMN (specially via precuneus/cuneus and MTG.L area). Conversely, the same component contains an altered network on IDP matrix, vFC approach, in the patients respect control group. On the contrary, it presents an abnormal interhemispheric symmetry network respect to the

altered circuitry with the sFC approach. It shows a decrease of IDP, less dispersion of phase-coupling (it could represent a loss of flexibility between regions), for patients with a corrected pvalue of network p=0.0158 (7 connections, t>2.68; df=53; p<0.0047). The most relevant loss of IDP is produced between the connections: *ACG.L-ANG.R-PCUN.R* (*purple Figure 3A.A & Table 3B*). In this case, the OPFC superior medial and ACG regions showed also a loss of flexibility of phase with the posterior part of DMN but via ANG.R and PCG.R areas. Besides, we observed that the posterior part of the DMN is especially altered. In particular, the RSN_2-1 (posterior DMN; *purple Figure 3A.B & Table 3B*) shows an altered subnetwork with a strong loss of flexibility in the patients with corrected p=0.0026 (8 connections with t>2.25; df=53; p<0.0143 where all connections hold out FDR) and another subnetwork with an increment of static FC with p=0.0276 (4 connections with t>1.78; df=53; p<0.0404). Here, the bilateral ANG-PCUN, together with PCG.R, shows alterations towards subcortical areas such as the thalamus or hippocampus by their right side (r*ed Figure 3A.B; table 3A*).

As regards FP networks, we observe a significant loss of functional connectivity and inflexibility of phase-coupling. For the sFC approach specially, a set of connections in the left FP network (RSN_S3; *red Figure 3B.B & Table 3A*) in the patient group is decreased respect to the control group, with a corrected p=0.0198 (7 connections with t>2.125; df=53; with lowermost connection non-corrected p<0.019), where the most significant altered connections are between *SFGdor.L-PreCG.L-SPG.L* regions. In this sense the right-FP *(RSN_S4; purple Figure 3B.D & Table 3B*), the IDP matrices of patients also show decrement of IDP in the connection: *DCG.R-PCG.R-IFGoperc.R* with corrected p=0.0354 (2 connections with t>4.2; df=53; p<0.0002), and again the left-FP (RSN_3; *purple Figure 3B.C & Table 3B*) shows a decrement of variability of phase-coupling among SFGdor and parietal regions together with PCUN.L and MTG.L, with a corrected p=0.0104 (4 connections with t>3.2; df=53; p<0.001).

Furthermore, the matrix of IDP also presents a loss of flexibility between the PF areas in the network PFL (RSN_1; *Figure 3B.A & Table 3B*), such as SFGdor, mPF areas and medial OPFC, and CUN.R, with corrected p=0.027 (4 connections with t>3; df=53; p<0.0021) (table 2, figure 2).

In sum, we discover hyperconnectivity and loss of flexibility between both the OPFC and ACC regions and the posterior DMN via: precuneus/cuneus, post cingulate and medial temporal regions; loss of flexibility between PFC areas and right cuneus region; and loss of functional connectivity and flexibility mainly between superior

frontal and parietal regions in patients with major depressive disorder respect to control group.

## 2. Classification between groups from descriptors

### 2.1 Classification through nodal descriptors

From the nodal features obtained through graph theory, bimodal models were used to classify each individual as depressives or controls (weighted and binarized on pos-FC matrices for sFC approach and weighted and cost-corrected on IPD matrices for vFC approach) via classification trees, using a LOOCV strategy where the current OOB subject received a training ensemble (*see methods*). For each iteration of Leave-One-Out, ergo for each one of the individuals, the ensemble of metrics with best scores in the models, that are created through each training set of the classification tree (branch nodes), were saved. Taking into consideration that in one hand an individual network can be typified by a different metrics ensemble, and that in the other hand each one of the metrics defines the behavior of a ROI inside a particular network, the process of classification was done for each one of the defined networks. So, each RSN matrix used to classify the groups was built from the rows that define the set of ROI involved in this RSN, and the columns that define a set of measures or nodal descriptors (*Table 4A for vFC approach, Table 4B for sFC approach*).

We observe that the regions included in the PFL network achieve the maximum accuracy for the classification of subjects with 83.33% using all nodal features (*Figure 4.B*). However, the same network shows 81.48% of accuracy even if we only use its nodal binary descriptors, from binarized matrices on sFC approach. Besides, because the LOO strategies usually tend to show up an over-training, we also analyze the metrics and trees obtained by iteration in its best case. So, we observe that a homogeneous ensemble of features was used for the individual classification (93% of the trees were built using the same features). From that point, the existence of a strong stability of used features is deduced, and instead of finding an ad-hoc model in each iteration, a quite general model for all the population is found.

In particular, the binary degree descriptor on the SFGmed.R region was always located at root, in the 100% of the trees, the local efficiency of binary approach on the PAL.R region usually appeared at the second level of the tree, in the 94.44% of the

cases, the nodal efficiency descriptor of binary approach on the AMYG.L was also located the second level the tree, in the 68.52% of cases, the nodal efficiency of weighted matrices on the MFG.L was almost always present, in the 98.15% of the trees, together with the nodal efficiency weighted on the CAU.R, it was found in the 92.59% of cases and finally, the weighted nodal efficiency on the ACG.R and finally the nodal efficiency of binary approach on the ORBsupmed.R were sometimes present in 31.48% of cases (*Figure 3A; Table 5 sFC approach*).

Furthermore, respect to metrics on the vFC approach, regions of the right FP network achieve the maximum accuracy in the classification using only cost-corrected nodal degree descriptors with 85.19% (*Figure 4.A*) . Besides, a homogeneous ensemble of features was also used for the individual classification (92.6% of the trees were built using the same features).

In particular, the TPOSup.R region was always located at root, in 100% of the trees. PreCG.R, IPL.R, IFGtriang.R always appeared at the second and third level of tree in 100% of cases too. The SPG.R was almost always located at the third level of the tree, in 92.59% of cases. And finally, MFG.L was sometimes presented in 7% of the trees (*Figure 4.A; Table 5 vFC approach*).

## 2.2 - Classification by means of network descriptors: DMN, right FP and PFL networks

Once built through graphs, global metrics made possible an assessment of the behavior and organization of the Whole Brain Network (WBN) and the RSNs ones of every individual through quantitative value. We determined which of these global variables could explain best major depression by means of a logistic binary regression model (see methods). So, we find out that the best model to classify the subjects between groups (Controls, Patients) by means of network descriptors. It is built by sex, age, posterior DMN on vFC approach and PFL together with right FP networks on sFC approach (*Tables 6s; Figure 5.E*).

In particular, this model presents a Nagelkerke $R^2$=0.453 with a model pvalue p=0.0004 (gl=5; $X^2$=22.44) and an overall percentage of classification of 70.4% (19/27 controls and 19/27 patients) using gender, age, global efficiency of PFL and average degree of right FP network on binarized pos-FC matrices, and also average strength on IDP matrices of posterior DMN. Neither do we observe co-linearity or correlation

between the variables of this model. Thus, this model would be showing three main altered components in major depression: the DMN, specially its posterior part, PFL, which includes PF and limbic areas, and the right hemisphere of PF networks.

## 3 – Clinical variables can be explained using network descriptors in patients

### 3.1 Efficiency descriptors on the PFL and posterior DMN explain the severity

Once the network descriptors were obtained, we determined which of these global variables could explain better the severity of depression (HDRS) in patients with MDD by means of a multiple lineal regression (see methods). Gender, age, dynamic posterior DMN and static PFL descriptors were thus used to build the model (*Table 7 – Top; Figure 5.A*).

In particular, the model presents an $R^2$=0.481 (F=5.093; ngl=4; dgl=22; p=0.005) where all its network metrics show a low co-linearity. We build the model using age, gender, global efficiency descriptors on IDP matrices of posterior DMN and local efficiency on weighted pos-FC matrices of PFL network. In sum, the HDRS in patients with MDD could be predicted from efficiency descriptors on the PFL and specific posterior part of DMN components.

### 3.2 The length of current episodes can be predicted by right FP and PF descriptors

Once the network descriptors were obtained, we determined which of these global variables could explain better the episodes of depression in patients by means of a multiple lineal regression. Gender, age, PF and right FP descriptors on sFC approach were thus used to build the model that best predicts the length of current episode (*Table 7 – 3$^{rd}$; Figure 5.C*).

In particular, the model presents a $R^2$=0.462 (F=4.722; ngl=4; dgl=22; p=0.007) where all its network metrics show a low co-linearity. In this case, the model is built by age, gender, local efficiency descriptors on weighted matrices of right-FP network and global efficiency descriptors on binarized matrices of PF network of the sFC approach. Moreover, we observe that a quadratic $R^2$=0.671 is adjusted on these variables. In sum, the length of current episodes in patients with MDD could be predicted from static efficiency descriptors on prefrontal and right FP components.

## 3.3 – The total number of episodes can be strongly explained by posterior DMN and right FPN

Once the network descriptors were obtained, we determined which of these global variables could explain better the total number of episodes of depression in patients by means of a multiple lineal regression. Gender, age, posterior DMN and right FP descriptors on sFC approach were thus used to build the model that best predicts the length of current episodes (*Table 7 – Bottom; Figure 5.D*).

In particular, the model presents an R²=0.602 (F=8.324; ngl=4; dgl=22; p=0.0001) where all its network metrics show a low co-linearity. In this case, the model is built by age, gender, average degree descriptors of right-FP network and local efficiency descriptors of posterior DMN on binarized matrices of the sFC approach. In sum, the total number of episodes in patients with MDD could be predicted from static descriptors on posterior DMN and right FP components.

## 3.4 – The DMN and PFL remain a clinical history of MDD in patients

Once the network descriptors were obtained, we determined which of these global variables could be used to know the initial age (*InitialDate*) of major depression in patients by means of a multiple lineal regression. So, gender, static DMN and dynamic PFL descriptors were used to build the model that best predicts the initial age of the major depression (*Table 7 – 2ⁿᵈ; Figure 5.B*).

Especially, the model presents an R²=0.566 (F=7.506; ngl=4; dgl=22; p=0.001) where all its network metrics show a low co-linearity. In this case, the model is built by gender, average degree descriptors of DMN together with local efficiency of posterior DMN on binarized matrices of the sFC approach and global efficiency of PFL on IDP matrices. In sum, possible historical traits about depression could be contained within DMN and PFL components.

## DISCUSSION

In the present study, dynamical and statical network descriptors of the BOLD signal at rest were designed to assess the putative relationship between clinical variables, which describe states of patients with MDD, and possible underlying changes in certain components that may encode the brain functions affected by depression. Additionally, local descriptors in these components were also assembled to discover the regions that might trigger alterations in the brain functions hobbled by depression. For a further understanding of the altered functions in major depression, not only descriptors based on constant measures of functional connectivity (static approach, sFC) should be considered, but another kind of measures based on moments of the BOLD signal, which describes time-dependent aspects (time-varying or dynamic approach, vFC), should also be included in the study. Thus, the descriptors of the sFC approach describe the functional connectivity with an underlying structural connectivity, and the descriptors of the vFC approach characterize cerebral functions in terms of temporary stability or synchronism.

The results show that static and dynamic network descriptors together unmask underlying spatiotemporal alterations in MDD. The brain functions encoded by the PFL, right FP and DMN, specially its posterior part, seem to be particularly affected in major depression. Apparently the results confirm that the descriptors which come from these networks can be useful to classify patients with respect to controls. Moreover, we observe that prediction models of clinical variables, such as the HDRS, length of the current episode, total number of episodes and initial date of depression can also be built from the combination of both static and dynamic descriptors of these networks.

All this suggests that the clinical phenomenon of major depression can be due to both synchronism and underlying structural problems among regions implicated in these RSN. In this sense, when classifying the individuals among the groups from nodal descriptors, we observe that it is possible to distinguish the subjects using only static nodal descriptors located within the PFL network, or using only dynamic nodal descriptors located within the right FP network. This fact somehow indicates two kinds of problems or alterations which cohabit in MDD.

# 1. Static and dynamic metrics on the BOLD signal at rest unmask connectivity problems among areas within the DMN, PF and FP networks

As for the spatiotemporal connectivity among regions, we can observe three principal RSN with a high concentration of alterations in the group of patients. Even though the sFC approach discovers alterations in the DMN, in left FP and in PFL networks, the dynamic measures show a loss of flexibility in the phase-coupling in all three networks. The understanding of each connectivity problem found among regions can contribute to explain specific depressive traits, but we consider that they should be taken into account together in MDD as some altered regions such as the Dorsal Nexus (DN) or DMN could trigger problems in the rest of systems. For this reason, the network descriptors can help to learn more from results.

## 1.1. The Index of Dispersion of Phase-coupling and Functional Connectivity detect hyperconnectivity and rigidity between the anterior and posterior brain areas of the DMN. It may trigger high levels of rumination and brooding in MDD

The results show a hyperconnectivity and loss of flexibility in the connectivity between the anterior and posterior part of brain, especially among specific areas of the DMN. Certain problems of FC among areas of DMN have been discussed in previous studies. In particular, Marc G. Berman et al. (2011) revealed pattern alterations between the subgenual and posterior cingulate cortex. Besides, these alterations were correlated with depressive rumination and brooding values. In this sense, X. Zhu et al. (2012) can only correlated anterior regions of the DMN, such as the medial PFC and ACC, to high levels of ruminations in MDD.

Thus, it suggests that areas such as the ACC, OPFC and superior medial PFC could be a putative altered hub in MDD which could be over coupling the PFC from posterior regions in the DMN structures, producing a high level of rumination and brooding in the patients with MDD. Peter Fransson and Guillaume Marrelec (2008) presented both the precuneus and posterior cingulate as areas with a high degree of interaction with the rest of the DMN. Curiously, these rigidity and hyperconnectivity of the DMN go in the same direction than the biological vulnerability described in the depression theory of N.L. Nixon et al. (2014). They showed that the MDD group presented a hyperconnectivity with a process of hypogyrification in the DMN (specially

the precuneus region), and this fact could support this idea of vulnerability in front of depression.

## 1.2. Index of Dispersion of Phase-coupling and pos-FC in resting state reveals an interhemispheric symmetry of the DMN with two levels of problems among its regions

The results expose that disturbed connections within the DMN seem to show an interhemispheric symmetry among the approaches. As Michael D. Fox et al. explained in 2005, the task-positive network (TPN) and structures such as the DMN could indicate a competitive, anti-correlated relationship between them while performing a cognitive task as well as a resting state. Then, Catie Chang and Gary H. Glover (2010) analyzed the posterior cingulate (PCC) with the TPN and the rest of DMN regions and then observed the presence of scale-dependent temporal variability. They suggested that this non-static FC could be due to a modulation of the cognitive state. Later, Paul Hamilton et al. (2011) argued that the functional alterations in resting-state, that were found in the task-positive network (TPN) and DMN, could be connected with an adaptive/maladaptive, depressive rumination in MDD.

This suggests the idea of two levels of interaction or organization in this network, where the connectivity problems might influence alterations towards other connected systems, producing the clinical phenomenon of depression. In this sense, Northoff et al. (2011) explained that the rs-fMRI signal from DMN regions at rest could be enabling stimulus-induced activity in sensory and limbic/paralimbic regions.

## 1.3. Both approaches also present problems between the posterior DMN and the Hippocampal-Thalamic Pathway. A putative path for the over general AM in MDD

Both approaches present strong spatiotemporal disruptions among the posterior DMN such as in Angular, Precuneus and PCC regions, and the hippocampal-thalamic pathway. John P. Aggleton et al. (2010) argued that the hippocampal-thalamic interactions would form part of an interdependent system which would be involved in long term memory functions, and that an alteration in one of these components might produce dysfunctional changes to distal sites across systems. More recently, several studies have invited to consider that the over general AM would be implicated somehow

with depression where would connect the visual areas with hyppocampal regions via the precuneus, PCC (X. Zhu et al. 2012; Cavanna and Trimble, 2006; Hassabis, Kumaran, and Maguire, 2007).

All this suggests that alterations between the posterior DMN and this pathway may contribute to problems in the normal control of the inhibition of negative episodic memory in depressed people where precuneus/PCC could be an important hub of this pathway. In this sense, Michael Greicius et al. (2009) implicated the PCC/retrosplenial in episodic memory processing. Moreover, this overgeneral AM in MDD might be somehow associated with depressed ruminations (Catherine Crane et al. 2007).

## 1.4. The loss of flexibility in the Dorsal Nexus: the DLPFC and OPFC may produce negative emotional judgments and anxiety problems in patients with MDD

The dynamic measures expose a loss of flexibility among interhemispheric regions of the DLPFC and OPFC in the PFL network of the group of patient. In this sense, Simone Grimm et al. (2008) found an imbalance between the left and right sides of the DLPFC in MDD. They suggested that this imbalance might produce a negative emotional judgment in patients. Furthermore, during the last two decades the alterations between OPFC and amygdalar regions, via cortico-striato-pallido-thalamic circuit, have been associated with anxiety disorders (Joseph L Price, Wayne C.Drevets, 2010). More concretely, Andreas Hahn et al. (2011) linked the decrease of FC among these regions with social anxiety disorder. Besides, Acioly L.T Lacerda et al. (2004) observed especially a decrease of OPFC gray matter volumes.

It was Yvette I. Sheline et al. (2010) who observed that the activity of the bilateral dorsal medial prefrontal cortex region was dramatically increased in depressive patients in relation to controls regarding the different brain networks analyzed. Besides, they demonstrated that the DN area is overlapped among different networks and argued that because of this, its abnormal increment of FC might explain part of the depressive symptoms.

As a consequence, we suggest that this rigidity of connectivity in this area may trigger alterations in of the rest of PFL, producing negative emotional judgments and problems of anxiety in patients with MDD.

## 1.5. The inflexibility in phase-coupling among FP regions might generate a maladaptive control in front of transmission errors in patients with MDD

The left SFGdor presents a strong loss of variability on phase-coupling within the circuitry constituted by other regions such as the bilateral inferior parietal and left medial temporal, in the left FP network. Aneta Brzezicka (2013) observed that FPN dysfunctions in MDD might come from an ineffective transmission of information between PFC and parietal regions, and alterations between executive network and the DMN. In this sense, Sylvester et al. (2013) observed that anxiety problems may be associated with alterations in the FPN and DMN. Moreover, we also observed a loss of phase-coupling between the PCC and inferior frontal operculum region. Nico U. F. Dosenbach et al. (2007) demonstrated that brain processes could be separated on the base of functional features. They determined that the intraparietal, DLPFC, inferior parietal, precuneus and midcingulate cortex of the FPN could be responsible for support control initiation, and provide of flexibility by adjusting a control in response to errors (adaptive control). Moreover, the adaptive control seems to be included in the attentional network (Corbetta et al. 2002). However, the cingulo opercular network, composed of the anterior insula/operculum, dorsal anterior cingulate cortex and thalamus contributes to the flexible control of human goal-directed behavior (maintaining cognitive faculties).

All this suggests that this decrement of flexibility in the transmission of information between these PFC areas and parietal regions might generate problems in the control of cognitive faculties, and in the adaptive control in response to feedbacks between frontal and intra/parietal regions. It can produce maladaptive traits in depression.

## 2. Static descriptors of the PFL and right FP network, and dynamic descriptors of the posterior DMN characterize MDD. Static nodal descriptors of the PFL or dynamic nodal descriptors of right FP network might be markers of the disease

Static and dynamic network descriptors were built to assess the possible global changes in the different networks produced by MDD. For this purpose, a binary logistic regression was used (see methods). The results show that the network descriptors that best explain the model come from the PFL, right FP and posterior DMN.

Additionally, nodal descriptors were used for each component to evaluate if there is any region which might be directly related to putative changes in this network. The results at this level go in the same direction than global descriptors.

The best classification which has been achieved about nodal descriptors with the sFC approach could mirror any underlying anatomical deficiencies into the PFL system. In the same sense, Peng Fang et al (2012) were able to classify many of major depressive patients using regions of the fronto-limbic network from DTI data by means of SVM and LOOCV methods. Furthermore, it has to be noted that many cortico-limbic regions associated with nodal descriptors achieved in the models, have been reported in different volumetric, structural and neurophysiological studies.

In particular, we would highlight regions as Anterior Cingulate Cortex, Amygdala, Frontal Superior Medial, Orbital Superior Medial, and Middle Frontal Cortex by the number of reported evidences and the role they play in the depression.

Several have already shown the existing relationship between the cortico-striato-pallido-thalamic circuitry and the amygdala towards the cortical subcircuits of the medial prefrontal area included in the Limbic system, and associated to mood disorders. Besides, other studies have presented projections from the basal and lateral amygdala to the orbital and medial prefrontal, insular and temporal cortical areas, the mediodorsal thalamic nucleus, and the medial and lateral hypothalamus at a neurophysiological level. Caspi et al. in 2003 identified that the serotonin transporter gene promoter area affecting 5-HT1A binding receptor would be associated to genetic factors, and which could increase the risk of developing MDD in a stressfu environment, and at the same time it could be related to a decrease of volume in the ACC (Pezawas et al. 2005). Recently, Cordova-Polomera A. and Tornador C. et al (2015) showed, in their study of twins with major depression, that both genes and environment modify different patterns in the amygdala resting-state connectivity, increasing the depression risk.

Furthermore, regions as the Caudate-putamen (Mayuresh S. Korgaonkar et al, 2014), OPFC area and Pallidum (Kyle S. Smith et al. 2019) are connected with Amygdala through the nucleus accumbens and might indicate problems of the Reward System via dopamine regulation in patients with major depression.

However, the best nodal descriptors of vFC values would reveal problems of space-time connectivity between regions of the right FP. Several studies have shown the involvement of the cerebellum, intra/parietal areas and the right DLPFC (Damen and Brunia 1988, Mohl and Pfurtscheller 1991) in task automatic timing, and researchers

have speculated that there must be some type of 'internal clock' between the sensorimotor, parietal areas and prefrontal regions. Jones Catherine et al (2004) specially showed that the right DLPFC side present a special selectivity in the phase wherewith it would indicate that these regions could be particularly involved especially in memory processes.

All this suggests that several components would be involved together in the major depression and, they would be mainly localized in the following networks: PFL, right FP and posterior DMN. Besides, it seems that static and dynamic nodal descriptors might gather two different level of anomalies in patients with MDD. Static local measures could cause general problems of efficiency in the PFL system, whereas as phase-coupling anomalies could trigger alterations in the strength of connectivity in the right FP component. The dynamic descriptors of the posterior DMN might show a general rigidity in this area.

## 3. Dynamic and static global descriptors characterize the traits of depression

Static and dynamic global descriptors were designer for each network to assess the relationship between global brain changes and clinical states of MDD in the group of patients. In the present study, the clinical variables such as the stage of the depression (HDRS), length of the episode, total number of episodes, and age at onset of the first depressive episode were used as dependent variables of the multiple lineal regression to describe the states of the disease in each patient. Basically, the resulting models were constructed from combinations among the network descriptors of the PFL, right FP and DMN, and especially its posterior part. Moreover, the models show certain connections if they are observed from their independent variables, descriptors of network.

The HDRS, level of severity and initial age of depression seem to be related inasmuch as they might be explained by fluctuations in the same components (the PFL network and posterior DMN). However, the initial date of the disorder seems to be over-represented by the whole DMN. This suggests that it may have a specific weight in explaining the clinical history of the patients. This fact could thus be connected somehow with a gradual hypogyrification of the DMN. Additional studies could perhaps establish a putative relationship among them.

In this sense, Baojuan Li et al. (2013) showed that the posterior DMN was normalized after antidepressant treatment, but the alteration persisted within the anterior

part. Moreover, they suggested the anterior part of DMN as a potential indicator for relapse in depression. Furthermore, rumination has been strongly linked with the whole the DMN in major depression: different studies have shown that people who present ruminative responses to depressive symptoms have higher levels of manifestations of disorder over time. In fact, Nolen-Hoekseman Susan (2000) observed a strong correlation between a high level of rumination and HDRS in major depressive. It suggests that the posterior and anterior part of the DMN could be involved in major depression, but in a different way: rumination could be a higher complex function which implies several components.

Moreover, we also observe a partial relationship between the length of depression and total number of depressive events via the right FPN. However, the length of depression in the MDD group seems to be especially more associated with the anterior part of the brain, unlike the total number of depressive events which would be more related with the posterior part of the DMN. This suggests that the length of the episodes might be connected somehow with negative emotional judgments, anxiety problems or areas which have been evaluated as a depressive risk of depressive disorder. The total number of episodes would however be more connected to overgeneral AM. Additional studies would be necessary to establish putative relationships.

In this sense, Ernst H.W. Koster et al. (review, 2011) argued the existence of a certain relationship between both rumination and brooding, and a valence-specific attentional bias in depression based on different studies (Donaldson, Lam and Mathews, 2007; Burwell and Shirk, 2007; Joormann, 2006). They also contended with relationship between cortical attention areas and the DMN in patients. Moreover, they considered that the existence of an information-processing unbalance might present a certain difficulty in breaking depressive ruminations, and the cognitive control deficits might be related to the persistence of depressive events. Thus, they suggested programs to improve attentional control as a protective effect in at-risk individuals. Philip Gorwood et al. (2008) argued that there is a correlation between both the intensity of past depression and number of episodes, and an accumulation of memory performance impairment. Recently, there has been an increase of evidences which invites us to consider the implication of autobiographical memory (AM) in neural changes associated with depression (Zhu et al. 2012). In fact, the episodic richness and imagery are attributed to the hippocampus and medial parietal cortex -posterior cingulate, cuneus and precuneus- (Cavanna and Trimble, 2006; Hassabis, Kumaran, and Maguire, 2007).

Zhu et al. observed that the AM was significantly correlated with the posterior part of the DMN and Zhou et al. (2010) found a hyperactivation between the posterior cingulate cortex and DLPFC at rest in depression. It suggests that the selection of negative autobiographical memories could be due to a selective attention towards negative events (Cristiano A. Köhler et al. 2015: C. Lemogne et al. 2006; G. G. Lloyd and W. A. Lishman et al. 1975). It has to be noted that the autobiographical memories are characterized by self-reflective autonoetic consciousness (Cristiano A. Köhler). Polzella et al. (1977) already argued, following the model of Thomas and Weaver (1975), that the right hemisphere uses visual information collection to estimate the duration and perception of time. In this sense, Stephen M. Rao (2001) illustrated that the activation of a dynamic network of the cortical-subcortical brain (the right inferior parietal cortex, bilateral premotor cortex, basal ganglia and cerebellum) is associated with different components of temporal information processing. Other studies related recurrent depressive episodes with a result of cumulative hippocampal injuries in women first (Yvette I. Sheline et al. 1999) and both women and men later (MacQueen GM et al. 2003; Bell-McGinty et al. 2002).

Furthermore, Michale D. Greicius et al. (2007) observed a positive correlation between the current length of depressive episodes and the ACC area into the anterior part of the DMN. Besides, it seems that rumination could also be used as a predictor of anxiety symptoms in patients with anxiety/depression and new onsets of depressive episodes (Nolen-Hoeksema Susan 2012). In this sense, several studies have strongly connected anxiety issues with alterations in the serotonin transporter, as well as depression and suicide victims with problems in the ventro prefrontal cortex and amygdala region or fronto-limbic system (Arango V et al. 1995; Mann JJ et al. 2000). Ramin V. Parsey et al. (2006) observed in a major depressive episode (MDE) a potential lower serotonin transporter binding potential in the amygdala and midbrain in major depressive patients compare to controls.

**CONCLUSION**

The results advocate for the use of both static metrics of functional connectivity and time-dependent aspects of BOLD signals in resting state, specially when studying the DMN, and its posterior part in particular, PFL and right FP networks which would lead to functional alterations in depression. This may have important implications considering the relevance of these RSN in the possible codification of important brain functions such as the expression of the emotions, affectivity, motivation, self-attribution of emotions, self-reference, working memory, attention, adaptive control, maintain of cognitive faculties and autobiographical or episodic memory processes, among others.

The present findings suggest that certain clinical depressive phenomenons (level of depression, length of the episode, total number of episodes and age at onset of the first depressive episode) could be partially explained by the combination of static and dynamic global alterations in these components. Moreover, we found a general loss of variability (rigidity) on phase-coupling together with underlying structural changes between regions into these RSN, such as the posterior part of the DMN or DN.

We hypothesize that this rigidity on phase-coupling over these areas could be related somehow with a gradual process of hypogyrification which might be proportional to the length of depression or at level of severity level. Future studies may clarify the relationship that exists between them.

## MATERIAL AND METHODS

### 1. Subjects

27 MDD patients were recruited from the Mood Disorders Unit of the University Hospital of Bellvitge. Eligible participants were adult outpatients with a primary diagnosis of MDD as assessed by the Structured Clinical Interview for DSM-IV Axis I Disorders-Clinician Version (SCID) that was conducted by two senior psychiatrists who reached a consensus for all items. All patients had a Hamilton Depression Scale (HAM-D 17) score equal to or greater than 18. Exclusion criteria included the presence or past history of other Axis I diagnoses, relevant medical or neurological disorders and abnormal clinical MRI upon radiological inspection. A group of 27 healthy volunteers comparable in gender, age, handedness and years of education also participated in the study. A complete medical interview was carried out to exclude subjects with relevant medical or neurological disorders, history of substance abuse and psychiatric illness. All patients and control subjects gave written informed consent to participate in the study, which was approved by the Research and Ethics Committee of the University Hospital of Bellvitge.

### 2. rs-fMRI acquisition and preprocessing

Image acquisition was accomplished with a 1.5 tesla Signa system (GE Healthcare, Milwaukee, WI, USA) equipped with an eight-channel phased-array head coil. The Protocol consisted in an echo planar BOLD contrast sequence and a high-resolution T1-weighted sequence. The acquisition parameters for functional data were: time of repetition [TR]= 2000 ms; time of echo [TE]= 50 ms; flip angle=15º; 240 mm field of view, a 64 x 64 matrix; slice thickness= 4 mm and inter-slice gap=1.5 mm. Twenty-two slices parallel to the anterior-posterior commissure line covered the entire brain. The sequence included four additional dummy volumes to facilitate the equilibrium of magnetization, thus totalling 120 volumes per session. The high-resolution T1-weighted anatomical image was a 3D fast spoiled gradient inversion-recovery prepared sequence with 130 contiguous slices in the axial plane (repetition time = 11.8 ms, echo time = 4.2 ms and flip angle = 15º, field of view= 300 mm , a 256x256 matrix and a slice thickness of 1.2 mm).

SPM8 (Welcome Trust Centre for Neuroimaging, University College London, UK; http://www.fil.ion.ucl.ac.uk/spm/) was chosen to perform image preprocessing. For every subject, functional series were realigned in a two-step procedure: firstly to the first image and then to the mean image. Next, movement effects regressed out from functional series at the voxel level using the Volterra expansion of the movement parameters. Subsequent to inspection for the presence of artifacts, high-resolution T1-weighted structural images were co-registered to the mean functional image and then segmented. The transformation from MNI to native space that resulted from segmentation was employed to warp the Automated Anatomical Labelling atlas (AAL) from MNI to every T1 image. AAL atlases in native space were restricted to subject's grey matter by the formula: *[Atlas.\*(GM>WM).\*(GM>CSF).\*(GM>0.1)]* where GM is the grey matter, WM is the white matter and CSF is the cerebrospinal fluid tissue probability maps and '.\*' refers to voxel to voxel product of images. The last atlases were used to calculate functional time series in AAL's areas. Finally, the preprocessed time series were band-pass filtered in 0.04-0.07 Hz range

## 3. Dynamic Functional Connectivity

Preprocessed time series were band-pass filtered in *0.04-0.07* Hz range. Then, the analytical signal (*st*) with an instant phase (*phi*) and amplitude (*A*) was extracted using Hilbert Transform *(s = Acos (phit))*. For each time instance *t*, the difference between the phases of the respective ROIs was calculated as $\Delta\varphi_{ij}(t)=\varphi_i(t)-\varphi_j(t)$, where *i* and *j* are the indices of each ROI. Then, instantaneous coupling matrices (ICM), *C(t)* were constructed using the phase differences normalized between 0 and 1, thereby representing perfect synchronization and perfect desynchronization respectively, such

$$C_{ij}(t) = \frac{2p}{D j_{ij}(t)}$$

that:

The variability in each pair in ICM, $C_{ij}(t)$ was considered at the nodal level. The variability of functional connectivity (vFC) was computed as: Variance/Mean - Index of Dispersion of Phase-coupling of a pair (IDP), and this was calculated for each subject.

$$IDP_{ij}=\sigma^2_{C_{ij}}\mu_{C_{ij}}$$

## 4. Group-ICA and Resting State Networks (RSN)

Group-ICA was performed using GIFT toolbox in MATLAB at voxel level (GIFT version 2.0.b, Matlab v10, Mathworks Inc. Sherborn, MA, USA). Out of 12, we finally selected 8 Independent Components (IC) based on the study of Smith et al. (2009). Besides, 4 IC: the DMN, and both bilateral FP and PFL Networks defined by Smith et al. were also added as template, resulting in total of 12 maps for the subsequent analyses (*Figure 2A-2B; Table 2*). They were initially selected as a control because of their tight involvement in studies about major depression. Besides, as they came from large number of controls, we considered that they could be used as templates for future studies. Once estimated the RSN, they were applied as masks on the input matrices (both vFC and sFC approaches) before brain connectivity analysis and the obtaining of both local and global metrics.

## 5. Looking for altered networks from a Network Based Statistical Analysis (NBS)

In order to locate pairs of connections and subnetworks within the connectome of each individual, matrices of functional connectivity (both pos-FC and IDP matrices) were used. A False Discovery Rate (FDR) approach was also used upon the probability distributions resulting from the non-parametric test, with permutations applied independently to every existing connection of the network. Furthermore an analysis based on the Network Based Statistic (NBS) (Zalesky et al. 2010; http://www.nitrc.org/projects/nbs/) approximation using the NBS toolbox (version 1.2) within every defined network (RSN) and across the whole brain (Whole Brain Network, WBN) was also used.

The NBS approximation has proved to be statistically more powerful compared to an FDR procedure if the difference in connectivity follows a pattern in which the altered connections in a group are connected components (Xueling Suo et al. 2015; Li et al. 2013; Zalesky et al. 2010; Zhang et al. 2011). In this type of univariate analysis, there is also a direct relation between statistical power and network resolution, because when subnetworks are analyzed, in general, the number of altered connected components inside altered regions generally increases, and therefore, the ability to detect the signal (above noise).

The NBS toolbox uses a non-parametric test with permutations (where we used 5000 permutations). In every permutation, it reallocates all the individuals randomly within one of the two groups, and a t-statistic is independently calculated for every connection. Initially, the user sets a t probability threshold for the network and the component that have the highest connections is calculated, establishing a size $M$ of network connections. The corrected p-value $p$ for each subnetwork was calculated as the proportion of connected components of $N$ permutations which had a bigger size than $M$.

By means of the NBS approximation, a t threshold was established minimizing the number of connected components where its p-value of network corrected was $p < 0.05$. The final connected component (sub-net) is compose by connections which all presented a $t > 1.68$, $df=53$. Finally, in order to find single connections that were significantly altered, the FDR procedure of the NBS toolbox was applied to each of the RSN and WBN, setting a $p < 0.05$, as a control of FWE, depending on the probability distribution of the non-parametric tests with 10000 permutations.

## 6. Descriptors design from graph theory features

### 6.1 Network Construction

A network is defined as a group of nodes linked together through edges creating a connection graph. In this study, nodes showed the different areas of the brain divided from the preprocessing step through the AAL atlas. 90 different areas or nodes were defined, 45 for each hemisphere. The nodes which represent areas of the cerebellum were originally dismissed.

### 6.2 Network Analysis

On one hand, Graph theory features allow to summarize infrastructure and organization of a brain network represented as an adjacency matrix (binary or weighted; it represents the probability of connectivity between two regions). The global functioning of each network was assessed by its infrastructure (average strength for matrices with weighted values, average degree for matrices with binary values), integration (global efficiency) and segregation (local efficiency). In the current study they are called global descriptors or network descriptors.

On the other hand, regional characteristics were evaluated by means of nodal strength (for matrices with weighted values) or nodal degree (for matrices with binary values), assessing the total connectivity of a node in a given network, and nodal efficiency, measuring the efficiency of the sub-network associated to a given node. They are called nodal descriptors. Nodes with a high nodal efficiency indicate a high tolerance of the network to the elimination of the given node, which is associated to a high clustering of the neighborhood of this node (Achard S. and Bullmore E. 2007). Formulation and calculation of the graph theory features used to assess each network were based on the definitions and code compiled by Rubinov and Sporns (2010).

In addition, we took into consideration that the brain is really sensitive to energetic shortage, and most of the energy is obtained by the glucose metabolism, in other words the brain is sensitive to the oxidative stress and it might produce problems in the interconnectivity among regions. When disorders are found, it is reasonable to find metabolical alterations in the connections affecting somehow their functions. In brain disorders, it would be expected some kind of defects in the networks with heavy costs or with a high density of connection such as long interconnection hubs would be expected. The hubs should be specially sensible to the loss of variability in phase-coupling. This idea could be used to assess the IDP matrices for the detection of hubs/nodes with certain rigidity in phase-coupling.

There are proofs that the metabolic cost of a node is proportional in one way or another to its own degree and/or centrality (degree, strength nodal) and the physical distance that it implies regarding other nodes (efficiency). The area under the curve ($AUC$) is a metric that provides a value which can be used to characterize the brain networks regardless of the selected threshold. In contrast with pos-FC where we can binarize matrices, we thus use a density/cost estimator that corrects them by the total of connections from all range of values in the IDP matrices.

## 7. Analyzing nodal characteristics using classification trees

In order to determine which features (graph metrics) could be used as predictors (descriptors) of major depression, a strategy of Leave-One-Out Cross Validation (LOOCV) with classification trees was used. To do that, several sets of metrics were used to build different models for each of the approaches, vFC and sFC. Consequently, before each interaction from the Leave-One-Out strategy, an input matrix was obtained

with an *N = 54* individuals (rows), split into the two groups (control or patient), and *M* number of features introduced in the study (columns). After every LOOCV iteration, an individual or row was removed from the original set, also called Out Of the Bag (OOB), and it was classified by means of a classification tree. This tree was trained with the model obtained in the training sample (the rest of the registers that builds the entry matrix with *N-1* individuals). At the end, we analyzed the membership of the individual among both groups.

The classification tree used in the process was the one provided by MATLAB v.10 (*classregtree*) maximizing the results from the "*splitmin*" argument (range [*10, 22*]). To conclude every iteration, the characteristics that better described the system (more frequents) were also extracted from the final model (classification tree)

## 8. Statistical analysis of the network metrics

In order to determine those putative global metrics, either MDD markers, as predictors for each clinical variable (*HDRS, length of the episodes, total number of episodes, initial date of depression*), multivariate analyses ANCOVA were used. The ANCOVA tests were built from the General Lineal Model (GLM, SPSS Chicago IL), where the main effects were used in the interaction among variables (factors and covariant) and the type II were employed for the squares addition. Besides, the variable 'gender' was defined like a factor, and 'age' like a covariant into the GLM.

Regarding the classification between groups, once these preselected network metrics were obtained, a binary logistic regression model was built from the global metrics which showed the best fit with the group variable (Controls, Patients). In this case, all subjects were used.

Then, regarding the prediction of clinical variables from these preselected network metrics, a multiple lineal regression model was built from the global metrics which showed the best fit for each clinical variable. In this case, only the patients were used.

**REFERENCES**

WHO (2001) The world health report. http://www.who.int; Chap 2,4

Wayne C. Drevets, Joseph L. Price, Maura L. Furey (2008) Brain structural and functional abnormalities in mood disorders: implications for neurocircuitry models of depression. Brain Struct Funct, 213 (1-2): 93–118. doi: 10.1007/s00429-008-0189-x

Ferrari, Alize J., Fiona J. Charlson, Rosana E. Norman, Scott B. Patten, Greg Freedman, Christopher J.L. Murray, Theo Vos, and Harvey A. Whiteford (2013) Burden of Depressive Disorders by Country, Sex, Age, and Year: Findings from the Global Burden of Disease Study 2010. PLoS Med, 10 (11): e1001547. doi:10.1371/journal.pmed.1001547.

Grimm S, Ernst J, Boesiger P, Schuepbach D, Hell D, Boeker H, Northoff G (2009) Increased self-focus in major depressive disorder is related to neural abnormalities in subcortical-cortical midline structures. Hum Brain Mapp, 30 (8):2617-27. doi: 10.1002/hbm.20693.

Grunebaum MF, Keilp J, Li S, Ellis SP, Burke AK, Oquendo MA, Mann JJ (2005): Symptom components of standard depression scales and past suicidal behavior. J Affect Disord 87:73–82.

Ingram RE (1990): Self-focused attention in clinical disorders: Review and a conceptual model. Psychol Bull 107:156–176.

Northoff G (2007): Psychopathology and pathophysiology of the self in depression Neuropsychiatric hypothesis. J Affect Disord 104:1–14.

Rimes KA, Watkins E (2005): The effects of self-focused rumination on global negative self-judgements in depression. Behav Res Ther 43:1673–1681.

Treynor E (2003): Rumination reconsidered: A psychometric analysis. Cogn Ther Res 27:247–259.

Zhu X, Wang X, Xiao J, Liao J, Zhong M, Wang W, Yao S (2012) Evidence of a dissociation pattern in resting-state default mode network connectivity in first-episode, treatment-naive major depression patients. Biol Psychiatry, 71 (7):611-7. doi: 10.1016/j.biopsych.2011.10.035.

Aneta Brzezicka (2013) Integrative deficits in depression and in negative mood states as a result of fronto-parietal network dysfunctions. Review Acta Neurobiol Exp 2013, (73) : 313-325

J. Paul Hamilton, Daniella J. Furman, Catie Chang, Moriah E. Thomason, Emily Dennis, Ian H. Gotlib (2011) Default-mode and task-positive network activity in Major Depressive Disorder: Implications for adaptive and maladaptive rumination. Biol Psychiatry, 70 (4): 327–333. doi: 10.1016/j.biopsych.2011.02.003.

Qiu C, Liao W, Ding J, Feng Y, Zhu C, Nie X, Zhang W, Chen H, Gong Q (2011) Regional homogeneity changes in social anxiety disorder: a resting-state fMRI study. Psychiatry Res, 194 (1):47-53. doi: 10.1016/j.pscychresns.2011.01.010.

Grimm S, Beck J, Schuepbach D, Hell D, Boesiger P, Bermpohl F, Niehaus L, Boeker H, Northoff G (2008) Imbalance between left and right dorsolateral prefrontal cortex in major depression is linked to negative emotional judgment: an fMRI study in severe major depressive disorder. Biol Psychiatry, 63 (4):369-76.

Jones CR, Rosenkranz K, Rothwell JC, Jahanshahi M (2004) The right dorsolateral prefrontal cortex is essential in time reproduction: an investigation with repetitive transcranial magnetic stimulation. Exp Brain Res, 158 (3):366-72.

Greicius MD, Supekar K, Menon V, Dougherty RF (2009) Resting-state functional connectivity reflects structural connectivity in the default mode network. Cereb Cortex, 19 (1):72-8. doi: 10.1093/cercor/bhn059.

Cordes D, Haughton VM, Arfanakis K, Carew JD, Turski PA, Moritz CH, Quigley MA, Meyerand ME (2001) Frequencies contributing to functional connectivity in the cerebral cortex in "resting-state" data. AJNR Am J Neuroradiol, 22:1326–1333.

Biswal B, Yetkin FZ, Haughton VM, Hyde JS (1995) Functional connectivity in the motor cortex of resting human brain using echo-planar MRI. Magn Reson Med, (34):537-541.

Hampson M, Peterson BS, Skudlarski P, Gatenby JC, Gore JC (2002) Detection of functional connectivity using temporal correlations in MR images. Hum Brain Mapp, 15:247-262.

Beckmann CF, DeLuca M, Devlin JT, Smith SM (2005) Investigations into resting-state connectivity using independent component analysis. Philos Trans R Soc Lond B Biol Sci, 360:1001-1013.

Seeley WW, Menon V, Schatzberg AF, Keller J, Glover GH, Kenna H, Reiss AL, Greicius MD (2007) Dissociable intrinsic connectivity networks for salience processing and executive control. J Neurosci, 27:2349–2356.

Greicius MD, Krasnow B, Reiss AL, Menon V (2003) Functional connectivity in the resting brain: a network analysis of the default mode hypothesis. Proc Natl Acad Sci U S A, 100:253–258.

De Luca M., Beckmann C. F., De Stefano N., Matthews P. M., Smith S. M. (2006) fMRI resting state networks define distinct modes of long-distance interactions in the human brain. Neuroimage 29, 1359–136710.1016/j.neuroimage.2005.08.035

David M. Cole, Stephen M. Smith, Christian F. Beckmann (2010) Advances and Pitfalls in the Analysis and Interpretation of Resting-State FMRI Data. Front Syst Neurosci, 4: 8. doi: 10.3389/fnsys.2010.00008.

Saini S., DeStefano N., Smith S., Guidi L., Amato M. P., Federico A., Matthews P. M. (2004). Altered cerebellar functional connectivity mediates potential adaptive plasticity in patients with multiple sclerosis. J. Neurol. Neurosurg. Psychiatr. 75, 840–84610.1136/jnnp.2003.016782

Lewis C. M., Baldassarre A., Committeri G., Romani G. L., Corbetta M. (2009). Learning sculpts the spontaneous activity of the resting human brain. Proc. Natl. Acad. Sci. U.S.A. 106, 17558–1756310.1073/pnas.0902455106

S.M. Smith, P.T. Fox, K.L. Miller, D.C. Glahn, P.M. Fox, C.E. Mackay, N. Filippini, K.E. Watkins, R. Toro, A.R. Laird, and C.F. Beckmann (2009) Correspondence of the brain's functional architecture during activation and rest. Proc Natl Acad Sci USA (PNAS), 106 (31):13040-13045

A.R. Laird, P.M. Fox, S.B. Eickhoff, J.A. Turner, K.L. Ray, D.R. McKay, D.C. Glahn, C.F. Beckmann, S.M. Smith, and P.T. Fox (2011) Behavioral interpretations of intrinsic connectivity networks. Journal of Cognitive Neuroscience.

Damoiseaux J. S., Rombouts S. A., Barkhof F., Scheltens P., Stam C. J., Smith S. M., Beckmann C. F. (2006) Consistent resting-state networks across healthy subjects. Proc. Natl. Acad. Sci. U.S.A. 103,13848–1385310.1073/pnas.0601417103

Lowe M. J., Mock B. J., Sorenson J. A. (1998). Functional connectivity in single and multislice echoplanar imaging using resting-state fluctuations. Neuroimage 7, 119–13210.1006/nimg.1997.0315

Fox M. D., Raichle M. E. (2007) Spontaneous fluctuations in brain activity observed with functional magnetic resonance imaging. Nat. Rev. Neurosci, 8, 700–71110.1038/nrn2201

Raichle M. E., MacLeod A. M., Snyder A. Z., Powers W. J., Gusnard D. A., Shulman G. L. (2001) A default mode of brain function. Proc. Natl. Acad. Sci. U.S.A. 98, 676–68210.1073/pnas.98.2.676

Shulman G. L., Fiez J. A., Corbetta M., Buckner R. L., Miezin F. M., Raichle M. E., Petersen S. E. (1997) Common blood flow changes across visual tasks: II. Decreases in cerebral cortex. J. Cogn. Neurosci. 9, 648–66310.1162/jocn.1997.9.5.648

Wicker B, Ruby P, Royet JP, Fonlupt P (2003) A relation between rest and the self in the brain?. Brain Res Brain Res Rev, 43 (2):224-30.

Vincent JL, Patel GH, Fox MD, Snyder AZ, Baker JT, Van Essen DC, Zempel JM, Snyder LH, Corbetta M, Raichle ME (2007) Intrinsic functional architecture in

the anaesthetized monkey brain. Nature, 447 (7140):83-6.

Deco G, Jirsa VK, McIntosh AR (2011) Emerging concepts for the dynamical organization of resting-state activity in the brain. Nat Rev Neurosci, 12 (1):43-56. doi: 10.1038/nrn2961.

Sheline YI, Barch DM, Price JL, Rundle MM, Vaishnavi SN, Snyder AZ, Mintun MA, Wang S, Coalson RS, Raichle ME (2009) The default mode network and self-referential processes in depression. Proc Natl Acad Sci USA., 106 (6):1942-7. doi: 10.1073/pnas.0812686106.

Sheline YI, Price JL, Yan Z, Mintun MA (2010) Resting-state functional MRI in depression unmasks increased connectivity between networks via the dorsal nexus. Proc Natl Acad Sci U S A., 107 (24):11020-5. doi: 10.1073/pnas.1000446107.

Michael D. Greicius, MPH, Benjamin H. Flores, Vinod Menon, Gary H. Glover, Hugh B. Solvason, Heather Kenna, MA, Allan L. Reiss, and Alan F. Schatzberg (2007) Resting-State Functional Connectivity in Major Depression: Abnormally Increased Contributions from Subgenual Cingulate Cortex and Thalamus. Biol Psychiatry, 62 (5): 429–437.

Berman MG, Peltier S, Nee DE, Kross E, Deldin PJ, Jonides J. Soc Cogn (2011) Depression, rumination and the default network. Affect Neurosci. 6 (5):548-55. doi: 10.1093/scan/nsq080.

J. Paul Hamilton, Michael C. Chen, and Ian H. Gotlib (2013) Neural Systems Approaches to Understanding Major Depressive Disorder: An Intrinsic Functional Organization Perspective. Neurobiol Dis, 52C: 4–11. doi: 10.1016/j.nbd.2012.01.015.

Bench CJ, Friston KJ, Brown RG, Scott LC, Frackowiak RSJ, Dolan RJ (1992) The Anatomy of Melancholia - Focal Abnormalities of Cerebral Blood-Flow in Major Depression. Psychological Medicine, 22 (3):607–615.

Mayberg HS, Lozano AM, Voon V, McNeely HE, Seminowicz D, Hamani C, et al. (2005) Deep brain stimulation for treatment-resistant depression. Neuron, 45 (5):651–660

Pizzagalli DA, Holmes AJ, Dillon DG, Goetz EL, Birk JL, Bogdan R, et al. (2009) Reduced Caudate and Nucleus Accumbens Response to Rewards in Unmedicated Individuals With Major Depressive Disorder. American Journal of Psychiatry, 166 (6):702–710.

Strigo IA, Simmons AN, Matthews SC, Craig AD, Paulus MP (2008) Association of Major Depressive Disorder With Altered Functional Brain Response During Anticipation and Processing of Heat Pain. Archives of General Psychiatry, 65 (11):1275–1284.

O'Reardon JP, Solvason HB, Janicak PG, Sampson S, Isenberg KE, Nahas Z, et al. (2007) Efficacy and safety of transcranial magnetic stimulation in the acute treatment of major depression: A multisite randomized controlled trial. Biological Psychiatry, 62 (11):1208–1216.

Gross M, Nakamura L, Pascual-Leone A, Fregni F. (2007) Has repetitive transcranial magnetic stimulation (rTMS) treatment for depression improved? A systematic review and meta-analysis comparing the recent vs. the earlier rTMS studies. Acta Psychiatrica Scandinavica, 116 (3):165–173.

Chad M. Sylvester, Deanna M. Barch, Maurizio Corbetta, Jonathan D. Power, Bradley L. Schlaggar, and Joan L. Luby (2013) Resting State Functional Connectivity of the Ventral Attention Network in Children With a History of Depression or Anxiety. J Am Acad Child Adolesc Psychiatry, 52 (12): 1326–1336.e5. doi: 10.1016/j.jaac.2013.10.001

Northoff G, Wiebking C, Feinberg T, Panksepp J. (2011) The 'resting-state hypothesis' of major depressive disorder a translational subcortical-cortical framework for a system disorder. Neurosci Biobehav Rev, 35 (9):1929-45. doi: 10.1016/j.neubiorev.2010.12.007.

Rao SM, Mayer AR, Harrington DL (2001) The evolution of brain activation during temporal processing. Nat Neurosci. 4 (3):317-23.

Brunia, C. & Damen, E. (1988) Distribution of slow brain potentials related to motor preparation and stimulus anticipation in a time estimation task. Electroencephalogr. Clin. Neurophysiol. 69, 234–243

Mohl, W. and Pfurtscheller, G. (1991) The role of the right parietal region in a movement time estimation task. Neuroreport, 2, 309–312.

Chang C, Glover GH (2010) Time-frequency dynamics of resting-state brain connectivity measured with fMRI. Neuroimage, 50 (1):81-98. doi: 10.1016/j.neuroimage.2009.12.011.

Gong Q, He Y (2015) Depression, neuroimaging and connectomics: a selective overview. Biol Psychiatry, 77 (3):223-35. doi: 10.1016/j.biopsych.2014.08.009

Rubinov M, Sporns O (2010) Complex network measures of brain connectivity: Uses and interpretations. NeuroImage 52:1059-69.

Zalesky A, Fornito A, Bullmore ET (2010) Network-based statistic: identifying differences in brain networks. Neuroimage, 53 (4):1197-207. doi: 10.1016/j.neuroimage.2010.06.041.

Zhang J, Wang J, Wu Q, Kuang W, Huang X, He Y, Gong Q (2011) Disrupted brain connectivity networks in drug-naive, first-episode major depressive disorder. Biol Psychiatry, 70:334–342.

Li Y, Jewells V, Kim M, Chen Y, Moon A, Armao D, Troiani L, Markovic-Plese S, Lin W, Shen D (2013) Diffusion tensor imaging based network analysis detects alterations of neuroconnectivity in patients with clinically early relapsing-remitting multiple sclerosis. Hum Brain Mapp, 34:3376–3391.

Suo X, Lei D, Li K, Chen F, Li F, Li L, Huang X, Lui S, Li L, Kemp GJ, Gong Q (2015) Disrupted brain network topology in pediatric posttraumatic stress disorder: A resting-state fMRI study. Hum Brain Mapp. 2015 Sep;36(9):3677-86. doi: 10.1002/hbm.22871.

Achard S, Bullmore E (2007) Efficiency and cost of economical brain functional networks. PLoS Computational Biology, 3: 174–183.

Fransson P, Marrelec G (2008) The precuneus/posterior cingulate cortex plays a pivotal role in the default mode network: Evidence from a partial correlation network analysis. Neuroimage, 42 (3):1178-84. doi: 10.1016/j.neuroimage.2008.05.059.

Nixon NL, Liddle PF, Nixon E, Worwood G, Liotti M, Palaniyappan L (2014) Biological vulnerability to depression: linked structural and functional brain network findings. Br J Psychiatry, 204:283-9. doi: 10.1192/bjp.bp.113.129965.

Sylvester CM, Corbetta M, Raichle ME, Rodebaugh TL, Schlaggar BL, Sheline YI, Zorumski CF, Lenze EJ (2012) Functional network dysfunction in anxiety and anxiety disorders. Trends Neurosci. 35 (9):527-35. doi: 10.1016/j.tins.2012.04.012.

Fox MD, Snyder AZ, Vincent JL, Corbetta M, Van Essen DC, Raichle ME (2005) The human brain is intrinsically organized into dynamic, anticorrelated functional networks. Proc Natl Acad Sci U S A. 102 (27):9673-8.

Aggleton JP, O'Mara SM, Vann SD, Wright NF, Tsanov M, Erichsen JT (2010) Hippocampal-anterior thalamic pathways for memory: uncovering a network of direct and indirect actions. Eur J Neurosci. 2010 Jun;31(12):2292-307. doi: 10.1111/j.1460-9568.2010.07251.x.

Cavanna AE, Trimble MR (2006) The precuneus: a review of its functional anatomy and behavioural correlates. Brain. 129 (Pt 3):564-83.

Hassabis D, Kumaran D, Maguire EA (2007) Using imagination to understand the neural basis of episodic memory. J Neurosci. 27 (52):14365-74.

Crane C, Barnhofer T, Mark J, Williams G. (2007) Cue self-relevance affects autobiographical memory specificity in individuals with a history of major depression. Memory, 15 (3):312-23.

Price JL, Drevets WC (2010) Neurocircuitry of mood disorders. Neuropsychopharmacology, 35 (1):192-216. doi: 10.1038/npp.2009.104.

Hahn A, Stein P, Windischberger C, Weissenbacher A, Spindelegger C, Moser E, Kasper S, Lanzenberger R (2011) Reduced resting-state functional connectivity between amygdala and orbitofrontal cortex in social anxiety disorder. Neuroimage, 56 (3):881-9. doi: 10.1016/j.neuroimage.2011.02.064.

Lacerda AL, Keshavan MS, Hardan AY, Yorbik O, Brambilla P, Sassi RB, Nicoletti M, Mallinger AG, Frank E, Kupfer DJ, Soares JC (2004) Anatomic evaluation of the orbitofrontal cortex in major depressive disorder. Biol Psychiatry, 55 (4):353-8.

Dosenbach NU, Fair DA, Miezin FM, Cohen AL, Wenger KK, Dosenbach RA, Fox MD, Snyder AZ, Vincent JL, Raichle ME, Schlaggar BL, Petersen SE (2007) Distinct brain networks for adaptive and stable task control in humans. Proc Natl Acad Sci U S A. 2007 Jun 26;104(26):11073-8.

Corbetta M, Shulman GL (2002) Control of goal-directed and stimulus-driven attention in the brain. Nat Rev Neurosci. 3 (3):201-15.

Fang P, Zeng LL, Shen H, Wang L, Li B, Liu L, Hu D (2012) Increased cortical-limbic anatomical network connectivity in major depression revealed by diffusion tensor imaging. PLoS One, 7 (9):e45972. doi: 10.1371/journal.pone.0045972.

Pezawas L, Meyer-Lindenberg A, Drabant EM, Verchinski BA, Munoz KE, Kolachana BS, Egan MF, Mattay VS, Hariri AR, Weinberger DR (2005) 5-HTTLPR polymorphism impacts human cingulate-amygdala interactions: a genetic susceptibility mechanism for depression. Nat Neurosci. 8 (6):828-34.

Caspi A, Sugden K, Moffitt TE, Taylor A, Craig IW, Harrington H, McClay J, Mill J, Martin J, Braithwaite A, Poulton R (2003) Influence of life stress on depression: moderation by a polymorphism in the 5-HTT gene. Science. 301 (5631):386-9.

Córdova-Palomera A, Tornador C, Falcón C, Bargalló N, Nenadic I, Deco G, Fañanás L (2015) Altered amygdalar resting-state connectivity in depression is explained by both genes and environment. Hum Brain Mapp, 36 (10):3761-76. doi: 10.1002/hbm.22876.

Korgaonkar MS, Fornito A, Williams LM, Grieve SM (2014) Abnormal structural

networks characterize major depressive disorder: a connectome analysis. Biol Psychiatry. 76(7):567-74. doi: 10.1016/j.biopsych.2014.02.018.

Smith KS, Tindell AJ, Aldridge JW, Berridge KC (2009) Ventral pallidum roles in reward and motivation. Behav Brain Res. 196 (2):155-67. doi: 10.1016/j.bbr.2008.09.038.

Li B, Liu L, Friston KJ, Shen H, Wang L, Zeng LL, Hu D (2013) A treatment-resistant default mode subnetwork in major depression. Biol Psychiatry, 74 (1):48-54. doi: 10.1016/j.biopsych.2012.11.007.

Nolen-Hoeksema S (2000) The role of rumination in depressive disorders and mixed anxiety/depressive symptoms. J Abnorm Psychol. 109 (3):504-11.

Koster EH, De Lissnyder E, Derakshan N, De Raedt R (2011) Understanding depressive rumination from a cognitive science perspective: the impaired disengagement hypothesis. Clin Psychol Rev. 31 (1):138-45. doi: 10.1016/j.cpr.2010.08.005.

Donaldson C, Lam D, Mathews A, (2007) Attention and rumination in major depression. Behaviour Research and Therapy,45, 2664−2678.

Buckner, R. L., & Carroll, D. C. (2007). Self-projection and the brain. Trends in Cognitive Science,11,49−57.

Joormann, J. (2006). The relation of rumination and inhibition: Evidence from a negative priming task.Cognitive Therapy and Research,30, 149−160.

Gorwood P, Corruble E, Falissard B, Goodwin GM (2008) Toxic effects of depression on brain function: impairment of delayed recall and the cumulative length of depressive disorder in a large sample of depressed outpatients. Am J Psychiatry. 165 (6):731-9. doi: 10.1176/appi.ajp.2008.07040574.

Zhou Y, Yu C, Zheng H, Liu Y, Song M, Qin W, Li K, Jiang T (2010) Increased neural resources recruitment in the intrinsic organization in major depression. J Affect Disord. 121 (3):220-30. doi: 10.1016/j.jad.2009.05.029.

Köhler CA, Carvalho AF, Alves GS, McIntyre RS, Hyphantis TN, Cammarota M (2015)

Autobiographical Memory Disturbances in Depression: A Novel Therapeutic Target?. Neural Plast. 2015;2015:759139. doi: 10.1155/2015/759139.

Lemogne C., Piolino P., Jouvent R., Allilaire J.-F., Fossati P (2006) Episodic autobiographical memory in depression: a review. L'Encéphale. 32 (5, part 1):781–788. doi: 10.1016/s0013-7006(06)76231-5.

Lloyd G. G., Lishman W. A (1975) Effect of depression on the speed of recall of pleasant and unpleasant experiences. Psychological Medicine. 5 (2):173–180. doi: 10.1017/s0033291700056440

Donald J Polzella, Frank DaPolito, Christine Hinsman (1977) Cerebral asymmetry in time perception. Perception and Psychophysics, 21 (2), 187-192

Thomas E A C, Weaver W B (1975) Cognitive processing and time perception. Perception and Psychophysics, 17:363-367.

Bell-McGinty, S., Butters, M.A., Meltzer, C.C., Greer, P.J., Reynolds, C.F. III, Becker, J.T. (2002) Brain morphometric abnormalities in geriatric depression: long-term neurobiological effects of illness duration. Am. J. Psychiatry. 159:1424–1427.

Sheline Y.I., Sanghavi M., Mintun M.A., Gado M.H. (1999) Depression duration but not age predicts hippocampal volume loss in medically healthy women with recurrent major depression. Journal of Neuroscience: the Official Journal of the Society for Neuroscience, 19 (12):5034–5043.

MacQueen G.M., Campbell S., McEwen B.S., Macdonald K., Amano S., Joffe R.T., Nahmias C., Young L.T. (2003) Course of illness, hippocampal function, and hippocampal volume in major depression. Proceedings of the National Academy of Sciences of the United States of America, 100 (3):1387–1392.

Arango V, Underwood MD, Gubbi AV, Mann JJ. (1995) Localized alterations in pre- and postsynaptic serotonin binding sites in the ventrolateral prefrontal cortex of suicide victims. Brain Res. 688 (1-2):121-33.

Mann JJ, Huang YY, Underwood MD, Kassir SA, Oppenheim S, Kelly TM, et al. (2000) A serotonin transporter gene promoter polymorphism (5-HTTLPR) and prefrontal cortical binding in major depression and suicide. Archives of General Psychiatry, 57:729–38.

Parsey RV, Olvet DM, Oquendo MA, Huang YY, Ogden RT, Mann JJ (2006) Higher 5-HT(1A) receptor binding potential during a major depressive episode predicts poor treatment response: preliminary data from a naturalistic study. Neuropsychopharmacology. 31:1745–9.
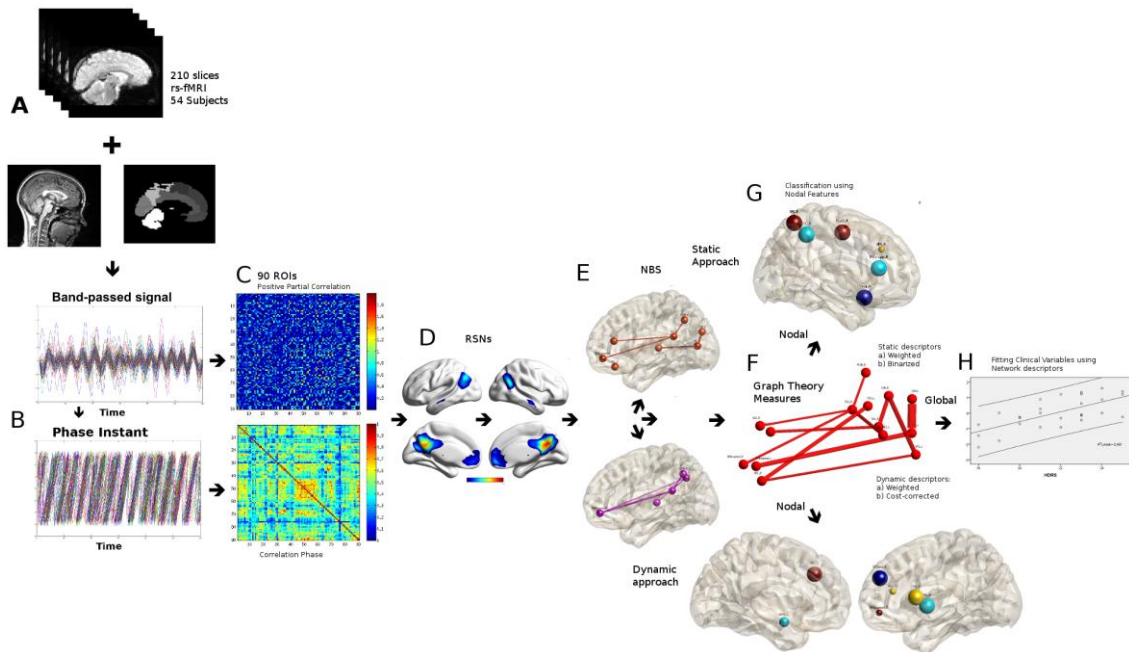
## FIGURES



**Figure 1. Pipeline.** Schematic representation of the pipeline used in the present study. **(A)** The 120 rs-fMRI volumes (slices) are co-registered to the anatomical T1, then each voxel is mapped to 90 regions of interest (ROI)s in the AAL atlas by subject in the study (27 Controls + 27 patients with MDD). **(B)** [For each subject]: After artifacts removal, the time series were obtained by the average of the BOLD signal activation probability in each ROI. Then, *(B, top)* a band-pass filter was applied obtaining the rs-fMRI narrow-band signal between 0.04-0.07Hz. Next, *(B, bottom)* an analytic component of the oscillatory activity (instantaneous phase) was extracted. **(C)** [For each subject]: Two types of functional connectivity normalized matrices were obtained, on the one hand *(C, top)* applying the positive values of partial correlation among the narrow-band signals (pos-FC), and on the other hand *(C, bottom)* applying correlation on instantaneous phase (IDP matrices). **(D)** [For each subject]: Next, different matrices by each RSN were obtained applying different masks on whole brain matrices (*i.e DMN, RSN_S2*). **(E)** [For each Subject, RSN matrix and approach]: Networks Based Statistic (NBS) was obtained on the different matrices; *(F, top)* NBS on pos-FC RSN matrices (*i.e RSN_S2*); *(F, bottom)* on IDP RSN matrices (*i.e RSN_S2*). **(F)** [For each subject, RSN and approach]: Graph-theoretical measures were obtained for each region (nodal variables, nodal descriptors) and network (global variables, network descriptors). **(G)** [For each approach]: Putative features associated to regions (possible markers) were obtained from classification trees on nodal descriptors; *(G, top)* classification between MDD and Control subjects: possible markers of depression on IDP matrices (vFC approach); *(G, down)* classification between MDD and Control subjects: possible markers of depression on pos-FC matrices (sFC approach). **(H)** The different models were obtained combining network descriptors (*i.e HDRS*).
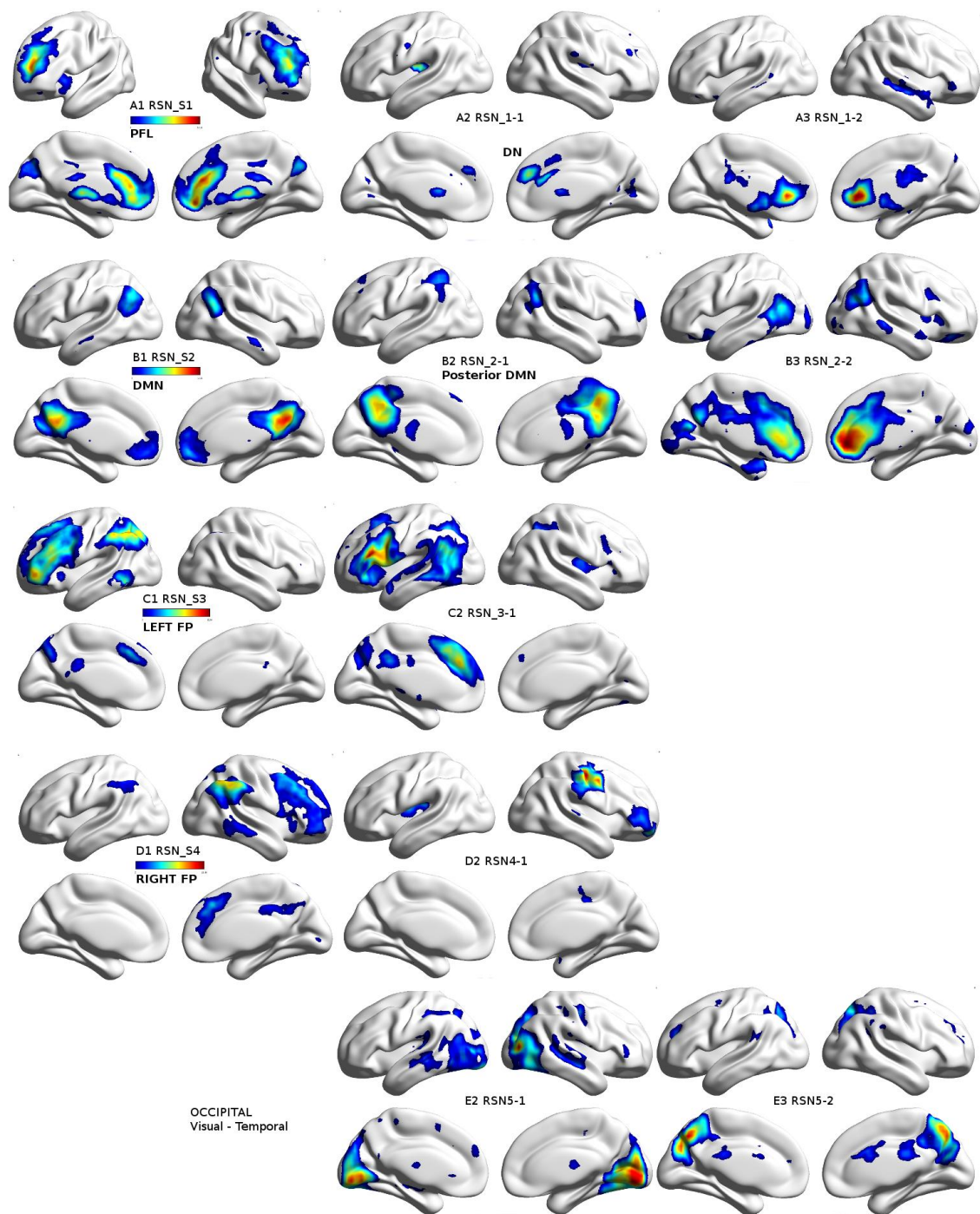
**Figure 2A. RSNs.** The different Resting State Networks (RSN)s were obtained from an Independent Component Analysis (ICA) from Smith et al. Study, and the BOLD signal of the control group was used with Group-ICA strategy. Blue indicates a low probability of the existence of this independent component (IC) within this area, however, yellow and red show the areas with a strong presence of this component. A priori, these areas should work together when they are performing similar tasks or brain complex functions. The nodal AAL definition of these networks is shown in Figure 2B and into table 2. **(A1)** This component is extracted from Smith et al. study and it is present in the Prefrontal and Limbic areas (Smith

et al.; In the study it is called PFL or RSN_S1). **(A2)** This component is extracted from the control group and it is mainly present in the Dorsal Nexus (In this study is called: DN or RSN 1-1). **(A3)** This component is extracted from the control group and it is present mainly in the prefrontal areas (In this study is called PF or RSN 1-2). **(B1)** This component is extracted from the Smith et al. study and it is present in the Default Mode Network (It is called DMN or RSN_S2). **(B2)** This component is extracted from the control group and it is present in the posterior part of DMN (In the current study is called posterior DMN or RSN 2-1). **(B3)** This component is extracted from the control group and it is mainly present in the anterior part of the PF or DMN. (In this study we define this component like anterior part of DMN or RSN 2-2). **(C1)** This component is extracted from the Smith et al. study and it is present in the left hemisphere, mainly within the left Frontal and Parietal areas. (It is called left-FP or RSN_S3). **(C2)** This component is extracted from the control group, and it seems to be a sub-network of the left-FP (It is called RSN 3-1). **(D1)** This component is extracted from the Smith et al. study and it is present in the right hemisphere, mainly within the right Frontal and Parietal areas (It is called right-FP or RSN_S4). **(D2)** This component is extracted from the control group, and it seems to be a sub-network of the right-FP (it is called RSN 4-1). **(E1** and **E2)** These components are extracted from the control group, and they located on the occipital and temporal areas (They are called RSN 5-1 and RSN 5-2).
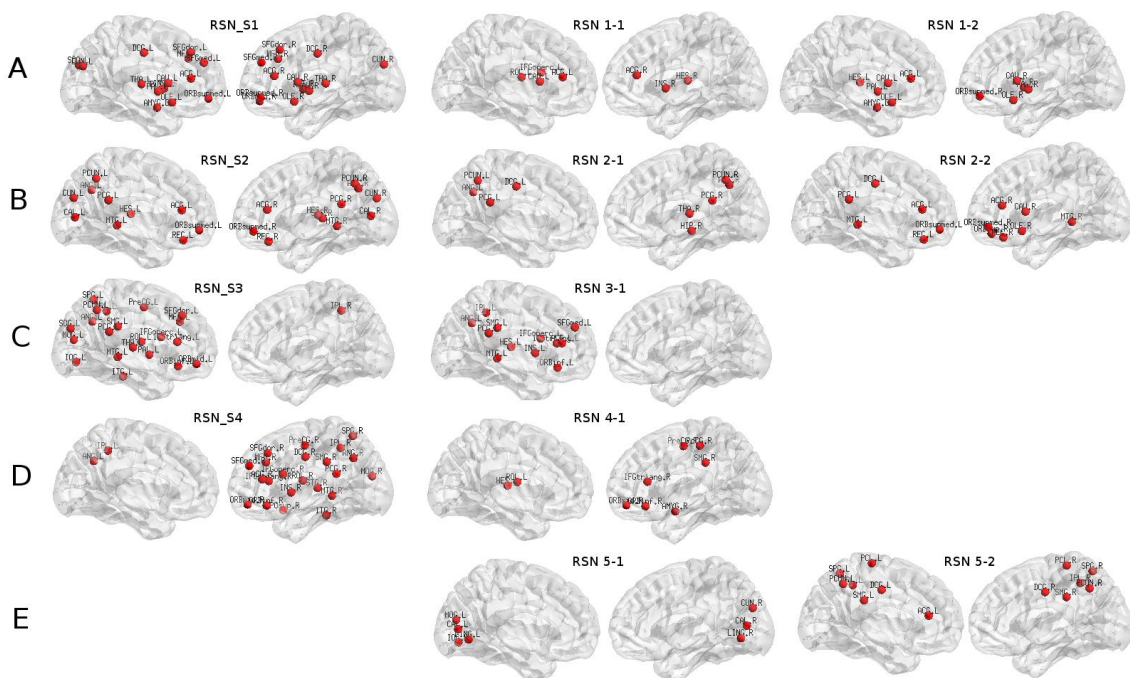


**Figure 2B. RSN - nodes.** After the ICs are extracted we define the networks at a node level from the IC average probability in each AAL region. [A-E] corresponds to the components shown in Figure 1A and Table 2. (A) These components seem to be working into Prefrontal and Limbic areas. (B) They are components seem to be working into the DMN. (C) They are components seem to be working into the Left FP areas or left hemisphere. (D) They are components seem to be working into the Right FP areas or right hemisphere. (E) They are components seem to be working into the occipital and temporal or visual areas.
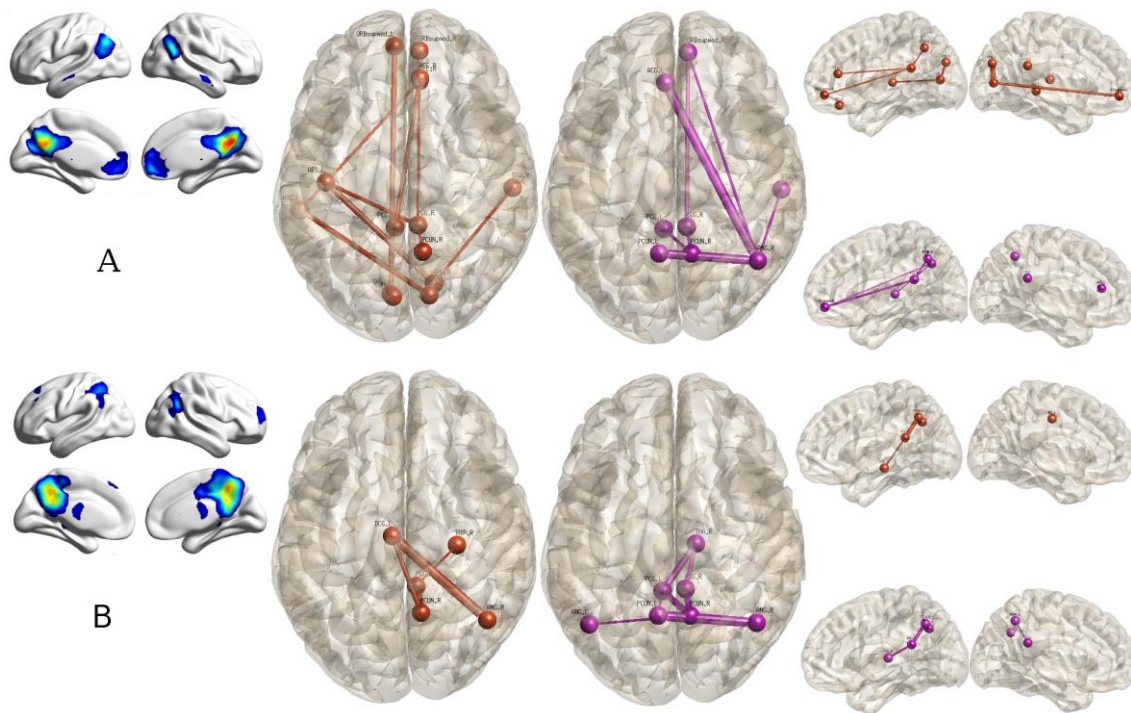
**Figure 3A. Default Mode Network alterations in the FC.** An NBS strategy is used to discover alterations in the FC between the control and the patient group in the different RSNs by both sFC and vFC approaches. The connectivity alterations are shown in Tables 3 (3A for the sFC approach, 3B for the vFC approach). **(A)** [RSN_S2]: The DMN shows hyperconnectivity between its anterior and posterior parts (*left, red*), and a loss of variability in phase-coupling (*right, purple*). Besides, they seem to be in an interhemispheric symmetry way. It suggests two levels of disruptions in the functional connectivity (FC) of the DMN in resting-state condition. Here, the NBS strategy reveals possible hubs for hyperconnectivity between areas, and rigidity of phase-coupling in the ORBsupmed and ACC for the anterior part and PCC, and the Precuneus for the posterior part. This hyperconnectivity could be due to a hypogryrification in MDD, and this support the idea of a vulnearbility at a biological level in front of depression. Besides, we hypothesize that it might be more severe depending on the level of HDRS and time  of depression. These abnormalities could produce depressive ruminations and brooding. **(B)**  [RSN 2-1]: A hyperconnectivity (*left, red*) and a decrease in the index of dispersion of the phase (*right, purple*) between the posterior part of brain (mainly PCC and Precuneus) and the Hippocampal-Thalamic pathway are found, using an NBS strategy on the posterior DMN. This suggests a putative anomaly in the path responsible for managing the episodic memories. It might trigger an over general AM in patients with MDD.
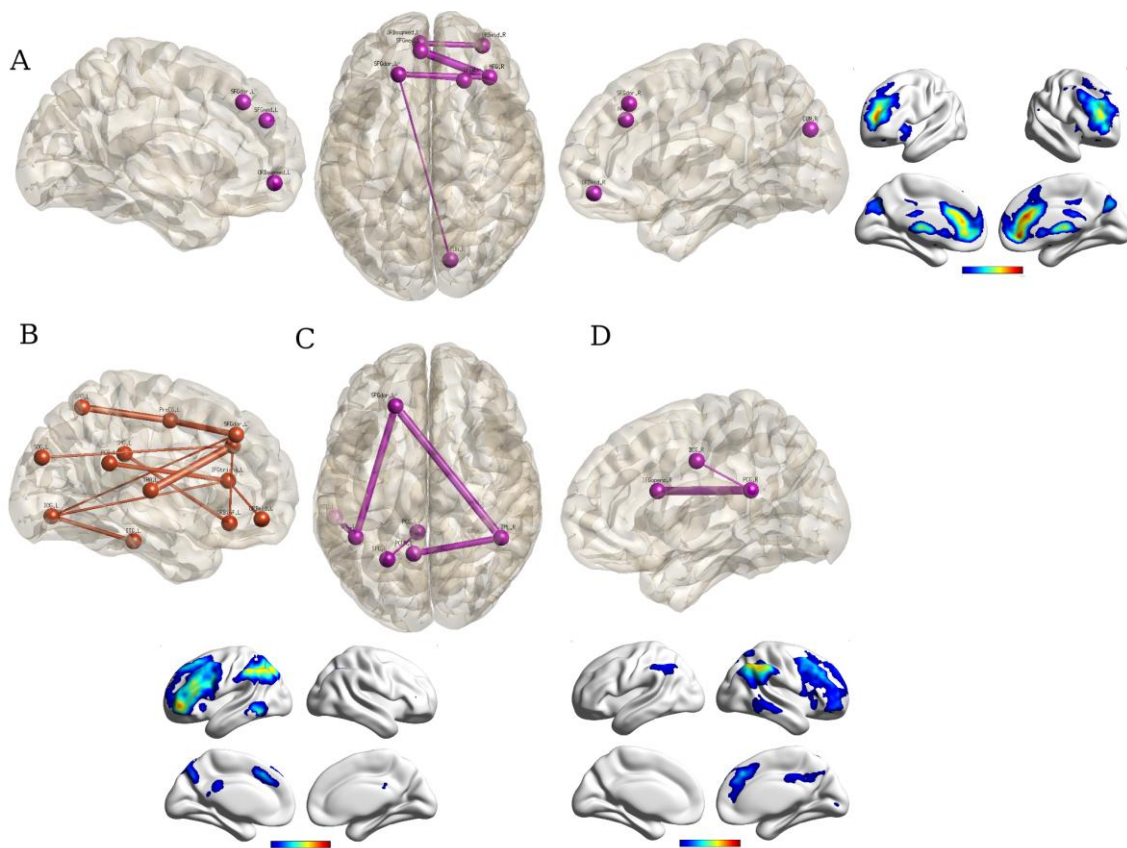
**Figure 3B. PFL and FP Network.** An NBS strategy is used to discover alterations in the FC the between control and the patient group in the different RSN with both sFC and vFC approaches. The connectivity alterations are shown in Tables 3 (3A sFC approach, 3B for the vFC approach). **(A)** [RSN_S1]: The PFL shows a loss of variability in phase-coupling among the DLPFC, OPFC and the right cuneus region. This might produce negative emotional judgment and anxiety problems in the patients. **(B)** [RSN_S3]: The left hemisphere, specially the left FP, shows general problems of connectivity. The static approach in the left FP unmasks a decrement of connectivity between parietal areas and frontal (specially with the left SFGdor area). Besides, we found a disconnectivity between MFG.L and both the left Thalamus and ORBinf areas. **(C)** [RSN_S3]: The left FP also shows a loss of variability in phase-coupling, mainly among the SFGdor.L and inferior parietal regions. **(A,B,C)** The left SFGdor could play a relevant role in the depressive maladaptive, negative emotional judgment and anxiety traits of depression. **(D)** [RSN_S4]: The NBS applied on the right FP unmasks a decrement in the index of dispersion in the phase among the right cingulate regions and IFGoperc.R. This may influence in the flexibility that should exist in the control of human goal-directed behavior (maintaining cognitive faculties). **(A,B,C,D)** The alterations in both static and dynamic measures suggest that the disconnection between frontal and parietal regions might produce a maladaptive control in front of errors of transmission in patients with MDD, generating problems in the control of cognitive faculties and in the adaptive response of feedbacks between frontal and intra/parietal regions.
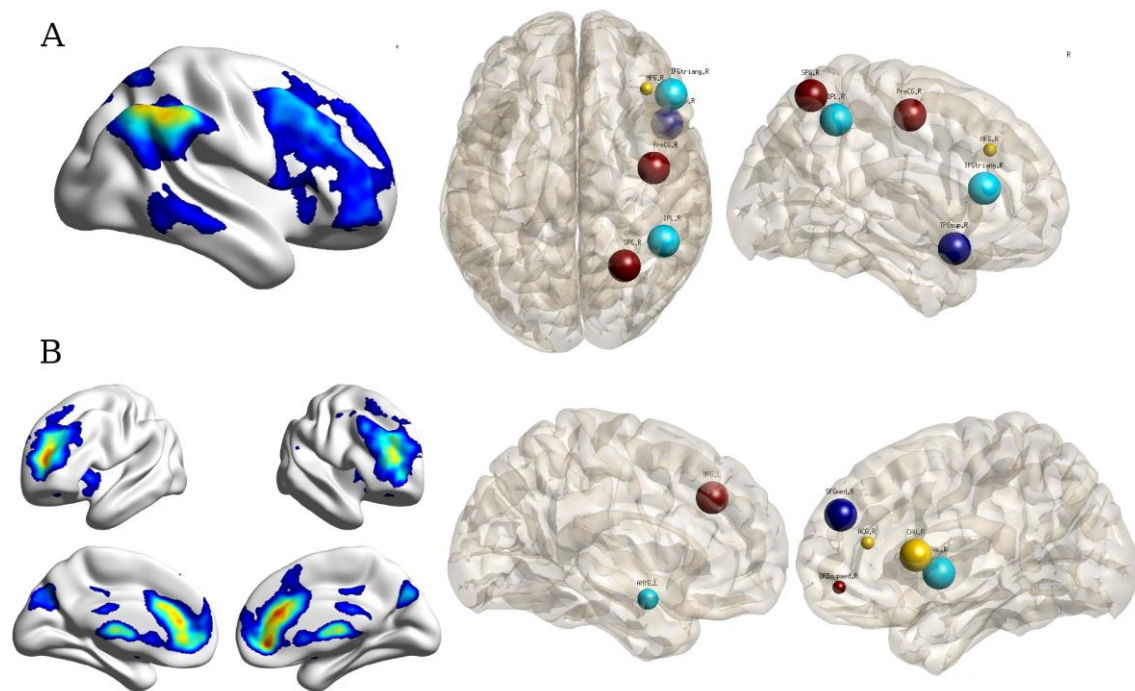
**Figure 4. Classification Tree.** A Classification Tree procedure with a LOOCV strategy are used together to classify individuals between the control and MDD group from nodal descriptors of graph theory by approach (static and dynamic). The descriptors obtained are shown into table 5, and their accuracy values using an LOOCV strategy are shown in the tables 4A-4B. The size defines the occurrence frequency of this metric in the model across the LOO iterations. This frequency is described in the table 5. Thus, small nodes represents a low occurrence of this metric, associated to one region, in the final model. In these cases, these nodes could not be realied on for the classification because of its presence in only some subjects. The color represents the priority the Classification Tree uses it to build the model (table 5). The root of the tree (high priority to build the model) is represented in strong blue, the first level of tree is represented in light blue, intermediate levels in yellow and the last levels of the tree in red. **(A)** The best classification using dynamic nodal descriptors is located on the right FP network. It shows 85.2% of accuracy. **(B)** The best classification using static nodal descriptors is located on the PFL. It shows 83.3% of accuracy. **(A,B)** They could be putative markers of the disorder.
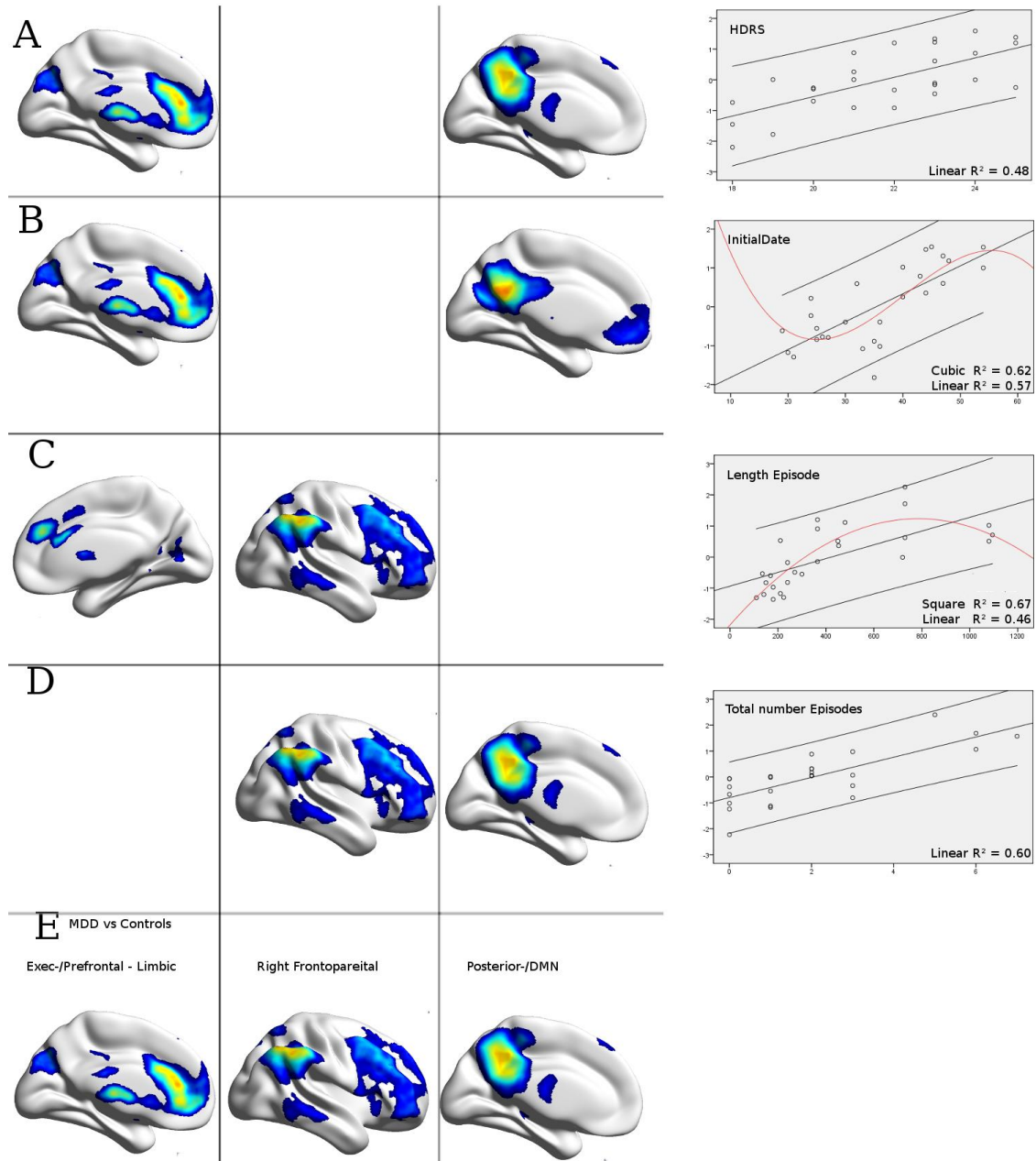
**Figure 5. Clinical variables are explained by the combination of network descriptors.** Static and dynamic network descriptors of RSN such as: DMN, specially the posterior part of DMN, PFL and the right FPN can explain partially different clinical variables of patients with MDD **(A,B,C,D)**. Besides these networks are also involved in the classification model built by binary logistic regression **(E)**. The global descriptors used to build the models and the R² are shown into the tables 6 and 7 (In concret, the classification model is described into the tables 6A-C, and the models which describe different clinical variables in patients are explained into the table 7). In the first column (left), those components that are related to prefrontal and limbic areas which contain some global descriptor in the model are shown; in the second the right FP and the thrid the DMN or posterior DMN components. **(A)** Aterations in the FC among areas or global abnormalities of the activity in the prefrontal and limbic areas (RSN_S1) together with problems in the posterior DMN (RSN 2-1) would partially explain the HDRS (R²=0.48). **(B)**

Alterations in the FC among areas or global abnormalities of the activity in the prefrontal and limbic areas (RSN_S1) together with problems DMN (RSN_S2) migh know historial traits of the major depression (linear model: R²=0.57, Cubic model: R²=0.62). **(C)** Alterations of activity in resting state in the DN (RSN 1-1) and the right hemisphere, specially into the right FP network (RSN_S4), might predict the current length of episode (Linear model: R²=0.46, using a square model: R²=0.67). **(D)** Alterations of activity at rest in the right hemisphere, specially in the right FP network (RSN_S4) together with problems in the posterior DMN (RSN 2-1) might predict the total number of episodes in a patient. **(A,B,C,D)** This networks descriptors could be used like markers to monitoring at strong phases of depression in the patients.**(E)** The major depression could be explained for alterations or global oscillatory problems in the global signal activity in the PFL, right FP and posterior DMN.

**TABLES**

| ID | AAL ID | ID ROI | x | y | z | ID | AAL ID | ID ROI | x | y | z |
|---|---|---|---|---|---|---|---|---|---|---|---|
| 1 | Precentral_L | PreCG.L | -38,65 | -5,68 | 50,94 | 46 | Cuneus_R | CUN.R | 13,51 | -79,36 | 28,23 |
| 2 | Precentral_R | PreCG.R | 41,37 | -8,21 | 52,09 | 47 | Lingual_L | LING.L | -14,62 | -67,56 | -4,63 |
| 3 | Frontal_Sup_L | SFGdor.L | -18,45 | 34,81 | 42,20 | 48 | Lingual_R | LING.R | 16,29 | -66,93 | -3,87 |
| 4 | Frontal_Sup_R | SFGdor.R | 21,90 | 31,12 | 43,82 | 49 | Occipital_Sup_L | SOG.L | -16,54 | -84,26 | 28,17 |
| 5 | Frontal_Sup_Orb_L | ORBsup.L | -16,56 | 47,32 | -13,31 | 50 | Occipital_Sup_R | SOG.R | 24,29 | -80,85 | 30,59 |
| 6 | Frontal_Sup_Orb_R | ORBsup.R | 18,49 | 48,10 | -14,02 | 51 | Occipital_Mid_L | MOG.L | -32,39 | -80,73 | 16,11 |
| 7 | Frontal_Mid_L | MFG.L | -33,43 | 32,73 | 35,46 | 52 | Occipital_Mid_R | MOG.R | 37,39 | -79,70 | 19,42 |
| 8 | Frontal_Mid_R | MFG.R | 37,59 | 33,06 | 34,04 | 53 | Occipital_Inf_L | IOG.L | -36,36 | -78,29 | -7,84 |
| 9 | Frontal_Mid_Orb_L | ORBmid.L | -30,65 | 50,43 | -9,62 | 54 | Occipital_Inf_R | IOG.R | 38,16 | -81,99 | -7,61 |
| 10 | Frontal_Mid_Orb_R | ORBmid.R | 33,18 | 52,59 | -10,73 | 55 | Fusiform_L | FFG.L | -31,16 | -40,30 | -20,23 |
| 11 | Frontal_Inf_Oper_L | IFGoperc.L | -48,43 | 12,73 | 19,02 | 56 | Fusiform_R | FFG.R | 33,97 | -39,10 | -20,18 |
| 12 | Frontal_Inf_Oper_R | IFGoperc.R | 50,20 | 14,98 | 21,41 | 57 | Postcentral_L | PoCG.L | -42,46 | -22,63 | 48,92 |
| 13 | Frontal_Inf_Tri_L | IFGtriang.L | -45,58 | 29,91 | 13,99 | 58 | Postcentral_R | PoCG.R | 41,43 | -25,49 | 52,55 |
| 14 | Frontal_Inf_Tri_R | IFGtriang.R | 50,33 | 30,16 | 14,17 | 59 | Parietal_Sup_L | SPG.L | -23,45 | -59,56 | 58,96 |
| 15 | Frontal_Inf_Orb_L | ORBinf.L | -35,98 | 30,71 | -12,11 | 60 | Parietal_Sup_R | SPG.R | 26,11 | -59,18 | 62,06 |
| 16 | Frontal_Inf_Orb_R | ORBinf.R | 41,22 | 32,23 | -11,91 | 61 | Parietal_Inf_L | IPL.L | -42,80 | -45,82 | 46,74 |
| 17 | Rolandic_Oper_L | ROL.L | -47,16 | -8,48 | 13,95 | 62 | Parietal_Inf_R | IPL.R | 46,46 | -46,29 | 49,54 |
| 18 | Rolandic_Oper_R | ROL.R | 52,65 | -6,25 | 14,63 | 63 | SupraMarginal_L | SMG.L | -55,79 | -33,64 | 30,45 |
| 19 | Supp_Motor_Area_L | SMA.L | -5,32 | 4,85 | 61,38 | 64 | SupraMarginal_R | SMG.R | 57,61 | -31,50 | 34,48 |
| 20 | Supp_Motor_Area_R | SMA.R | 8,62 | 0,17 | 61,85 | 65 | Angular_L | ANG.L | -44,14 | -60,82 | 35,59 |
| 21 | Olfactory_L | OLF.L | -8,06 | 15,05 | -11,46 | 66 | Angular_R | ANG.R | 45,51 | -59,98 | 38,63 |
| 22 | Olfactory_R | OLF.R | 10,43 | 15,91 | -11,26 | 67 | Precuneus_L | PCUN.L | -7,24 | -56,07 | 48,01 |
| 23 | Frontal_Sup_Medial_L | SFGmed.L | -4,80 | 49,17 | 30,89 | 68 | Precuneus_R | PCUN.R | 9,98 | -56,05 | 43,77 |
| 24 | Frontal_Sup_Medial_R | SFGmed.R | 9,10 | 50,84 | 30,22 | 69 | Paracentral_Lobule_L | PCL.L | -7,63 | -25,36 | 70,07 |
| 25 | Frontal_Med_Orb_L | ORBsupmed.L | -5,17 | 54,06 | -7,40 | 70 | Paracentral_Lobule_R | PCL.R | 7,48 | -31,59 | 68,09 |
| 26 | Frontal_Med_Orb_R | ORBsupmed.R | 8,16 | 51,67 | -7,13 | 71 | Caudate_L | CAU.L | -11,46 | 11,00 | 9,24 |
| 27 | Rectus_L | REC.L | -5,08 | 37,07 | -18,14 | 72 | Caudate_R | CAU.R | 14,84 | 12,07 | 9,42 |
| 28 | Rectus_R | REC.R | 8,35 | 35,64 | -18,04 | 73 | Putamen_L | PUT.L | -23,91 | 3,86 | 2,40 |
| 29 | Insula_L | INS.L | -35,13 | 6,65 | 3,44 | 74 | Putamen_R | PUT.R | 27,78 | 4,91 | 2,46 |
| 30 | Insula_R | INS.R | 39,02 | 6,25 | 2,08 | 75 | Pallidum_L | PAL.L | -17,75 | -0,03 | 0,21 |
| 31 | Cingulum_Ant_L | ACG.L | -4,04 | 35,40 | 13,95 | 76 | Pallidum_R | PAL.R | 21,20 | 0,18 | 0,23 |
| 32 | Cingulum_Ant_R | ACG.R | 8,46 | 37,01 | 15,84 | 77 | Thalamus_L | THA.L | -10,85 | -17,56 | 7,98 |
| 33 | Cingulum_Mid_L | DCG.L | -5,48 | -14,92 | 41,57 | 78 | Thalamus_R | THA.R | 13,00 | -17,55 | 8,09 |
| 34 | Cingulum_Mid_R | DCG.R | 8,02 | -8,83 | 39,79 | 79 | Heschl_L | HES.L | -41,99 | -18,88 | 9,98 |
| 35 | Cingulum_Post_L | PCG.L | -4,85 | -42,92 | 24,67 | 80 | Heschl_R | HES.R | 45,86 | -17,15 | 10,41 |
| 36 | Cingulum_Post_R | PCG.R | 7,44 | -41,81 | 21,87 | 81 | Temporal_Sup_L | STG.L | -53,16 | -20,68 | 7,13 |
| 37 | Hippocampus_L | HIP.L | -25,03 | -20,74 | -10,13 | 82 | Temporal_Sup_R | STG.R | 58,15 | -21,78 | 6,80 |
| 38 | Hippocampus_R | HIP.R | 29,23 | -19,78 | -10,33 | 83 | Temporal_Pole_Sup_L | TPOsup.L | -39,88 | 15,14 | -20,18 |
| 39 | ParaHippocampal_L | PHG.L | -21,17 | -15,95 | -20,70 | 84 | Temporal_Pole_Sup_R | TPOsup.R | 48,25 | 14,75 | -16,86 |
| 40 | ParaHippocampal_R | PHG.R | 25,38 | -15,15 | -20,47 | 85 | Temporal_Mid_L | MTG.L | -55,52 | -33,80 | -2,20 |
| 41 | Amygdala_L | AMYG.L | -23,27 | -0,67 | -17,14 | 86 | Temporal_Mid_R | MTG.R | 57,47 | -37,23 | -1,47 |
| 42 | Amygdala_R | AMYG.R | 27,32 | 0,64 | -17,50 | 87 | Temporal_Pole_Mid_L | TPOmid.L | -36,32 | 14,59 | -34,08 |
| 43 | Calcarine_L | CAL.L | -7,14 | -78,67 | 6,44 | 88 | Temporal_Pole_Mid_R | TPOmid.R | 44,22 | 14,55 | -32,23 |
| 44 | Calcarine_R | CAL.R | 15,99 | -73,15 | 9,40 | 89 | Temporal_Inf_L | ITG.L | -49,77 | -28,05 | -23,17 |
| 45 | Cuneus_L | CUN.L | -5,93 | -80,13 | 27,22 | 90 | Temporal_Inf_R | ITG.R | 53,69 | -31,07 | -22,32 |

**Table 1. ROIs of AAL atlas.** The definition of the 90 regions of the atlas AAL used in the study and their positions (x,y,z) in the brain into the MNI space.

| RSN_S1 PFL | RSN_S2 DMN | RSN_S3 L_FP | RSN_S4 R_FP | RSN 5-1 Visual |
|---|---|---|---|---|
| SFGdor.L | ORBsupmed.L | PreCG.L | PreCG.R | CAL.L |
| SFGdor.R | ORBsupmed.R | SFGdor.L | SFGdor.R | CAL.R |
| MFG.L | REC.L | MFG.L | MFG.R | CUN.R |
| MFG.R | REC.R | ORBmid.L | ORBmid.R | LING.L |
| ORBmid.R | ACG.L | IFGoperc.L | IFGoperc.R | LING.R |
| OLF.L | ACG.R | IFGtriang.L | IFGtriang.R | MOG.L |
| OLF.R | PCG.L | ORBinf.L | ORBinf.R | IOG.L |
| SFGmed.L | PCG.R | ROL.L | ROL.R | RSN 5-2 VM |
| SFGmed.R | CAL.L | PCG.L | SFGmed.R | ACG.L |
| ORBsupmed.L | CAL.R | SOG.L | INS.R | DCG.L |
| ORBsupmed.R | CUN.L | MOG.L | ACG.R | DCG.R |
| INS.L | CUN.R | IOG.L | DCG.R | SPG.L |
| INS.R | ANG.L | SPG.L | PCG.R | SPG.R |
| ACG.L | ANG.R | IPL.L | MOG.R | IPL.L |
| ACG.R | PCUN.L | IPL.R | SPG.R | IPL.R |
| DCG.L | PCUN.R | SMG.L | IPL.L | SMG.L |
| DCG.R | HES.L | ANG.L | IPL.R | SMG.R |
| AMYG.L | HES.R | PCUN.L | SMG.R | PCUN.L |
| CUN.L | STG.R | PAL.L | ANG.L | PCUN.R |
| CUN.R | MTG.L | THA.L | ANG.R | PCL.L |
| SOG.L | MTG.R | MTG.L | STG.R | PCL.R |
| CAU.L | RSN_2-1 Post-DMN | ITG.L | TPOsup.R | |
| CAU.R | DCG.L | RSN 3-1 | MTG.R | |
| PUT.L | PCG.L | IFGoperc.L | ITG.R | |
| PUT.R | PCG.R | IFGtriang.L | RSN 4-1 | |
| PAL.L | HIP.R | ORBinf.L | PreCG.R | |
| PAL.R | ANG.L | SFGmed.L | ORBmid.R | |
| THA.L | ANG.R | INS.L | IFGtriang.R | |
| THA.R | PCUN.L | ACG.L | ORBinf.R | |
| RSN 1-1 DN | PCUN.R | PCG.L | ROL.L | |
| IFGoperc.L | THA.R | IPL.L | AMYG.R | |
| ROL.L | RSN_2-2 Pre-DMN | SMG.L | PoCG.R | |
| INS.R | ORBsup.R | ANG.L | SMG.R | |
| ACG.L | OLF.R | HES.L | HES.L | |
| ACG.R | ORBsupmed.L | MTG.L | | |
| CAU.L | ORBsupmed.R | | | |
| HES.R | REC.L | | | |
| RSN 1-2 PF | REC.R | | | |
| OLF.L | ACG.L | | | |
| OLF.R | ACG.R | | | |
| ORBsupmed.R | DCG.L | | | |
| ACG.L | PCG.L | | | |
| AMYG.L | CAU.R | | | |
| CAU.L | MTG.L | | | |
| CAU.R | MTG.R | | | |
| PUT.R | | | | |
| PAL.L | | | | |
| PAL.R | | | | |
| HES.L | | | | |

**Table 2. RSN - ROIs.** The definition of the resting state networks (RSNs) at ROI level used in the study described in the figure 2A and 2B. The ROIs are defined into the Table 1.

| MDD > HC | | MDD > HC | | MDD < HC | |
|---|---|---|---|---|---|
| RSN_S2 Net1 | t=1,93 | RSN 2-1 Post-DMN | t=1,78 | RSN S3 Left FP. Net1 | t=2,13 |
| PCG.L-REC.R | 2,38 | PCG.R-HIP.R | 1,78 | PreCG.L-SFGdor.L | 2,75 |
| ORBsupmed.R-PCG.R | 2,01 | DCG.L-ANG.R | 2,05 | ORBmid.L-IFGtriang.L | 2,18 |
| ACG.R-PCG.R | 1,93 | DCG.L-PCUN.R | 1,87 | PCG.L-IFGtriang.L | 2,51 |
| CAL.R-CUN.R | 2,41 | PCG.R-PCUN.R | 1,99 | SFGdor.L-IOG.L | 2,13 |
| PCG.R-PCUN.R | 1,99 | | | IFGtriang.L-IOG.L | 2,17 |
| PCG.R-HES.L | 2,27 | | | PreCG.L-SPG.L | 2,87 |
| CAL.R-HES.L | 2,66 | | | IOG.L-ITG.L | 2,44 |
| CAL.R-STG.R | 2,11 | | | RSN S3 Left FP. Net2 (Lef | t=2,14 |
| MTG.L-REC.R | 2,02 | | | MFG.L-THA.L | 3,14 |
| MTG.L-CUN.R | 2,54 | | | MFG.L-SOG.L | 2,19 |
| RSN_S2 Net2 (Left CAL) | t=2,56 | | | MFG.L-ORBinf.L | 2,14 |
| ORBsupmed.L-CAL.L | 2,56 | | | SMG.L-ORBinf.L | 2,34 |
| CAL.L-CUN.L | 3,57 | | | | |

**Table 3A. NBS – sFC approach.** The NBS strategy allows to detect functional connectivity problems between groups when they are forming connected components (altered sub-networks on a system). This strategy can be used both on Whole Brain Network (WB) and RSNs. The input are usually matrices of correlations between the activity of regions. In this case, we show altered connections with their respectives ttest one-tailed values (non-corrected) for each RSN (ttest one-tailed value corrected). We want to learn those connections which show an increment or decrement of functional connectivity in the MDD. The representation of this table is in the figures 3A.A, 3A.B (connections in red color) and in the 3B.B. We apply an threshold of t>1.67 to be sure that each connection has a pvalue p<0.05. Depending on the method used to calculate the input matrices for the NBS strategy, the interpretation of results will be different. In this case, we discover alterations on pos-FC. So, this table indicates likely an increment or a loss of connectivity in resting-state between regions. The results show an general hiperconnectivity (MDD>HC) into the DMN and a loss of connectivity (MDD<HC) among frontal and parietal regions.

| vFC approach | | | | | | | |
|---|---|---|---|---|---|---|---|
| MDD < HC | | MDD < HC | | MDD < HC | | MDD < HC | |
| RSN_S2 | t=2,68 | RSN 2-1 Post-DMN | t=2,25 | RSN S3 Left FP. Net1 | t=3,23 | RSN_S1 PFC. Net1 | t=3,00 |
| ORBsupmed.R-PCG.R | 2,75 | PCG.L-PCUN.L | 2,43 | SFGdor.L-IPL.L | 3,34 | SFGdor.R-SFGdor.L | 3,01 |
| ORBsupmed.R-ANG.R | 2,69 | PCUN.L-ANG.R | 2,95 | SFGdor.L-IPL.R | 3,43 | MFG.R-SFGdor.L | 3,54 |
| ACG.L-ANG.R | 2,99 | PCG.L-PCUN.R | 2,72 | PCUN.L-IPL.R | 3,31 | MFG.R-SFGmed.L | 3,96 |
| PCUN.L-ANG.R | 2,95 | PCG.R-PCUN.R | 2,73 | IPL.L-MTG.L | 3,23 | SFGdor.L-CUN.R | 3,00 |
| PCG.L-PCUN.R | 2,72 | ANG.L-PCUN.R | 2,41 | RSN S3 Left FP. Net2 | T=3,00 | RSN S1 PFC. Net2 | t=3,51 |
| PCG.R-PCUN.R | 2,73 | ANG.R-PCUN.R | 2,66 | PCG.L-SPG.L | 3,00 | ORBsupmed.L-ORBmid.R | 3,51 |
| STG.R-ANG.R | 2,68 | PCG.L-THA.R | 2,72 | RSN S4 Right FP | T=4,21 | | |
| | | PCG.R-THA.R | 2,54 | PCG.R-IFGoperc.R | 4,43 | | |
| | | | | PCG.R-DCG.R | 4,21 | | |

**Table 3B. NBS – vFC approach.** The NBS strategy allows to detect functional connectivity problems between groups when they are forming connected components (altered sub-networks on a system). This strategy can be used both on Whole Brain Network (WB) and RSNs. The input are usually matrices of correlations between the activity of regions. In this case, we show anomalies in the phase-coupling with their respectives ttest one-tailed values (non-corrected) for each RSN (ttest one-tailed value corrected). We want to learn those connections which show an increment or decrement of variability in the phase-coupling. The representation of this table is in the figures 3A.A, 3A.B (connections in purple), 3B.A, 3B.C, 3B.D. We apply an threshold of t>1.67 to be sure that each connection has a $P<0.05$ (non-corrected) between groups. Depending on the method used to calculate the input matrices for the NBS strategy, the interpretation of results will be different. In this case, we unmask problems on the IDP matrices. So, this table indicates likely an increment or a loss of index of dispersion in the phase between regions at rest. The results show an general loss of variability in the phase-coupling (loss of flexibility in the transmission of information, rigidity) into the DMN (MDD < HC).

| RSN | All Nodal graph | All Nodal Weighted | All Nodal Corrected | All Nodal Strength | All Nodal Efficiency | Corrected Strength | Strength | Nodal cost Efficiency | Nodal Efficiency |
|---|---|---|---|---|---|---|---|---|---|
| RSN_S2 | 0.5741 | 0.7037 | 0.6852 | 0.5556 | 0.6296 | 0.6481 | 0.7037 | 0.7037 | 0.7222 |
| RSN 2-1 | 0.6296 | 0.7593 | 0.4259 | 0.6296 | 0.6481 | 0.4259 | 0.6852 | 0.4815 | 0.6667 |
| RSN 2-2 | 0.6481 | 0.6111 | 0.5741 | 0.4259 | 0.7593 | 0.5370 | 0.5556 | 0.7037 | 0.5926 |
| RSN 1-1 | 0.6481 | 0.6111 | 0.6852 | 0.5741 | 0.8333 | 0.6296 | 0.6481 | 0.4630 | 0.6481 |
| RSN 1-2 | 0.5185 | 0.6481 | 0.6667 | 0.5926 | 0.5741 | 0.7778 | 0.5556 | 0.4815 | 0.5926 |
| RSN 4-1 | 0.6481 | 0.7037 | 0.6852 | 0.6111 | 0.6481 | 0.4444 | 0.6481 | 0.6667 | 0.7037 |
| RSN 3-1 | 0.7593 | 0.6667 | 0.6852 | 0.5556 | 0.6667 | 0.6852 | 0.6111 | 0.5370 | 0.6667 |
| RSN 5-2 | 0.5370 | 0.5000 | 0.4815 | 0.5556 | 0.6667 | 0.5370 | 0.5000 | 0.4630 | 0.3889 |
| RSN 5-1 | 0.6481 | 0.5000 | 0.5185 | 0.7593 | 0.6296 | 0.5926 | 0.5741 | 0.4630 | 0.5741 |
| RSN_S1 | 0.5370 | 0.6111 | 0.5741 | 0.3519 | 0.5370 | 0.5926 | 0.4630 | 0.4259 | 0.6296 |
| RSN_S4 | 0.7593 | 0.6667 | 0.8148 | 0.8333 | 0.5185 | 0.8519 | 0.7037 | 0.4444 | 0.6296 |
| RSN_S3 | 0.5370 | 0.6852 | 0.6111 | 0.3704 | 0.4444 | 0.5370 | 0.4630 | 0.7407 | 0.5370 |
| Whole Brain | 0.6852 | 0.7222 | 0.7222 | 0.7222 | 0.6667 | 0.7407 | 0.8333 | 0.5556 | 0.6111 |

**Table 4A. Classification Tree by RSN – vFC approach.** A strategy of classification by means of Classification Tree with LOOCV on nodal measures from graph theory was used for unmasking possible markers in the major depression. Each feature is associated to one region which describes the role of this area into its network (graph). An input matrix (*NxM*) was used for this strategy where *N=54* individuals, split into the two groups (control or patient), and *M* is the number of measures. However, the value of each measure depends on its network and the M depends on both the number of measures and regions. The goal was to find the best combination of network and its nodal measures that best separate the individuals among both groups. So, each value in this table represents the accuracy value for one combination. In this case, the measures are extracted from graph theory on IDP matrices (dynamic approach). The values under the column "*All Nodal graph*" indicates that those models were built using all nodal measures (both *nodal efficiency and strength*) both on corrected and on weighted matrices. The models under "*All Nodal weighted*" used all nodal measures on weighted IDP matrices. "*All Nodal corrected*" indicates that those models used all nodal measures on corrected IDP matrices. "*All Nodal Strength*": it was strength nodal measures which come from both weighted and corrected IDP matrices. "*All Nodal Efficiency*": it was nodal efficiency which come from both weighted and corrected IDP matrices. "*Corrected Strength*": these models only used the nodal strength measures that come from corrected IDP matrices. "*Strength*": these models only used nodal strength on weighted IDP matrices. "*Nodal cost Efficiency*": these models only used the nodal efficiency on corrected IDP matrices. "*Nodal Efficiency*": these models only used the nodal efficiency on weighted IDP matrices. The results in the dynamic approach show that the right FP network, in general, gets a good ratios of accuracy, specially the model that uses only corrected nodal strength measures (red). It is represented in the figure 4.A. Nodal efficiency into the DN and nodal strength of whole brain show also good ratio of accuracy 83.3% (blue).

| RSN | All Nodal graph | All Nodal Weighted | All Nodal Binarized | All Nodal Strength | All Nodal Efficiency | Degree | Strength | Nodal Bin Efficiency | Nodal Efficiency |
|---|---|---|---|---|---|---|---|---|---|
| RSN_S2 | 0.7037 | 0.4074 | 0.7778 | 0.6296 | 0.7037 | 0.5741 | 0.6296 | 0.7037 | 0.7037 |
| RSN 2-1 | 0.6481 | 0.6296 | 0.6481 | 0.6481 | 0.6481 | 0.6111 | 0.6481 | 0.6481 | 0.7037 |
| RSN 2-2 | 0.7778 | 0.7778 | 0.6111 | 0.7778 | 0.6667 | 0.4074 | 0.7778 | 0.7222 | 0.5370 |
| RSN 1-1 | 0.5556 | 0.5741 | 0.5926 | 0.5185 | 0.6667 | 0.7222 | 0.5185 | 0.6667 | 0.6852 |
| RSN 1-2 | 0.3704 | 0.3889 | 0.4815 | 0.5185 | 0.4630 | 0.6481 | 0.5556 | 0.5185 | 0.4259 |
| RSN 4-1 | 0.4815 | 0.5000 | 0.5000 | 0.5370 | 0.5741 | 0.3333 | 0.5741 | 0.4815 | 0.5741 |
| RSN 3-1 | 0.6296 | 0.3333 | 0.5370 | 0.5556 | 0.3704 | 0.7407 | 0.5741 | 0.5741 | 0.4259 |
| RSN 5-2 | 0.6852 | 0.4630 | 0.3704 | 0.3889 | 0.4259 | 0.7037 | 0.3889 | 0.3519 | 0.4630 |
| RSN 5-1 | 0.6481 | 0.6481 | 0.6296 | 0.4259 | 0.6667 | 0.7407 | 0.4259 | 0.7222 | 0.5556 |
| RSN_S1 | 0.8333 | 0.6111 | 0.8148 | 0.5926 | 0.7037 | 0.5926 | 0.4444 | 0.7778 | 0.7407 |
| RSN_S4 | 0.3889 | 0.5556 | 0.5926 | 0.5556 | 0.4259 | 0.7222 | 0.4815 | 0.6481 | 0.5556 |
| RSN_S3 | 0.6852 | 0.6852 | 0.5185 | 0.7222 | 0.4259 | 0.4259 | 0.7222 | 0.5370 | 0.5741 |
| Whole Brain | 0.7037 | 0.46296 | 0.7593 | 0.7963 | 0.5000 | 0.7963 | 0.4259 | 0.6481 | 0.4630 |

**Table 4B. Classification Tree by RSN – sFC approach.** A strategy of classification by means of Classification Tree with LOOCV on nodal measures from graph theory was used for unmasking possible markers in the major depression. The goal was to find the best combination of network and its nodal measures that best separate the individuals among both groups. So, each value in this table represents the accuracy value for one combination. In this case, the measures are extracted from graph theory on pos-FC matrices (static approach). The values under the column "*All Nodal graph*" indicates that those models were built using all nodal measures (both *nodal efficiency and nodal degree*) both on binarized and on weighted matrices. The models under "*All Nodal weighted*" used all nodal measures on weighted pos-FC matrices. "*All Nodal Binarized*" indicates that those models used all nodal measures on binarized pos-FC matrices. "*All Nodal Strength*": it was strength nodal measures which come from both weighted and binarized pos-FC matrices. "*All Nodal Efficiency*": it was nodal efficiency which come from both weighted and binarized pos-FC matrices. "*Degree*": these models only used the nodal degree that come from binarized pos-FC matrices. "*Strength*": these models only used nodal strength on weighted IDP matrices. "*Nodal Bin Efficiency*": these models only used the nodal efficiency on binarized pos-FC matrices. "*Nodal Efficiency*": these models only used the nodal efficiency on weighted pos-FC matrices. The results in the static approach show that the best model to classify the subjects of this study is build by binarized and weighted nodal measures of PFL (red). It is represented in the figure 4.B.

| sFC approach : RSN_S1 (PFL): 83.3% of accuracy | | | |
|---|---|---|---|
| ROI | Frequency | Tree Level | Feature |
| SFGmed.R | 54/54 | root | Degree |
| PAL.R | 54/54 | 1st | Binarized nodal Efficiency |
| AMYG.L | 15/54 | 1st | Binarized nodal Efficiency |
| CAU.R | 54/54 | intermediate | Weighted nodal Efficiency |
| ACG.R | 7/54 | intermediate | Weighted nodal Efficiency |
| MFG.L | 54/54 | last | Weighted nodal Efficiency |
| ORBsupmed.R | 7/54 | last | Weighted nodal Efficiency |
| vFC approach : RSN_S3 (right-FP): 85.2% of accuracy | | | |
| ROI | Frequency | Tree Level | Feature |
| TPOsup.R | 54/54 | root | Corrected Strength |
| IFGtriang.R | 54/54 | 1st | Corrected Strength |
| IPL.R | 54/54 | 1st | Corrected Strength |
| MFG.R | 9/54 | intermediate | Corrected Strength |
| PreCG.R | 54/54 | last | Corrected Strength |
| SPG.R | 54/54 | last | Corrected Strength |

**Table 5. Classification Tree – ROIs description.** Only the best descriptors that classify the individuals between groups by approach (sFC static; vFC dynamic) are shown. The classification model is built by using binary trees with Leave-One-Out strategy (LOO). The accuracy values that correspond to each approach are into the Table 4A and 4B (red). The column "ROI" describes the regions present in the best model for each approach. "Frequency" is the frequency of occurrence of this region a long of LOO strategy in this approach. "Tree Level": describes the priorty level of this region to build the best tree model for this approach (level of information that can be explained by this region in that model). "Feature": is the measure used in this classification model on this particular region in this approach. The results from classification tree using static measures on FC (under a point of view of static functional connectivity among regions) show that the features that describe ROIs in the PFL are the best descriptors to classify the individual in the current study, however the features that describe ROIs in the right-PF are the best descriptors to classify the subjects between groups under a dynamic point of view (analyzing the phase coupling among regions in a possible transmission of information).

| Before to equation | Correlation | | | | | Predict | |
|---|---|---|---|---|---|---|---|
| Variables | Gender | Age | Efficiency **PFL** (Binarized pos-FC) | Average Degree **right-FP** (Binarized pos-FC) | Average Strength **Posterior-DMN** (Weighted IDP) | Score test | pvalue *P* |
| Gender | 1,0000 | -,0359 | -,1606 | -,3187 | ,1080 | 1,5429 | ,2142 |
| Age | -,0359 | 1,0000 | ,0008 | -,1793 | -,1468 | ,0388 | ,8438 |
| Efficiency **PFL** (Binarized pos-FC) | -,1606 | ,0008 | 1,0000 | ,3074 | -,2955 | 5,7234 | ,0167 |
| Average Degree **right-FP** (Binarized pos-FC) | -,3187 | -,1793 | ,3074 | 1,0000 | -,2031 | 4,6714 | ,0307 |
| Average Strength **Posterior-DMN** (Weighted IDP) | ,1080 | -,1468 | -,2955 | -,2031 | 1,0000 | 7,5597 | ,0060 |

**Table 6A. Global descriptors before to logistic regression (correlation & predict pvalue).** A binary logistic model was built to classify the subjects between Control and MDD groups. The correlation values of the independent variables used into this binary logistic regression model and their predict score test in the model before to equation are shown in this table. The table show that all global metrics ("*Variables*") which describe the behaviour of the whole networks would be statistically significant. Gender and Age a priori would not be statistically significant in the model. On the other hand, we observe that any independent variable of the model present moderate or strong correlation between them before to equation.

| Observed | | Predicted | | | Nagelkerke R² | Chi-square (X²) | df | *P* |
|---|---|---|---|---|---|---|---|---|
| | | Group | | Percentage Correct | | | | |
| | | Control | Patient | | | | | |
| Group | Control | 19 | 8 | 70,4 | 0,453 | 22,443 | 5 | 0,00043 |
| | Patient | 8 | 19 | 70,4 | | | | |
| Overall | | | | 70,4 | | | | |

**Table 6B. Binary Logistic Regression – Classification & Results of equation.**
A binary logistic model was built to classify the subjects between Control and MDD groups. The overall percent of cases that are correctly predicted by the model, the pseudo-R² and chi-square together with its significant level of the binary logistic regression model are shown in this table. In specially, *"Observed"* indicates the number 0's and 1's that are observed in the dependent variable (group) however the *"Predicted"* show the predict values (results) of this model. The results show that an moderate capacity of prediction of subjects in the group (70,4%; R²=0.45; p=0.0004) using global metrics (descriptors) on the PFL, posterior part DMN and right-FP . We observed equilibrate capacity to predict both control case and patients (19/27, 19/27).

| Variables | B | S.E | X² | df | P |
|---|---|---|---|---|---|
| Gender | -1,342 | ,849 | 2,498 | 1 | ,11398 |
| Age | -,007 | ,035 | ,044 | 1 | ,83347 |
| Efficiency PFL (Binarized pos-FC) | 127,922 | 55,072 | 5,395 | 1 | ,02019 |
| Average Degree right-FP (Binarized pos-FC) | 2,076 | ,843 | 6,069 | 1 | ,01376 |
| Average Strength Posterior-DMN (Weighted IDP) | -5,914 | 2,546 | 5,397 | 1 | ,02018 |
| Constant | -116,510 | 45,213 | 6,641 | 1 | ,00997 |

**Table 6C. Variables in the equation.** The dependent variables into the binary logistic regression model are shown in this table. The overall and the significiant value of this model are shown in the table 6B. "B": are the coefficient values for the model for predicting the group from the these independent variables *(they are in log-odds unit)*. "S.E" is the standard errors associated with the coefficients. *"df":* degree of freedon for each of the test of the coefficients. "X² and P": are the Wald Chi-square and the 2-pvalue used in the testing the null hypothesis for each parameter of this model. The results show that all global metrics on RSN such as: PFL, right-FP and posterior DMN, are parameters stastistically significant for this model. So, despise the model have a moderate level for predicting group, a priori these global metrics would be indicating that these three RSN might be involved in the major depression and might be used like a general markers to monitoring the major depression in patients.

| Linear Model | R | R² | Adjusted R² | S.E (e) | ndf - ddf | F | P | Variables | B | S.E | Beta | t | P | VIF | Tolerance |
|---|---|---|---|---|---|---|---|---|---|---|---|---|---|---|---|
| HDRS | ,693 | ,481 | ,386 | 1,719 | 4 – 22 | 5,093 | ,005 | Constant | 4,183 | 4,431 | | ,944 | ,3554 | | |
| | | | | | | | | Gender | 1,011 | ,966 | ,182 | 1,046 | ,3067 | 1,288 | ,777 |
| | | | | | | | | Age | ,009 | ,033 | ,048 | ,283 | ,7796 | 1,228 | ,814 |
| RSN 2-1 | | | | | | | | Global Efficiency posterior-DMN (Weighted IDP) | 36,638 | 13,759 | ,434 | 2,663 | ,0142 | 1,124 | ,890 |
| RSN_S1 | | | | | | | | Local Efficiency PFL (Weighted pos-FC) | 50,440 | 13,402 | ,600 | 3,764 | ,0011 | 1,076 | ,930 |
| Linear Model | R | R² | Adjusted R² | S.E (e) | ndf - ddf | F | P | Variables | B | S.E | Beta | t | P | VIF | Tolerance |
| InitialDate | ,752 | ,566 | ,487 | 7,506 | 4 – 22 | 7,174 | ,001 | Constant | 153,118 | 39,665 | | 3,860 | ,0008 | | |
| | | | | | | | | Gender | -8,192 | 4,008 | -,309 | -2,044 | ,0531 | ,861 | 1,162 |
| RSN 2-1 | | | | | | | | Local Efficiency Posterior-DMN (Binarized pos-FC) | 24,177 | 7,595 | ,456 | 3,183 | ,0043 | ,962 | 1,040 |
| RSN_S1 | | | | | | | | Global Efficiency PFL (Weighted IDP) | -201,080 | 89,374 | -,327 | -2,250 | ,0348 | ,936 | 1,068 |
| RSN_S2 | | | | | | | | Global Efficiency DMN (Binarized pos-FC) | -9,171 | 3,581 | -,379 | -2,561 | ,0178 | ,900 | 1,111 |
| Linear Model | R | R² | Adjusted R² | S.E (e) | ndf - ddf | F | P | Variables | B | S.E | Beta | t | P | VIF | Tolerance |
| LengthEpi | ,680 | ,462 | ,364 | 244,999 | 4 – 22 | 4,722 | ,007 | Constant | 1695,124 | 393,049 | | 4,313 | ,0003 | | |
| | | | | | | | | Gender | -264,368 | 133,618 | -,341 | -1,979 | ,0605 | ,825 | 1,212 |
| | | | | | | | | Age | 4,070 | 4,843 | ,152 | ,841 | ,4097 | ,747 | 1,338 |
| RSN 1-1 | | | | | | | | Global Efficiency PF-DN (Binarized pos-FC) | -609,512 | 294,900 | -,348 | -2,067 | ,0507 | ,863 | 1,159 |
| RSN_S4 | | | | | | | | Local Efficiency Right-FP (Weighted pos-FC) | -3554,301 | 1160,101 | -,488 | -3,064 | ,0057 | ,965 | 1,036 |
| Linear Model | R | R² | Adjusted R² | S.E (e) | ndf - ddf | F | P | Variables | B | S.E | Beta | t | P | VIF | Tolerance |
| TotalEpi | ,776 | ,602 | ,530 | 1,365 | 4 – 22 | 8,324 | ,000 | Constant | -27,003 | 7,077 | | -3,815 | ,0009 | | |
| | | | | | | | | Gender | 2,576 | ,764 | ,512 | 3,373 | ,0027 | ,784 | 1,276 |
| | | | | | | | | Age | ,093 | ,026 | ,537 | 3,645 | ,0014 | ,832 | 1,201 |
| RSN_S4 | | | | | | | | Average Degree Right-FP (Binarized pos-FC) | 2,011 | ,569 | ,508 | 3,534 | ,0019 | ,874 | 1,144 |
| RSN 2-1 | | | | | | | | Local Efficiency Posterior-DMN (Binarized pos-FC) | -3,897 | 1,398 | -,387 | -2,787 | ,0107 | ,938 | 1,066 |

**Table 7. Multiple Linear Regressions Models from Network descriptors.** Multiple Linear regression were built from network descriptors, that characterize different RSNs (DMN, especially the Posterior part of the DMN, PFL and your DN area and right FP), for predicting different clinical variables such as: the level of severity of major depression (HDRS), initial age of the first episode of depression, the length of current episode of depression, the total number of episodes, in patients with MDD. The overall fits statistics, the level of significance from ANOVA (F-test) and the description of the parameters, together with their coefficients and pvalues, which compose the different models are shown in this table. The results show that HDRS of patients can be moderately explained by global metrics on posterior-DMN and PFL at 48.1%. The prefrontal and limbic areas would be specially relevants in this model (Beta=0.6, contribution in this model). Besides the parameters of the model (independent variables) a priori do not show collineality (tolerance > 0.1 and VIF < 10; *partial correlation controled by gender and age between the network metric of posterior-DMN and the PFL pcorr=-0.159 p=0.45*) and all global metrics values are statistically significative in the model p<0.05. The age and gender do not seem to have much influence in the model. The results also show that initial age of depression ("*initialDate*") in patients can be quite explained by global metrics on DMN, specially by its posterior area, and PFL at 56.7%. The

descriptor of the posterior-DMN component seems to be the most relevant in this model (Beta=0.456). Besides, parameters of this model do not seem to be collineality (tolerance > 0.1 and VIF < 10; *partial correlation controled by gender among these globals metrics: pcorr(DMN-posteriror_DMN)=0.188 p=0.37; pcorr(DMN-FPL)=-0.135 p=0.52; pcorr(PFL-posterior_DMN)=0.022 p=0.916*) and all global metrics values are statistically significative in the model p<0.05. The gender may have some influence in the model. As well, the results show that length of current episode ("*LengthEpi*") of patients can be moderately predicted by global metrics on DN area and right-FP at 46.2%. The right FP network might be the most relevant in this model (Beta=-0.488, negative contribution in this model). Besides the parameters of the model do not show collineality (tolerance > 0.1 and VIF < 10; *partial correlation controled by gender and age between both network metrics pcorr=0.086 p=0.68*) and all global metrics values are statistically significative in the model. The age does not seem to have much influence in the model but the gender seems that might have some weight in the prediction of this variable (*Beta=-0.34, p=0.06*). Finally, the results show that total number of episodes ("*TotalEpi*") can be quite explained by network descriptors of posterior-DMN and specially right-FP (Beta=0.5) with a fits $R^2$=0.6. In this case all variables, including gender and age, are statistically significatives in the model, and even the gender and age would be contributing significantly to explain the variability. Besides the parameters of the model do not show collineality (tolerance > 0.1 and VIF < 10) and the partial correlation controled by gender and age between both network metrics pcorr=0.085 p=0.69). The representation of this model are shown in the figure 5.

**CHAPTER III**

# Altered amygdalar resting-state connectivity in depression is explained by both genes and environment

Aldo Córdova-Palomera[1,2,*]; Cristian Tornador[3,*]; Carles Falcón[4,5]; Nuria Bargalló[2,4,6]; Igor Nenadic[7]; Gustavo Deco[3,8]; Lourdes Fañanás[1,2,**].

*[1]Unidad de Antropología, Departamento de Biología Animal, Facultad de Biología and Instituto de Biomedicina (IBUB), Universitat de Barcelona; Av. Diagonal, 643, 08028. Barcelona, Spain. [2]Centro de Investigaciones Biomédicas en Red de Salud Mental (CIBERSAM); C/Doctor Esquerdo, 46, 28007. Madrid, Spain. [3]Center for Brain and Cognition, Computational Neuroscience Group, Department of Information and Communication Technologies, Universitat Pompeu Fabra; C/ Roc Boronat, 138, 08018. Barcelona, Spain. [4]Medical Image core facility, the Institut d'Investigacions Biomèdiques August Pi i Sunyer (IDIBAPS); C/Rosselló, 149-153, 08036. Barcelona, Spain. [5]Centro de Investigación Biomédica en Red en Bioingeniería, Biomedicina y Nanomedicina (CIBER-BBN); C/ Poeta Mariano Esquillor, s/n., 50018. Zaragoza, Spain. [6]Centro de Diagnóstico por Imagen, Hospital Clínico; C/Villarroel, 170. 08036 - Barcelona, Spain. [7]Department of Psychiatry and Psychotherapy, Jena University Hospital, Friedrich Schiller University Jena; Philosophenweg 3, 07743. Jena, Germany. [8]Institució Catalana de la Recerca i Estudis Avançats (ICREA), Universitat Pompeu Fabra; Passeig Lluís Companys, 23, 08010. Barcelona, Spain.*

**Running title:** Amygdalar resting-state in depression: genes and environment

\* These two authors contributed equally to this work.

**\*\* *Correspondence:***

*Prof. Dr. Lourdes Fañanás Saura*

*Unitat d'Antropologia*

*Dep. Biologia Animal, Facultat Biologia*

*Universitat de Barcelona*

*Av. Diagonal, 645. Barcelona, Spain, 08028.*

*Telephone number: (+34) 93 402 1461.*

*Advisor report on the contribution of the Ph.D. candidate to the article.*

Prof. Dr. Gustavo Deco associate professor at the Universitat Pompeu Fabra of Barcelona, and supervisor of the present doctoral thesis by Cristian Tornador Antolin, hereby certifies that the participation of the Ph.D. candidate in the article "Altered amygdalar resting-state connectivity in depression is explained by both genes and environment" included the following tasks:

- Participation in study design
- MRI data pre- and post- processing.
- Statistical analysis.
- Writing parts of the manuscript
- Critical revision

Prof. Dr. Phil. Dr. Rer. Nat. Habil. Gustavo Deco

Barcelona, 2015

Córdova-Palomera A, Tornador C, Falcón C, Bargalló N, Nenadic I, Deco G, Fañanás L. Altered amygdalar resting-state connectivity in depression is explained by both genes and environment. Hum Brain Mapp. 2015 Oct;36(10):3761-76. doi: 10.1002/hbm.22876.

**CHAPTER IV**

# Environmental factors inducing depression alter
# the cerebellar resting-state synchronization

Aldo Córdova-Palomera[1,2,a]; Cristian Tornador[3,a]; Carles Falcón[4,5]; Nuria Bargalló[2,6,7]; Igor Nenadic[8]; Gustavo Deco[3,9,b]; Lourdes Fañanás[1,2,b,*].

*Under review in Hum Brain Mapp*

[1]*Unidad de Antropología, Departamento de Biología Animal, Facultad de Biología and Instituto de Biomedicina (IBUB), Universitat de Barcelona; Av. Diagonal, 643, 08028. Barcelona, Spain.* [2]*Centro de Investigaciones Biomédicas en Red de Salud Mental (CIBERSAM); C/Doctor Esquerdo, 46, 28007. Madrid, Spain.* [3]*Center for Brain and Cognition, Computational Neuroscience Group, Department of Information and Communication Technologies, Universitat Pompeu Fabra; C/ Roc Boronat, 138, 08018. Barcelona, Spain.* [4]*BarcelonaBeta Brain Research Center, Pasqual Maragall Foundation; C/Dr Aiguader, 88, 08003. Barcelona, Spain.* [5]*Centro de Investigación Biomédica en Red en Bioingeniería, Biomedicina y Nanomedicina (CIBER-BBN); C/ Poeta Mariano Esquillor, s/n., 50018. Zaragoza, Spain.* [6]*Medical Image core facility, the Institut d'Investigacions Biomèdiques August Pi i Sunyer (IDIBAPS); C/Rosselló, 149-153, 08036. Barcelona, Spain.* [7]*Centro de Diagnóstico por Imagen, Hospital Clínico; C/Villarroel, 170. 08036 - Barcelona, Spain.* [8]*Department of Psychiatry and Psychotherapy, Jena University Hospital, Friedrich Schiller University Jena; Philosophenweg 3, 07743. Jena, Germany.* [9]*Institució Catalana de la Recerca i Estudis Avançats (ICREA), Universitat Pompeu Fabra; Passeig Lluís Companys, 23, 08010. Barcelona, Spain.*

**Short title:** Cerebellar rsfMRI, environment and depression

[a] ACP and CT contributed equally to this work.

[b] GD and LF contributed equally to this work.

[*] *Correspondence:*

*Prof. Dr. Lourdes Fañanás Saura*

*Unitat d'Antropologia*

*Dep. Biologia Animal, Facultat Biologia. Universitat de Barcelona*

*Av. Diagonal, 645. Barcelona, Spain, 08028.*

*Telephone number: (+34) 93 402 1461. Fax number: (+34) 93 403 5740.*

*E-mail address: lfananas@ub.edu.*

***Keywords:*** *Cerebellum, resting-state fMRI, depression, environment, imaging genetics, signal processing, Hilbert transform, MZ twins*

*Advisor report on the contribution of the Ph.D. candidate to the article.*

Prof. Dr. Gustavo Deco associate professor at the Universitat Pompeu Fabra of Barcelona, and supervisor of the present doctoral thesis by Cristian Tornador Antolin, hereby certifies that the participation of the Ph.D. candidate in the article "Environmental factors inducing depression alter the cerebellar resting-state synchronization" included the following tasks:

- Participation in study design
- MRI data pre- and post- processing.
- Statistical analysis.
- Writing parts of the manuscript
- Critical revision

Prof. Dr. Phil. Dr. Rer. Nat. Habil. Gustavo Deco

Barcelona, 2015

**Abstract**

Hosting nearly eighty percent of all human neurons, the cerebellum is functionally connected to large regions of the brain. Accumulating evidences suggest that some cerebellar resting-state alterations may constitute a key candidate mechanism for psychopathology, particularly with regards to depression liability. While there is some evidence linking cerebellar function and depression, two topics remain largely unexplored. First, the potential genetic or environmental roots of this putative association have not been elicited. Secondly, different mathematical representations of resting-state fMRI patterns can embed diverse information of relevance for health and disease, though many of these representations have not been studied in detail regarding the cerebellum and depression.

Here, high-resolution fMRI scans were examined to estimate functional connectivity patterns across twenty-six cerebellar regions in a sample of 48 identical twins (24 pairs) informative for depression liability (8 discordant, 6 concordant and 10 healthy pairs). A network-based statistic approach was employed to analyze cerebellar functional networks built using three methods: the conventional approach of filtered BOLD fMRI time-series, and two analytic components of this oscillatory activity (amplitude envelope and instantaneous phase).

Results using fMRI wave amplitude envelopes indicate that the environmental liability for depression is associated with altered resting-state activity across a network involving eight cerebellar subdivisions, including portions of the vermis and the crus. The findings indicate that some environmental factors may lead to depression through alterations of the neural oscillatory activity of the cerebellum during the resting-state. These effects may be observed particularly when exploring the amplitude envelope of fMRI oscillations.

## 1. Introduction

Although the cerebellum embodies only 10% of total brain mass, it hosts almost 70 billion neurons, nearly 80% of all neural cells in the human brain (Azevedo, et al., 2009). Through resting-state oscillatory activity, the cerebellum is functionally connected to large regions of the cerebral cortex, including not only the motor areas but also the prefrontal and parietal cortices (O'Reilly, et al., 2010). These observations may partly explain the biological relevance of cerebellar resting-state activity disruptions observed across several psychiatric disorders (Anticevic, et al., 2014; Bernard, et al., 2014; E, et al., 2014; Kucyi, et al., 2015; Van Overwalle, et al., 2015). Notably, recent research findings have consistently suggested cerebellar resting-state connectivity changes in depression, making it one of the best candidate mechanisms to elicit the neural alterations of the depressed brain (Dutta, et al., 2014; Guo, et al., 2013a; Guo, et al., 2013b; Guo, et al., 2012; Kaiser, et al., 2015).

Both cerebellar resting-state connectivity and depression liability, when considered independently, are caused by the confluence of many genetic and environmental factors (Fu, et al., 2015; Glahn, et al., 2010; Sullivan, et al., 2000). Although disengaging genes and environment has a prominent value in psychiatric research (Caspi and Moffitt, 2006), whether the association between cerebellar functionality and depression can be explained by genetic or non-genetic factors remains largely unexplored. Genetically-informative studies need to be implemented to elicit this topic for two main reasons. First, it has been proposed that some alternative phenotypes (i.e., endophenotypes) would have a tougher connection with the genetic basis of psychopathology than phenomenologically-derived clinical diagnoses (Glahn, et al., 2014; Gottesman and Gould, 2003). This should be highlighted here since a novel study has found that some resting-state networks including cerebellar regions are likely to serve as endophenotypes in brain research (Fu, et al., 2015).

Thus, it is feasible hypothesizing that some genetic factors determining cerebellar resting-state activity may also modify depression risk. Secondly, the link between the cerebellum and depression may perhaps be due to non-genetic (i.e., environmental) factors. One could thus postulate that some environmental factors alter the cerebellar functionality and then lead to depressive psychopathology. This would have significant implications as there are several well-identified environmental risk factors for depression –such as adverse

infancy experiences and stressful adult life events (Kendler, et al., 2003; Moffitt, et al., 2007)– whose underlying neurobiology has been only partly explained. Discerning environmental mechanisms triggering specific neurobiological correlates of depression would have many epidemiological and public health implications (Duncan and Keller, 2011; Freeman and Stansfeld, 2008; Lundberg, 1998).

The mentioned alterations in cerebellar resting-state connectivity observed in depressive psychopathology suggest a number of (potential) functional disruptions. Importantly, although using diverse neuroimaging techniques to assess resting-state patterns, several authors have agreed that there are many differences in cerebellar function between depressed and healthy individuals (Dutta, et al., 2014). These different imaging analysis methods allow evaluating putative functional alterations from several viewpoints. While each of them might have its own potential relevance in the clinical settings (Lee, et al., 2013), one of the most promising approaches to study resting-state neural activity *in vivo* is the examination of spatio-temporal synchrony patterns between regions using network theory (Richiardi, et al., 2011; Smith, et al., 2013; van den Heuvel and Hulshoff Pol, 2010). In terms of large-scale neuronal networks, the brain disturbances reported in the literature of depression would indicate modifications of the information processing performance through the cerebellum.

Typically, the study of resting-state functional brain networks is based upon the extraction of low-frequency periodic time series from a set of pre-defined anatomical regions. Robust first-order correlations in temporal activation patterns of two anatomically-segregated regions (nodes) are considered a functional connection (edge) (De Vico Fallani, et al., 2014; van den Heuvel and Hulshoff Pol, 2010). Highly synchronized (correlated) wave amplitudes of two brain regions during resting-state are thus interpreted as a strong edge linking those two regions. Although this method has certainly led to remarkable clinical and neurobiological findings (Lee, et al., 2013), recent findings have highlighted that neural synchronization patterns observed through neuroimaging can occur at different levels, and that each of these levels may have different behavioral significance (Guggisberg, et al., 2014). For instance, Guggisberg, et al. (2014) have recently described three types of synchronization that may have large implications for behavior analysis. Namely, along with the aforesaid amplitude correlation mechanism –probably the most

used–, neural coupling can also take place as amplitude envelope correlation or as oscillation phase synchronization.

These three different types of synchronization have mostly been used in magneto- and electroencephalography. Their potential relevance to analyze resting-state fMRI brain scans has been specially highlighted during recent years, since *i*) they allow increasing temporal resolution of hemodynamic (fMRI) signals (Glerean, et al., 2012), *ii*) they may explain an important extent of the relationship between brain structure and function (Ponce-Alvarez, et al., 2015) and *iii*) they could partly explain brain deficits in psychopathology (Cordova-Palomera, et al., 2015). In biological terms, these observations on synchronization phenomena observed in fMRI signals would parallel the compelling evidence showing that higher-order brain function may be closely related to neural communication established from coherent oscillatory activity of brain regions at specific frequencies (Fries, 2005; Fries, 2009). Namely, distinct components of neuronal activity waves can encode and transmit information efficiently, although these components may not be directly deduced by examining raw fMRI time series.

Considering these elements, the present study was aimed at examining the putative association between cerebellar resting-state fMRI alterations and both the genetic and the environmental factors leading to depressive psychopathology. High resolution fMRI brain scans were used to extract cerebellar resting-state time series from a group of 48 monozygotic (MZ) twins (24 pairs) informative for depression. As co-twins of a MZ pair have almost identical DNA sequences, their phenotypic similarities and differences were investigated to gain insights on putative familial and environmental influences. An anatomically-restricted 26-node network comprising different subdivisions of the cerebellum (including the vermis) was examined. Functional connections (edges) between regions were defined using three complementary conceptions of neural synchrony (Guggisberg, et al., 2014): *i*) amplitude correlation –the conventional method–, *ii*) amplitude envelope correlation and *iii*) phase synchrony.

## 2. Methods

### 2.1. Sample description

The participants of this study were selected from a larger group of 115 Spanish Caucasian adult twin pairs (230 individuals) from the general population, who gave their consent to be contacted for research purposes. All the subjects were contacted by telephone and invited to participate in a general study of adult cognition and psychopathology. Trained psychologists administered a battery of neurocognitive and psychological tests to the twins. Also, they were interviewed for medical records. Exclusion criteria applied were a medical history of neurological disturbance, presence of sensory or motor alterations, current substance misuse or dependence and age under 18 and over 65 years. After a detailed description of the study aims and design, all participants signed a written informed consent form approved by the local Ethics Committee. All procedures were conducted in accordance with the Declaration of Helsinki.

Zygosity of all pairs was evaluated by genotyping 16 highly polymorphic microsatellite loci from DNA samples (SSRs; PowerPlex® 16 System Promega Corporation). Identity on all the markers can be used to assign monozygosity with greater than 99% accuracy (Guilherme, et al., 2009). In the whole sample (115 duos), 86 twin pairs were MZ.

From the former collection of participants, using the previously obtained data, a subset of 54 individuals (27 MZ twin pairs) was selected, as they were informative for psychopathological traits and agreed to participate in the MRI part of the present study. These 54 participants met the following criteria: *i*) age at scan between 20 and 56 years, *ii*) both twins right-handed, and *iii*) none of the twins manifested liability for DSM-IV-R psychiatric diagnoses other than depression and/or anxiety. No participant had a history of major medical illnesses.

Next, due to image artifacts or lack of data about six participants, the final sample (i.e., the subset included in all statistical analyses) consisted of 48 individuals (20 males, mean age: 33.6 years).

## 2.2. Psychometric measures

The liability for psychopathology in this general population sample was evaluated by a clinical psychologist in a face-to-face interview. Briefly, the Structural Clinical Interview for DSM-IV Axis I Disorders (SCID-I) (First, 1997) was applied in a face-to-face interview to screen for the presence of any lifetime depression or related anxiety spectrum disorder. In this sample, six individuals with a history of (mainly) anxious psychopathology were included in the psychopathology-affected group. This apparently wide category of outcomes was used in recognition of the evidence on comorbidity, shared etiopathology and diagnostic criteria overlap between depressive and anxious disorders (Mosing, et al., 2009; Ressler and Mayberg, 2007; Wittchen, et al., 2002; Zbozinek, et al., 2012), as well as considering findings of some similar resting-state alterations across both diagnoses (Oathes, et al., 2015; Pannekoek, et al., 2015). Of note, repeating the statistical analyses removing predominantly anxious individuals did not alter the significance of the results.

The participants were also asked to report if they had received psychological or pharmacological treatment or had consulted a mental health professional since they first participated in the study. Only one individual had life-time exposure to psychopharmacological treatment for depression. However, excluding this individual from the group analyses did not change the significance of the results.

In the whole sample, there were ten healthy, six concordant and eight discordant pairs for lifetime DSM-IV diagnoses. Furthermore, current depression status and other psychiatric symptoms were evaluated using the Brief Symptom Inventory (BSI) (Derogatis and Melisaratos, 1983; Ruiperez, et al., 2001). The BSI is a self-administered 46-item screening instrument designed to identify the experience of psychopathological symptoms during the last 30 days. It includes six subscales (depression, phobic anxiety, paranoid ideation, obsession-compulsion, somatization and hostility) and is designed to be used in both clinical and non-clinical samples. Items are rated on a five-point scale of distress, according to self-perception of symptom severity. Table I shows a descriptive summary of the data from the current sample. As displayed, twins with no lifetime history of DSM-IV diagnosis had fewer self-reported symptoms –lower BSI scores– in both the depressive subscale and the whole questionnaire. Moreover, neurocognitive information for this

sample was collected by means of the Wechsler Adult Intelligence Scale (Sattler, 2001; Wechsler, et al., 1997). The intelligence quotient (IQ) of each participant was estimated from five subtests of this battery (block design, digit span, matrix reasoning, information and vocabulary). As shown in Table I, the distribution of IQ scores was similar to those reported in demographically analogous samples (Lynn and Meisenberg, 2010). No intra-group differences were found in the IQ scores, likely indicating that neurocognitive effects on resting-state brain signals (Douw, et al., 2011; Wang, et al., 2011) do not influence the subsequent statistical analyses of this study.

## 2.3. MRI acquisition and pre-processing

The brain scans were acquired at the MRI Unit of the Image Platform (IDIBAPS, Hospital Clínic de Barcelona), using a TIM TRIO 3T scanner with an 8-channel head coil (Siemens, Erlangen, Germany). The resting-state fMRI images comprised 210 echo-planar (EPI) blood-oxygen-level dependent (BOLD) sensitive volumes (TR = 2790 ms, TE = 30 ms, 45 axial slices parallel to anterior-posterior commissure plane acquired in interleaved order, 3.0 mm slice thickness and no gap, FOV = $2075 \times 1344$ mm$^2$, voxel size = 2,67 x 2,67 x 3 mm$^3$). Moreover, high-resolution 3D structural datasets were acquired for anatomical reference, using a T1-weighted magnetization prepared rapid gradient echo, with the next parameters: 3D T1-weighted MPRAGE sequence, TR = 2300 ms, TE = 3.03 ms, TI = 900 ms, Flip Angle = 9°, 192 slices in the sagittal plane, matrix size=256×256, 1 mm$^3$ isometric voxel.

Resting-sate time series were obtained using standard image processing protocols implemented in the Statistical Parametric Mapping software, version 8 (SPM8) (Friston, et al., 1995), running under MATLAB (The Mathworks, Natick, MA). After correction of slice-timing differences and head-motion, the fMRI images were co-registered to the 3D (T1) anatomical reference and to the mean functional image. Then, the images were spatially normalized to the standard stereotaxic space MNI (Evans, et al., 1993). Artifacts related to blood pulsation, head movement and instrumental spikes were removed from the BOLD time series in MNI space, using independent component analysis as implemented in GIFT (Calhoun, et al., 2009; Sui, et al., 2009). No global signal regression or spatial

smoothing was applied. Mean BOLD time series were extracted from the 116 regions of interest (ROIs) in the standard Automatic Anatomical Labeling (AAL) atlas, which comprises 90 cerebral and 26 cerebellar regions (Tzourio-Mazoyer, et al., 2002). The atlas had previously been masked with the binarized subjective tissue probability maps to detach the mean value of the regions from the gray matter via a conventional protocol (Power, et al., 2014; Villain, et al., 2010). The following mask was used: [Atlas * (GM>WM) * (GM>CSF) * (GM>0.1)], where GM stands for gray matter, WM is the white matter and CSF stands for cerebrospinal fluid. Next, the BOLD time series for each region were band-pass filtered within the resting-state fMRI narrowband going from 0.04 to 0.07 Hz (Achard, et al., 2006; Glerean, et al., 2012). A schematic representation of these steps is shown in sections A-D of Figure I.

## 2.4. Extraction of functional connectivity networks for each individual

Three different approaches were used here to estimate functional connectivity from the band-passed time series described above. First, a conventional approach to examine correlations between fMRI BOLD time series was used (Smith, et al., 2013), with twenty-six $x(t)$ series per individual (one for each cerebellar AAL ROI). A partial correlation matrix was obtained for the 26 ROIs from the 210 slices scanned over time. Each partial correlation coefficient from this matrix represents the magnitude of the association between every pair of ROIs, controlling for the effect of the other variables (i.e., the remaining ROIs). This step produced a $26 \times 26$ matrix representing the functional connectivity between each pair of brain ROIs, which was then normalized using Fischer's z transform (Fox, et al., 2005; Jenkins and Watts, 1968). Subsequently, following a previous technical report (Schwarz and McGonigle, 2011), a soft threshold procedure was implemented to remove negative edges, since their particular network topology can drastically alter the properties of brain fMRI connectivity networks. The sequence of sections D, G and J in Figure I schematize this procedure, applied to data from a healthy participant.

Other two functional connectivity brain networks were retrieved for each participant. In order to get them, the analytic components of the resting-state BOLD signals from the 26 ROIs were computed following previously published protocols (Glerean, et al.,

2012; Guggisberg, et al., 2014). Briefly, the analytic representation of each real valued band-passed (0.04 - 0.07 Hz) BOLD time series was computed by further processing their band-passed time series, using the Hilbert transform. Explicitly, let $x(t)$ be the band-passed BOLD time series of a particular ROI. Its analytical representation is the complex function

$$x_a(t) = x(t) + i\,H\big[x(t)\big],$$

where $i$ stands for $\sqrt[2]{1}$, and $H[\cdot]$ is the Hilbert transform. The new signal $x_a(t)$ has the same Fourier transform as $x(t)$, although it is defined only for positive frequencies. Similarly, let $x(t)$ be expressed as an amplitude-modulated signal $a(t)$ with carrier frequency $\phi(t)$, so that $x(t) = a(t)\cos[\phi(t)]$. Then, its Hilbert transform gives

$$x_a(t) = a(t)e^{i\phi(t)},$$

where $|a(t)|$ represents the instantaneous envelope and $\phi(t)$ stands for the instantaneous phase. In the present study, both $|a(t)|$ and $\phi(t)$ are later used to estimate two new 26 × 26 partial correlation matrices as described above, which are later z-transformed and soft-thresholded. Sections E, F, H, I, K and L in Figure I represent this procedure applied to data from one participant.

## 2.5 Inter-subject analysis of the functional connectivity networks

A network-based statistic (NBS) approach (Zalesky, et al., 2010) was implemented to examine potentially altered connections (edges) between every pair of ROIs (nodes). Briefly, NBS performs a statistical examination of potentially altered network edges that may differ across groups or conditions. It controls the family-wise error rate when statistical tests are conducted at single edges comprising a whole graph, on the basis of conventional cluster-based thresholding of statistical parametric maps (Zalesky, et al., 2010). Since edge weights in the connectivity matrices studied here represent oscillatory coupling events between pairs of ROIs, the edge-based strategy of NBS allowed assessing potential coupling alterations across combinations of cerebellar regions. These oscillatory patterns were examined through independent analyses, implemented for each of the three partial correlation matrices: amplitude, amplitude envelope and instantaneous phase

(corresponding to $x(t)$, $\|h(t)\|$ and $\phi(t)$).

The design matrices used for NBS were based upon previous literature on regression models of clustered data (Begg and Parides, 2003), which can be applied to separate familial and environmental components of phenotype associations in twin studies (Carlin, et al., 2005). More explicitly, the regression model

$$Y_{ij} = \beta_0 + \beta_B \mu_{i.} + \beta_W (X_{ij} - \mu_{i.})$$

was implemented. Subindex $i \in \{1, ..., n\}$ stands for pair number (here, $n = 24$ MZ pairs) and $j \in \{1, 2\}$ refers to co-twin number (randomly assigned). The diagnostic status was coded as the numeric value 0 (healthy) or 1 (depressed) for each individual. An individual's diagnostic is thus represented as $X_{ij} \in \{0, 1\}$ in the equation, and a pair's familial liability for depression is expressed as $\mu_{i.} = (X_{i1} + X_{i2})/2$. The binary codification of the diagnostic status thus allows the familial liability (genes plus shared environment) to take only three values $\mu_{i.} \in \{0, 0.5, 1\}$, corresponding to no familial liability (healthy pairs, $\mu_{i.} = 0$), moderate familial load (discordant pairs, $\mu_{i.} = 0.5$) or high familial predisposition (concordant pairs, $\mu_{i.} = 1$). This value is then used to estimate a regression coefficient for the familial factors ($\beta_B$). Furthermore, the value $X_{ij} - \mu_{i.}$ is computed to represent the unique environmental influences from non-shared events within a twin pair ($\beta_W$). This arithmetic difference may only take three different values: $X_{ij} - \mu_{i.} = 1 - 1 = 0$, for concordant pairs, $X_{ij} - \mu_{i.} = 0 - 0 = 0$ for healthy pairs, and $X_{ij} - \mu_{i.} = 1 - 0.5 = 0.5$ for affected co-twins from a discordant pair and $X_{ij} - \mu_{i.} = 0 - 0.5 = -0.5$ for healthy co-twins from a discordant pair. Namely, both concordant and healthy pairs are assumed to have no environment-specific differences in depression liability, whereas affected (healthy) discordant co-twins are considered to have high (low) environmentally-induced risk. Lastly, $Y_{ij}$ represents the edge weight of each connection between the 26 different nodes in the cerebellum. Thus, the equation is solved for all edges separately, although the method implemented by NBS already exploits the fact that the connections with an effect of interest may usually be interconnected (Zalesky, et al., 2010). Moreover, to control for potential confounding demographics (Table I), all analyses were adjusted for gender and age.

Complementarily, a confirmatory analysis was conducted using R's software

packages *rms* and *mztwinreg* (Córdova-Palomera, 2015; Harrel, 2013; R Development Core Team, 2011). Namely, the cerebellar subgraph comprising the altered edges from the above procedure was retrieved, and total edge weight –a global measure of oscillatory synchronization of the potentially-altered connections– was computed. This value ( $Y_{ij}$ ) was used as outcome in the equation mentioned above. It was then solved via ordinary least squares, and the Huber-White method was implemented to adjust the variance-covariance matrix of these regression fits, in order to account for the non-independence of twin data (i.e., heteroskedasticity).

## 3. Results

As stated above, recent evidences suggest that the resting-state connectivity of the cerebellum may be influenced by the environment, which would be indexed as MZ twin dissimilarities (Fu, et al., 2015). Since the following analyses were mainly edge-based –to examine resting-state coupling between pairs of regions–, a first preliminary step consisted in the analysis of intrapair correlations in global connectivity metrics describing the links between cerebellar subdivisions. As shown in Table II, there were large intrapair differences within the MZ pairs across these measures. The table indicates that the largest intrapair correlation coefficient for the different network metrics considered was 0.38, suggesting that most of the variance in this population should be attributed to unique environmental influences. Importantly, none of these correlation coefficients was statistically significant. Namely, co-twins from every MZ pair have largely different cerebellar synchronization patterns. This prominent role of the environment in modulating cerebellar synchronization provides further support to the ensuing analyses separating the variance into genetic and non-genetic factors.

Next, NBS analyses were conducted to examine putative resting-state synchronization disruptions in the depressed cerebellum, dividing the depression liability into familial and unique environmental, and using three different time series analysis methods. When applying either the conventional approach or the instantaneous phase coupling methods, NBS analysis revealed no association between cerebellar resting-state activity and depression liability. In contrast, there were statistically significant results for the cerebellar resting-state network built from amplitude envelope correlations between the twenty-six regions of interest (Figure 2). As noticed in Figure 2-B, there was a seven-edge network that showed statistically significant differences in resting-state activation depending on the environmental liability for depression (NBS $p$-value for $\beta_W$ of the sub-network: 0.002; $F = 10.36$). As discussed above, the statistical significance of all the $p$-values retrieved from the NBS software tool is already controlling for the family-wise error rate (section 2.5). Although three different NBS analyses were implemented (conventional approach, amplitude envelope and instantaneous phase), the significance of the previous finding ($p = 0.002$) would survive even an additional –and perhaps overly conservative–

multiple testing adjustment stage (i.e., $p_{\text{adjusted}} = 0.002 \times 3$ independent tests $= 0.006$).

Further exploratory analysis revealed that these network edges formed stronger connections between nodes in the individuals with high environmental load for depression (i.e., affected co-twins from discordant pairs) than in the rest of the study population (Figure 2-C). This would indicate that an increased environmental liability for psychopathology would be related to hyper-synchronized activity across a set of cerebellar ROIs, including portions of the left and right crura, parts of the vermis and other subdivisions of both cerebellar hemispheres.

Since the NBS approach does not provide a direct adjust for heteroscedasticity, and in order to obtain further insights on the results for this set of edges, a confirmatory procedure was conducted. Namely, a linear regression model (section 2.5) was implemented to analyze the seven cerebellar edges shown altered by NBS. This new step provided evidence suggesting that the previous finding is statistically robust even after adjusting for the correlated nature of twin data (familial factors: $\beta_B = 0.11$, standard error $= 0.17$, $t = 0.62$, $p = 0.541$; unique environment: $\beta_W = 1.34$, standard error $= 0.29$, $t = 4.71$, $p < 0.0001$; adjusted $R^2$ for the whole model: 0.45). The results of this step are depicted in the barplot of Figure 2-D, which shows that, after adjusting for gender and age, the affected co-twins from discordant pairs have more than twice the total network edge weight than the rest of the participants.

## 4. Discussion

In this study, a genetically-informative design was implemented to evaluate the putative relationship between depression liability and different cerebellar resting-state synchronization patterns, as measured by fMRI. Three different coupling types (amplitude, amplitude envelope and instantaneous phase correlation) among the distinct anatomical subdivisions of the cerebellum were analyzed in relation to both familial and unique environmental factors underlying depression liability. Overall, there were large differences in cerebellar synchronization –at all three levels– within MZ twin pairs, likely indicating a major environmental modulation. When considering the amplitude envelope of the resting-state fMRI activity patterns, the temporal correlations between paired cerebellar ROIs showed an association with the environmental factors leading to depression. In contrast, depression risk –either familial or environmental– was not related to the cerebellar coupling patterns of either the amplitude or the instantaneous phase.

The results suggest that some analytic properties of the resting-state fMRI BOLD signal may be associated with differential exposure to environmental factors leading to depression. Although association does not necessarily imply causation (Huang, 2014), this finding somehow indicates that the environment may increase depression risk through alterations of the temporal coupling between different cerebellar regions.

Specifically, when analyzing the amplitude envelope of the resting-state fMRI patterns, individuals with high environmental risk load for depression showed a set of overly synchronized cerebellar regions. This hyper-synchronization pattern is analogous to other neural coupling impairments observed across different neuropsychiatric pathologies. For example, the complexity of the neural oscillatory activity is decreased in schizophrenia, as indexed by high synchrony between different cerebral regions (Andreou, et al., 2014; Billeci, et al., 2013; Sokunbi, et al., 2013). Perhaps the boundary expression of neural hyper-synchronization leading to a functional impairment is observed in the epileptic brain (Stamoulis, et al., 2010; Zhang, et al., 2014). Physically, the redundancy in information through different sources (i.e., ROIs having very similar oscillatory patterns) is linked to a reduction in communicational complexity (Shannon, 1997).

To the best of our knowledge, this is the first genetically-informative study of cerebellar resting-state functional networks in depression examining not only the network formed by BOLD wave amplitudes, but also those derived from their analytic components. Although functional connectivity has largely been studied in the literature using amplitude correlation to define brain networks, the investigation of the analytic components (i.e., amplitude envelope or instantaneous phase) of BOLD oscillatory patterns is relatively new in psychiatric research (Cordova-Palomera, et al., 2015; Glerean, et al., 2012). Remarkably, previous reports with different resting-state fMRI analysis techniques have similarly highlighted a role for the cerebellum in depressive psychopathology (Dutta, et al., 2014; Guo, et al., 2013a; Guo, et al., 2013b; Guo, et al., 2012; Kaiser, et al., 2015).

The fact that the observed association is mainly driven by the environment should be emphasized, particularly since there is evidence of important environmentally-induced physiological changes in the cerebellum (Foti, et al., 2011; Greenough, et al., 1986; Morel, et al., 2002; Vazquez-Sanroman, et al., 2013). These non-genetic factors may explain part of the relatively high influence of the environment on depression liability (i.e., an heritability estimate around 40%) (Sullivan, et al., 2000). Although the evidences on the environment and the cerebellum come mainly from animal research developed in laboratory settings, extensive epidemiological literature on depression has demonstrated a significant role for specific environmental factors leading to depression in humans. Interestingly, environmental factors typically associated with adult depression, such as early stressful experiences, have recently been suggested in a literature review as potential modifiers of the cerebellar functionality (Blanco, et al., 2015).

Overall, these results indicate that the non-genetic factors leading to depression alter the cerebellar synchronization. They also point out that different resting-state cerebral phenotypes –extracted using different time-series analysis techniques– may or not be linked to particular behaviors. When examining the neurobiological correlates linking an environmental exposure with depression, it might be appropriate using the amplitude envelop of low-frequency resting-state fMRI BOLD oscillations to build biological networks from the cerebellum.

**Additional considerations**

The previous results suggest that the environment leading to depression modifies the cerebellar network. Similarly, according to these analyses, the familial influences on depression risk may not be related to cerebellar oscillatory coupling. Recent findings indicate that MZ co-twin resemblance –here denoted by the familial factors– is mostly due to genetic variation (Polderman, et al., 2015). Hence, the outcomes from this study may suggest a lack of association between the genetic load for depression and the cerebellar synchrony. Data on brain networks from resting-state fMRI suggest a genetic regulation of some functional connections between the cerebellum –as a single anatomical unit– and other brain regions (Glahn, et al., 2010). The present results cannot be directly compared with this evidence due to differences in parcellation schemes and time-series analysis techniques. Despite this, the studies may be complementary, since the results shown here only indicate that the phenotypic variance observed in depression due to the genes does not seem related to the genetic variance responsible of cerebellar resting-state activity.

It is also important noticing that a large extent of the brain network literature is based upon widespread anatomical parcellation schemes excluding the cerebellum (Desikan, et al., 2006; Tzourio-Mazoyer, et al., 2002), and high-resolution fMRI scans are needed in order to map all its subdivisions correctly. Thus, many literature reports do not evaluate cerebellar regions when studying resting-state fMRI. Having included 26 cerebellar ROIs as the very focus of this study may have improved the specificity of the findings.

Lastly, some limitations of this study should be mentioned. First, the sample size was relatively small. However, having found statistically sound associations may suggest the existence of relatively robust effects. Also, the parcellation scheme used to derive the brain connectivity matrices was built upon the 26 cerebellar ROIs from the AAL atlas. Consequently, these results are not directly comparable with independent studies using other parcellation schemes. Although it is an important point, this issue is not specific of the current report. The choice of parcellation schemes is a key subject with enormous consequences for brain connectomics (de Reus and van den Heuvel, 2013). Future studies may combine finer-grained parcellations with higher-resolution neuroimaging scans.

**Acknowledgements**

**Conflict of Interest**

The authors declare that they have no conflict of interest.

## References

Achard, S., Salvador, R., Whitcher, B., Suckling, J., Bullmore, E. (2006) A resilient, low-frequency, small-world human brain functional network with highly connected association cortical hubs. The Journal of neuroscience : the official journal of the Society for Neuroscience, 26:63-72.

Andreou, C., Nolte, G., Leicht, G., Polomac, N., Hanganu-Opatz, I.L., Lambert, M., Engel, A.K., Mulert, C. (2014) Increased Resting-State Gamma-Band Connectivity in First-Episode Schizophrenia. Schizophrenia bulletin.

Anticevic, A., Hu, S., Zhang, S., Savic, A., Billingslea, E., Wasylink, S., Repovs, G., Cole, M.W., Bednarski, S., Krystal, J.H., Bloch, M.H., Li, C.S., Pittenger, C. (2014) Global resting-state functional magnetic resonance imaging analysis identifies frontal cortex, striatal, and cerebellar dysconnectivity in obsessive-compulsive disorder. Biological psychiatry, 75:595-605.

Azevedo, F.A., Carvalho, L.R., Grinberg, L.T., Farfel, J.M., Ferretti, R.E., Leite, R.E., Jacob Filho, W., Lent, R., Herculano-Houzel, S. (2009) Equal numbers of neuronal and nonneuronal cells make the human brain an isometrically scaled-up primate brain. The Journal of comparative neurology, 513:532-41.

Begg, M.D., Parides, M.K. (2003) Separation of individual-level and cluster-level covariate effects in regression analysis of correlated data. Statistics in medicine, 22:2591-602.

Bernard, J.A., Dean, D.J., Kent, J.S., Orr, J.M., Pelletier-Baldelli, A., Lunsford-Avery, J.R., Gupta, T., Mittal, V.A. (2014) Cerebellar networks in individuals at ultra high-risk of psychosis: impact on postural sway and symptom severity. Human brain mapping, 35:4064-78.

Billeci, L., Sicca, F., Maharatna, K., Apicella, F., Narzisi, A., Campatelli, G., Calderoni, S., Pioggia, G., Muratori, F. (2013) On the application of quantitative EEG for characterizing autistic brain: a systematic review. Frontiers in human neuroscience, 7:442.

Blanco, L., Nydegger, L.A., Camarillo, G., Trinidad, D.R., Schramm, E., Ames, S.L. (2015) Neurological changes in brain structure and functions among individuals with a history of childhood sexual abuse: A review. Neuroscience and biobehavioral

reviews, 57:63-69.

Calhoun, V.D., Liu, J., Adali, T. (2009) A review of group ICA for fMRI data and ICA for joint inference of imaging, genetic, and ERP data. NeuroImage, 45:S163-72.

Carlin, J.B., Gurrin, L.C., Sterne, J.A., Morley, R., Dwyer, T. (2005) Regression models for twin studies: a critical review. International journal of epidemiology, 34:1089-99.

Caspi, A., Moffitt, T.E. (2006) Gene-environment interactions in psychiatry: joining forces with neuroscience. Nature reviews. Neuroscience, 7:583-90.

Córdova-Palomera, A. 2015. mztwinreg: Regression Models for Monozygotic Twin Data.

Cordova-Palomera, A., Tornador, C., Falcon, C., Bargallo, N., Nenadic, I., Deco, G., Fananas, L. (2015) Altered amygdalar resting-state connectivity in depression is explained by both genes and environment. Human brain mapping.

de Reus, M.A., van den Heuvel, M.P. (2013) The parcellation-based connectome: limitations and extensions. NeuroImage, 80:397-404.

De Vico Fallani, F., Richiardi, J., Chavez, M., Achard, S. (2014) Graph analysis of functional brain networks: practical issues in translational neuroscience. Philosophical transactions of the Royal Society of London. Series B, Biological sciences, 369.

Derogatis, L.R., Melisaratos, N. (1983) The Brief Symptom Inventory: an introductory report. Psychological medicine, 13:595-605.

Desikan, R.S., Segonne, F., Fischl, B., Quinn, B.T., Dickerson, B.C., Blacker, D., Buckner, R.L., Dale, A.M., Maguire, R.P., Hyman, B.T., Albert, M.S., Killiany, R.J. (2006) An automated labeling system for subdividing the human cerebral cortex on MRI scans into gyral based regions of interest. NeuroImage, 31:968-80.

Douw, L., Schoonheim, M., Landi, D., Van der Meer, M., Geurts, J., Reijneveld, J., Klein, M., Stam, C. (2011) Cognition is related to resting-state small-world network topology: an magnetoencephalographic study. Neuroscience, 175:169-177.

Duncan, L.E., Keller, M.C. (2011) A critical review of the first 10 years of candidate gene-by-environment interaction research in psychiatry. The American journal of psychiatry, 168:1041-9.

Dutta, A., McKie, S., Deakin, J.F. (2014) Resting state networks in major depressive disorder. Psychiatry research, 224:139-151.

E, K.H., Chen, S.H., Ho, M.H., Desmond, J.E. (2014) A meta-analysis of cerebellar contributions to higher cognition from PET and fMRI studies. Human brain mapping, 35:593-615.

Evans, A.C., Collins, D.L., Mills, S., Brown, E., Kelly, R., Peters, T.M. (3D statistical neuroanatomical models from 305 MRI volumes). In; 1993. IEEE. p 1813-1817.

First, M.B. (1997) Structured clinical interview for DSM-IV axis I disorders : SCID - I : clinician version : administration booklet. Washington, D.C. American Psychiatric Press.

Foti, F., Laricchiuta, D., Cutuli, D., De Bartolo, P., Gelfo, F., Angelucci, F., Petrosini, L. (2011) Exposure to an enriched environment accelerates recovery from cerebellar lesion. Cerebellum, 10:104-19.

Fox, M.D., Snyder, A.Z., Vincent, J.L., Corbetta, M., Van Essen, D.C., Raichle, M.E. (2005) The human brain is intrinsically organized into dynamic, anticorrelated functional networks. Proceedings of the National Academy of Sciences of the United States of America, 102:9673-8.

Freeman, H.L., Stansfeld, S.A. (2008) The impact of the environment on psychiatric disorder. London ; New York. Routledge. x, 330 p. p.

Fries, P. (2005) A mechanism for cognitive dynamics: neuronal communication through neuronal coherence. Trends in cognitive sciences, 9:474-80.

Fries, P. (2009) Neuronal gamma-band synchronization as a fundamental process in cortical computation. Annual review of neuroscience, 32:209-24.

Friston, K.J., Holmes, A.P., Poline, J.B., Grasby, P.J., Williams, S.C., Frackowiak, R.S., Turner, R. (1995) Analysis of fMRI time-series revisited. NeuroImage, 2:45-53.

Fu, Y., Ma, Z., Hamilton, C., Liang, Z., Hou, X., Ma, X., Hu, X., He, Q., Deng, W., Wang, Y., Zhao, L., Meng, H., Li, T., Zhang, N. (2015) Genetic influences on resting-state functional networks: A twin study. Human brain mapping.

Glahn, D.C., Knowles, E.E., McKay, D.R., Sprooten, E., Raventos, H., Blangero, J., Gottesman, II, Almasy, L. (2014) Arguments for the sake of endophenotypes: examining common misconceptions about the use of endophenotypes in psychiatric genetics. American journal of medical genetics. Part B, Neuropsychiatric genetics : the official publication of the International Society of Psychiatric Genetics,

165B:122-30.

Glahn, D.C., Winkler, A.M., Kochunov, P., Almasy, L., Duggirala, R., Carless, M.A., Curran, J.C., Olvera, R.L., Laird, A.R., Smith, S.M., Beckmann, C.F., Fox, P.T., Blangero, J. (2010) Genetic control over the resting brain. Proceedings of the National Academy of Sciences of the United States of America, 107:1223-8.

Glerean, E., Salmi, J., Lahnakoski, J.M., Jaaskelainen, I.P., Sams, M. (2012) Functional magnetic resonance imaging phase synchronization as a measure of dynamic functional connectivity. Brain connectivity, 2:91-101.

Gottesman, II, Gould, T.D. (2003) The endophenotype concept in psychiatry: etymology and strategic intentions. The American journal of psychiatry, 160:636-45.

Greenough, W.T., McDonald, J.W., Parnisari, R.M., Camel, J.E. (1986) Environmental conditions modulate degeneration and new dendrite growth in cerebellum of senescent rats. Brain research, 380:136-43.

Guggisberg, A.G., Rizk, S., Ptak, R., Di Pietro, M., Saj, A., Lazeyras, F., Lovblad, K.O., Schnider, A., Pignat, J.M. (2014) Two Intrinsic Coupling Types for Resting-State Integration in the Human Brain. Brain topography.

Guilherme, R., Drunat, S., Delezoide, A.L., Oury, J.F., Luton, D. (2009) Zygosity and chorionicity in triplet pregnancies: new data. Human reproduction, 24:100-5.

Guo, W., Liu, F., Liu, J., Yu, L., Zhang, Z., Zhang, J., Chen, H., Xiao, C. (2013a) Is there a cerebellar compensatory effort in first-episode, treatment-naive major depressive disorder at rest? Progress in neuro-psychopharmacology & biological psychiatry, 46:13-8.

Guo, W., Liu, F., Xue, Z., Gao, K., Liu, Z., Xiao, C., Chen, H., Zhao, J. (2013b) Abnormal resting-state cerebellar-cerebral functional connectivity in treatment-resistant depression and treatment sensitive depression. Progress in neuro-psychopharmacology & biological psychiatry, 44:51-7.

Guo, W.B., Liu, F., Xue, Z.M., Xu, X.J., Wu, R.R., Ma, C.Q., Wooderson, S.C., Tan, C.L., Sun, X.L., Chen, J.D., Liu, Z.N., Xiao, C.Q., Chen, H.F., Zhao, J.P. (2012) Alterations of the amplitude of low-frequency fluctuations in treatment-resistant and treatment-response depression: a resting-state fMRI study. Progress in neuro-psychopharmacology & biological psychiatry, 37:153-60.

Harrel, F. 2013. rms: Regression Modeling Strategies.

Huang, S. (2014) When correlation and causation coincide. BioEssays : news and reviews in molecular, cellular and developmental biology, 36:1-2.

Jenkins, G.M., Watts, D.G. (1968) Spectral analysis and its applications. San Francisco,. Holden-Day. xviii, 525 p. p.

Kaiser, R.H., Andrews-Hanna, J.R., Wager, T.D., Pizzagalli, D.A. (2015) Large-Scale Network Dysfunction in Major Depressive Disorder: A Meta-analysis of Resting-State Functional Connectivity. JAMA psychiatry, 72:603-11.

Kendler, K.S., Hettema, J.M., Butera, F., Gardner, C.O., Prescott, C.A. (2003) Life event dimensions of loss, humiliation, entrapment, and danger in the prediction of onsets of major depression and generalized anxiety. Archives of general psychiatry, 60:789-96.

Kucyi, A., Hove, M.J., Biederman, J., Van Dijk, K.R., Valera, E.M. (2015) Disrupted functional connectivity of cerebellar default network areas in attention-deficit/hyperactivity disorder. Human brain mapping, 36:3373-86.

Lee, M.H., Smyser, C.D., Shimony, J.S. (2013) Resting-state fMRI: a review of methods and clinical applications. AJNR. American journal of neuroradiology, 34:1866-72.

Lundberg, A. (1998) The environment and mental health : a guide for clinicians. Mahwah, N.J. Lawrence Erlbaum Associates. xi, 233 p. p.

Lynn, R., Meisenberg, G. (2010) National IQs calculated and validated for 108 nations. Intelligence, 38:353-360.

Moffitt, T.E., Caspi, A., Harrington, H., Milne, B.J., Melchior, M., Goldberg, D., Poulton, R. (2007) Generalized anxiety disorder and depression: childhood risk factors in a birth cohort followed to age 32. Psychological medicine, 37:441-52.

Morel, M.P., Dusart, I., Sotelo, C. (2002) Sprouting of adult Purkinje cell axons in lesioned mouse cerebellum: "non-permissive" versus "permissive" environment. Journal of neurocytology, 31:633-47.

Mosing, M.A., Gordon, S.D., Medland, S.E., Statham, D.J., Nelson, E.C., Heath, A.C., Martin, N.G., Wray, N.R. (2009) Genetic and environmental influences on the co-morbidity between depression, panic disorder, agoraphobia, and social phobia: a twin study. Depression and anxiety, 26:1004-11.

O'Reilly, J.X., Beckmann, C.F., Tomassini, V., Ramnani, N., Johansen-Berg, H. (2010) Distinct and overlapping functional zones in the cerebellum defined by resting state functional connectivity. Cerebral cortex, 20:953-65.

Oathes, D.J., Patenaude, B., Schatzberg, A.F., Etkin, A. (2015) Neurobiological signatures of anxiety and depression in resting-state functional magnetic resonance imaging. Biological psychiatry, 77:385-93.

Pannekoek, J.N., van der Werff, S.J., van Tol, M.J., Veltman, D.J., Aleman, A., Zitman, F.G., Rombouts, S.A., van der Wee, N.J. (2015) Investigating distinct and common abnormalities of resting-state functional connectivity in depression, anxiety, and their comorbid states. European neuropsychopharmacology : the journal of the European College of Neuropsychopharmacology.

Polderman, T.J., Benyamin, B., de Leeuw, C.A., Sullivan, P.F., van Bochoven, A., Visscher, P.M., Posthuma, D. (2015) Meta-analysis of the heritability of human traits based on fifty years of twin studies. Nature genetics, 47:702-9.

Ponce-Alvarez, A., Deco, G., Hagmann, P., Romani, G.L., Mantini, D., Corbetta, M. (2015) Resting-state temporal synchronization networks emerge from connectivity topology and heterogeneity. PLoS computational biology, 11:e1004100.

Power, J.D., Mitra, A., Laumann, T.O., Snyder, A.Z., Schlaggar, B.L., Petersen, S.E. (2014) Methods to detect, characterize, and remove motion artifact in resting state fMRI. NeuroImage, 84:320-41.

R Development Core Team. 2011. R: A Language and Environment for Statistical Computing. Vienna, Austria: R Foundation for Statistical Computing.

Ressler, K.J., Mayberg, H.S. (2007) Targeting abnormal neural circuits in mood and anxiety disorders: from the laboratory to the clinic. Nature neuroscience, 10:1116-24.

Richiardi, J., Eryilmaz, H., Schwartz, S., Vuilleumier, P., Van De Ville, D. (2011) Decoding brain states from fMRI connectivity graphs. NeuroImage, 56:616-26.

Ruiperez, M., Ibáñez, M.I., Lorente, E., Moro, M., Ortet, G. (2001) Psychometric properties of the Spanish version of the BSI: Contributions to the relationship between personality and psychopathology. Eur J Psychol Assess, 17:241.

Sattler, J.M. (2001) Assessment of children: cognitive applications. San Diego. J.M. Sattler.

Schwarz, A.J., McGonigle, J. (2011) Negative edges and soft thresholding in complex

network analysis of resting state functional connectivity data. NeuroImage, 55:1132-46.

Shannon, C.E. (1997) The mathematical theory of communication. 1963. M.D. computing : computers in medical practice, 14:306-17.

Smith, S.M., Vidaurre, D., Beckmann, C.F., Glasser, M.F., Jenkinson, M., Miller, K.L., Nichols, T.E., Robinson, E.C., Salimi-Khorshidi, G., Woolrich, M.W., Barch, D.M., Ugurbil, K., Van Essen, D.C. (2013) Functional connectomics from resting-state fMRI. Trends in cognitive sciences, 17:666-82.

Sokunbi, M.O., Fung, W., Sawlani, V., Choppin, S., Linden, D.E., Thome, J. (2013) Resting state fMRI entropy probes complexity of brain activity in adults with ADHD. Psychiatry research, 214:341-8.

Stamoulis, C., Gruber, L.J., Chang, B.S. (2010) Network dynamics of the epileptic brain at rest. Conference proceedings : ... Annual International Conference of the IEEE Engineering in Medicine and Biology Society. IEEE Engineering in Medicine and Biology Society. Conference, 2010:150-3.

Sui, J., Adali, T., Pearlson, G.D., Calhoun, V.D. (2009) An ICA-based method for the identification of optimal FMRI features and components using combined group-discriminative techniques. NeuroImage, 46:73-86.

Sullivan, P.F., Neale, M.C., Kendler, K.S. (2000) Genetic epidemiology of major depression: review and meta-analysis. The American journal of psychiatry, 157:1552-62.

Tzourio-Mazoyer, N., Landeau, B., Papathanassiou, D., Crivello, F., Etard, O., Delcroix, N., Mazoyer, B., Joliot, M. (2002) Automated anatomical labeling of activations in SPM using a macroscopic anatomical parcellation of the MNI MRI single-subject brain. NeuroImage, 15:273-89.

van den Heuvel, M.P., Hulshoff Pol, H.E. (2010) Exploring the brain network: a review on resting-state fMRI functional connectivity. European neuropsychopharmacology : the journal of the European College of Neuropsychopharmacology, 20:519-34.

Van Overwalle, F., D'Aes, T., Marien, P. (2015) Social cognition and the cerebellum: A meta-analytic connectivity analysis. Human brain mapping.

Vazquez-Sanroman, D., Sanchis-Segura, C., Toledo, R., Hernandez, M.E., Manzo, J.,

Miquel, M. (2013) The effects of enriched environment on BDNF expression in the mouse cerebellum depending on the length of exposure. Behavioural brain research, 243:118-28.

Villain, N., Fouquet, M., Baron, J.C., Mezenge, F., Landeau, B., de La Sayette, V., Viader, F., Eustache, F., Desgranges, B., Chetelat, G. (2010) Sequential relationships between grey matter and white matter atrophy and brain metabolic abnormalities in early Alzheimer's disease. Brain : a journal of neurology, 133:3301-14.

Wang, L., Song, M., Jiang, T., Zhang, Y., Yu, C. (2011) Regional homogeneity of the resting-state brain activity correlates with individual intelligence. Neuroscience letters, 488:275-8.

Wechsler, D., Cordero Pando, A., Yela Granizo, M., Zimmerman, I.L., Woo-Sam, J.M., Glasser, A.J. (1997) WAIS escala de inteligencia de Wechsler para adultos. Madrid ; Barcelona. TEA Ediciones.

Wittchen, H.U., Kessler, R.C., Beesdo, K., Krause, P., Hofler, M., Hoyer, J. (2002) Generalized anxiety and depression in primary care: prevalence, recognition, and management. The Journal of clinical psychiatry, 63 Suppl 8:24-34.

Zalesky, A., Fornito, A., Bullmore, E.T. (2010) Network-based statistic: identifying differences in brain networks. NeuroImage, 53:1197-207.

Zbozinek, T.D., Rose, R.D., Wolitzky-Taylor, K.B., Sherbourne, C., Sullivan, G., Stein, M.B., Roy-Byrne, P.P., Craske, M.G. (2012) Diagnostic overlap of generalized anxiety disorder and major depressive disorder in a primary care sample. Depression and anxiety, 29:1065-71.

Zhang, Z., Liao, W., Wang, Z., Xu, Q., Yang, F., Mantini, D., Jiao, Q., Tian, L., Liu, Y., Lu, G. (2014) Epileptic discharges specifically affect intrinsic connectivity networks during absence seizures. Journal of the neurological sciences, 336:138-45.

## Figure legends

**Figure I.** Schematic representation of the construction of three functional networks for one cerebellum.

A: The 210 resting-state fMRI volumes (slices) are co-registered to the anatomical T1 3D reference volume, and each voxel is mapped to one of the 116 ROIs in the AAL atlas (including the cerebellum). B: The anatomical atlas allows segmenting the brain into 90 cerebral and 26 cerebellar ROIs, and after artefact removal, a time series of the mean (BOLD) activation probability for each of the 116 ROIs is obtained. C: For each ROI, a raw time series is retrieved using the 210 fMRI slices acquired through 9:56 minutes of scan. D: A band-pass filter is applied to obtain the resting-state fMRI narrowband signal (0.04 - 0.07 Hz). E: The amplitude envelope of each band-passed wave is estimated for later analysis. F: Similarly, the Hilbert transform also allows calculating the instantaneous phase of the waves. G, H, I: Three partial correlation matrices are obtained from the previous time-series (band-passed and Hilbert-transformed amplitude envelope and phase); they are z-transformed to normalize correlation values across individuals. Warm (cold) colours in these matrices represent large (small) correlation values between ROIs. The left tail of these correlation matrices (i.e., edges with negative z-scores) are set to 0 following a soft-thresholding procedure. J, K, L: Graph-theoretical measures of edge weight are obtained for each pair of cerebellar regions, to be analyzed using NBS.

**Figure II.** Environmental factors associated with depression risk are linked to cerebellar synchronization disruptions.

A: The amplitude envelope obtained from the Hilbert-transformed resting-state signal allowed identifying a functional network in the cerebellum potentially altered due to environmental liability for depression. B: A cerebellar synchronization sub-network comprising seven edges, built from oscillatory amplitude envelopes, was shown altered by the NBS approach. C: There are marked network edge differences across individuals depending on environmental risk liability for depression. The leftmost plot corresponds to low environmental risk –averaged from five healthy co-twins from discordant pairs–, the plot in the middle depicts subjects with average environmental risk –average of five brains from randomly chosen concordant and healthy pairs–, and the rightmost plot shows participants with high environmental liability –five affected co-twins from discordant pairs–. D: The barplot shows the mean and standard deviations of the total edge weights of the seven-edge network across the different environmental depression liabilities (red: low environmental risk; green: regular environmental risk; blue: high environmental risk). The values in the bars were retrieved by residualizing regression procedures from all 48 individuals, adjusting by age, gender and familial depression liability.

**Table I.** Demographic, psychopathological and neurocognitive data for DSM-IV diagnostic concordant, discordant and healthy MZ twin pairs.

*Notes:* SD, standard deviation; IQ, intellectual quotient; BSI, Brief Symptom Inventory; [a], Kruskal-Wallis X-squared, as these variables were continuous; *, statistically significant *p*-value.

| | CONCORDANT (12 subjects, 10 female) | | DISCORDANT (16 subjects, 10 female) | | HEALTHY (20 subjects, 8 female) | | Group comparison |
|---|---|---|---|---|---|---|---|
| | Mean (SD) | Range | Mean (SD) | Range | Mean (SD) | Range | X-squared[a]; *p* |
| **Age** | 42.5 (13) | 22-54 | 37 (10.9) | 20-50 | 30.3 (7.3) | 19-39 | 5.9; 0.052 |
| **IQ** | 105.1 (12.5) | 87-127 | 108.1 (11.8) | 87-131 | 110.5 (5.5) | 103-118 | 1.9; 0.393 |
| **Current psycho-pathology (total BSI)** | 27.9 (16.5) | 6-57 | 20.9 (13.3) | 4-45 | 10.6 (9.3) | 1-33 | 8.7; 0.013* |
| **Current depressive symptoms** | 6.9 (6.5) | 1-20 | 3.5 (2.7) | 0-9 | 1.7 (1.8) | 0-6 | 6.4; 0.04* |

**Table II.** Edge-based parameters describing the twenty-six-node cerebellar networks.

Three different approaches were used to build fMRI connectivity networks. First, the amplitude correlation method for band-passed low-frequency oscillations (a) (Smith, et al., 2013); afterward, the Hilbert-transformed signal allowed extracting the amplitude envelope (b) and the instantaneous phase (c) correlation methods (Glerean, et al., 2012; Guggisberg, et al., 2014). The results indicate edge weights considering both the connected network component, removing all zero entries of the matrix (d), and all edges accounting for the zeroed matrix entries (e). S.D., standard deviation.

| | INDIVIDUAL LEVEL | | | | | |
|---|---|---|---|---|---|---|
| | *Conventional (amplitude correlation)[a]* | | *Amplitude envelope correlation[b]* | | *Instantaneous phase correlation[c]* | |
| | *Mean (S.D.)* | *Range* | *Mean (S.D.)* | *Range* | *Mean (S.D.)* | *Range* |
| **Total edge weight** | 53.69 (4.51) | 45.75-64.55 | 31.54 (2.18) | 27.71-36.47 | 21.67 (2.13) | 16.52-27.41 |
| **Average edge weight (connected)[d]** | 0.31 (0.03) | 0.25-0.39 | 0.18 (0.01) | 0.16-0.21 | 0.12 (0.01) | 0.1-0.16 |
| **Average edge weight (all cells)[e]** | 0.16 (0.01) | 0.13-0.19 | 0.09 (0.01) | 0.08-0.11 | 0.06 (0.01) | 0.05-0.08 |
| **Maximum edge weight** | 1.12 (0.23) | 0.79-2.21 | 0.81 (0.51) | 0.54-3.94 | 0.57 (0.22) | 0.36-1.87 |
| | INTRAPAIR DIFFERENCES | | | | | |
| | *Spearman's Rho* | *p-value* | *Spearman's Rho* | *p-value* | *Spearman's Rho* | *p-value* |
| **Total edge weight** | -0.14 | 0.5 | 0.09 | 0.66 | 0.25 | 0.25 |
| **Average edge weight (connected)** | -0.17 | 0.42 | 0.28 | 0.19 | 0.25 | 0.25 |
| **Average edge weight (all cells)** | -0.38 | 0.07 | 0.15 | 0.48 | -0.07 | 0.73 |
| **Maximum edge weight** | -0.14 | 0.5 | 0.09 | 0.66 | 0.25 | 0.25 |
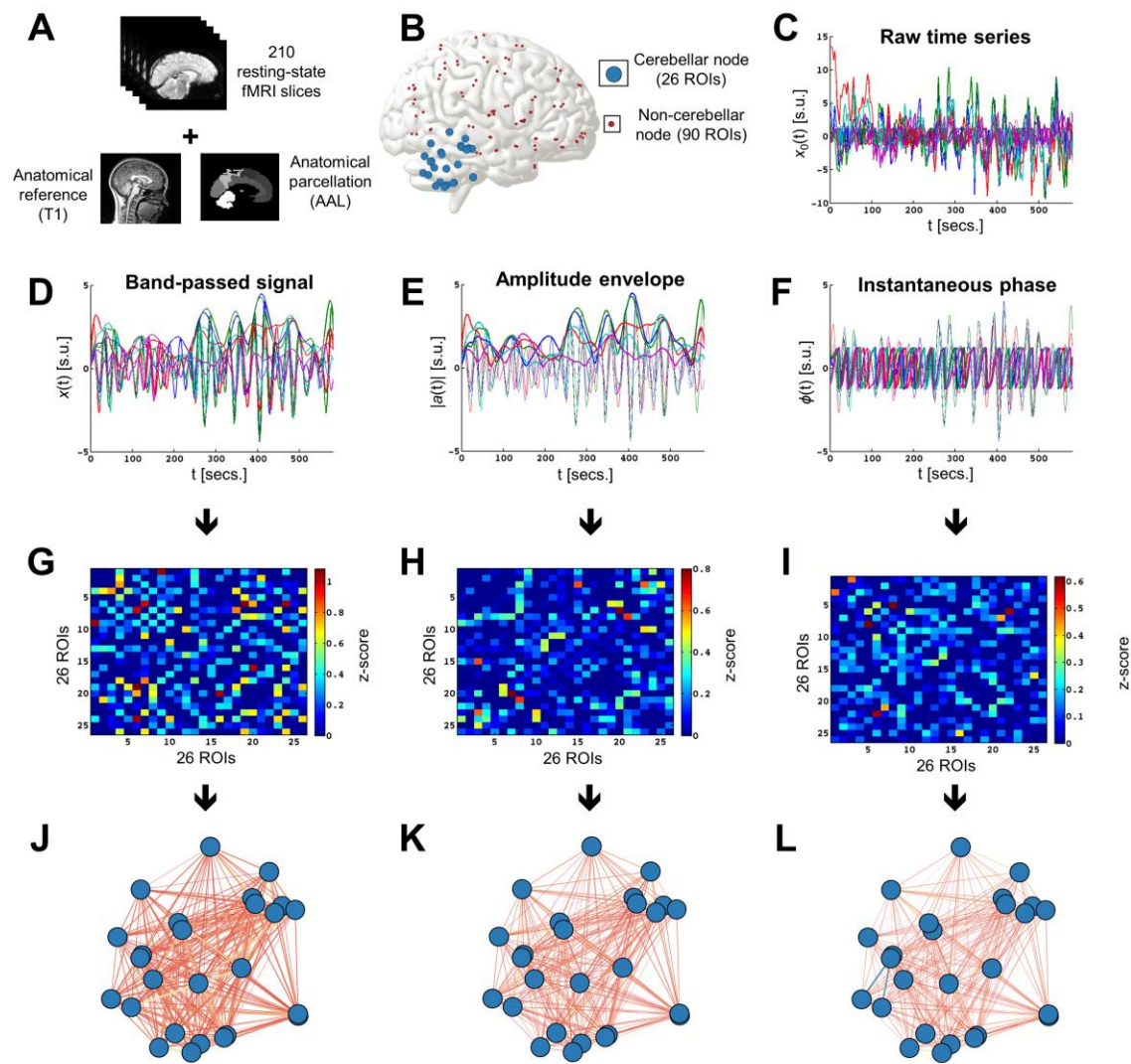
**Figure 1**

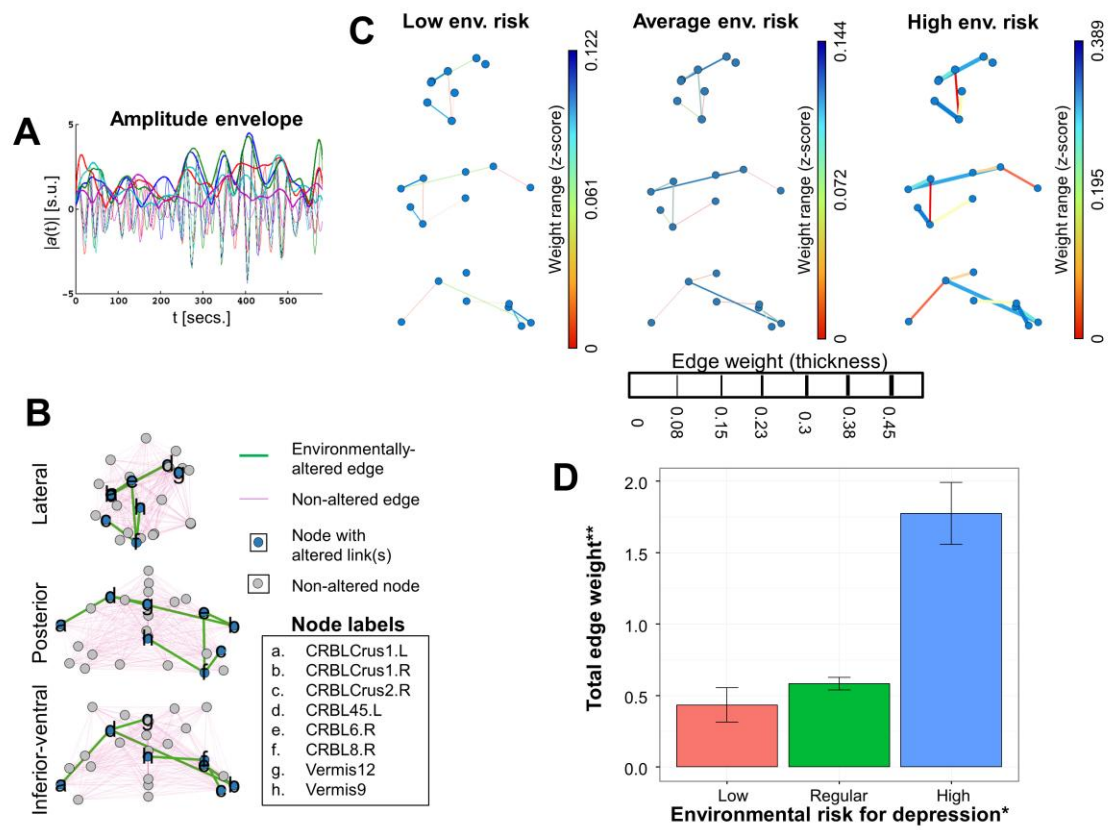**Figure 2**

Rs-fMRI has become a noninvasive powerful tool to discover possible anomalies in brain connectivity patterns in patients with mental health disorders. The ongoing fluctuations in resting-state condition might reflect an evolutionarily conserved aspect of cerebral organization (Vincent JL et al. 2007). This could be closely related to an underlying anatomical structural connectivity (review Gustavo Deco, Viktor K. Jirsa and Anthony R. Mcintosh 2011). However, rs-fMRI studies have still not been part of the clinical routine, mostly because of certain inconsistencies among studies about mental health disorders.

As far as MDD is concerned, different studies have presented inconsistencies in the whole brain functional connectivity (Berman et al. 2014; Guo et al. 2011; Li Wang et al. 2013) as well as in the functional connectivity between areas of specific brain networks (cognitive control and affective network: Sheline et al. 2010; DMN discrepancies: Xueling Zhu et al. 2012; Grecius et al. 2007; Marc G. Berman et al. (2011), Zhou et al. (2010); Sheline et al. 2010).

Most of the studies on rs-fMRI data evaluate the clinical phenomenon of MDD from measurements based on averaged measures such as the correlation coefficient that exists among BOLD time series of the different brain regions. The fact that correlation is a global measure on the whole temporal series masks temporal aspects of FC which could be key to an efficient transmission of the information between brain regions.

In this sense, previous studies suggested that organized networks, such as the DMN or areas involved in memory processes, would be coordinated for temporary adjustments embedded in BOLD signals. That is the reason why a static approach does not seem to be satisfactory for a complete characterization of Resting State Networks - RSNs-(Catherine et al. 2004; Catie Chang and Gary H. Glover 2010).

Chapters 1 and 2 present an evaluation of both static and dynamic features of time series regarding rs-fMRI data obtained from patients with MDD. These results demonstrate the coexistence of abnormalities in both dynamic and static aspects of the BOLD signal at rest in patients with major depression. This suggests two levels of alteration in the functional connectivity of depressed people. More specifically, it is suggested in chapter 1 that the global increment of synchronism observed in patients could be due to local modifications of the connectivity between specific regions of the DMN and FPN. Changes in behavioral patterns among these regions could induce alterations of global signals in these networks at least. The study is subsequently

extended in chapter 2, where the contribution of static and dynamic factors to the building of activity in RSNs is evaluated in relation to clinical depression activity via network descriptors (measures which estimate the efficiency features and structural characteristics of the network connectivity).

More specifically, the results of chapter 1 show that patients with MDD present an amplification of global synchronization at the level of the whole brain. Furthermore, the patients show an increment of overall average functional connectivity (static FC, sFC) among regions of the DMN, and a loss of variability in functional connectivity (dynamic FC, vFC) among specific regions of the FPN and DMN.

This suggests that these anomalies discovered in certain regions of the DMN and FPN could trigger in some way in this amplification in the global synchronization in MDD. Moreover, we discover that the average BOLD signal in parietal and OPFC regions fluctuates with the global average signal and shows correlation with global synchronization patterns. This observation seems to reveal consistency with recent studies where clinical implications of global signal fluctuations are demonstrated (Yang et al. 2014).

In chapter 2, the results expose structural changes in the functional connectivity of the DMN, specially in its posterior part, of the FPL and FPN networks. These alterations could trigger depressive traits such as: maladaptive, high level of rumination, brooding, overgeneral autobiographical or episodic memories, negative emotional judgment and anxiety problems.

More specifically, a hyperconnectivity, together with a loss of variability in phase-coupling (inflexibility/rigidity in the phase in the resting-state oscillations), is observed between the posterior (Posterior cingulate cortex, Pre/Cuneus and Angular regions) and the anterior part of the brain (mPFC, OPFC and ACC) , specially among the DMN areas. Besides, if we consider that the severity level (HDRS) and the age of onset of the disorder are directly correlated with the network descriptors which characterize these two areas, we can estimate that patients with MDD present a gradual disconnection between these two parts of the brain producing a gradual increment of rumination and brooding. In previous studies, the hyperconnectivity in DMN has been associated to a gradual process of hypogyrification in these areas in MDD. This supports the idea of vulnerability at a biological level in front of depression (N.L Nixon et al. 2014). If that were the case, it would indicate that patients with high severity levels of the disorder, or who remain in high states of depression could be more likely to

suffer from the disorder again. However, additional studies are necessary to confirm this hypothesis.

Moreover, these disruptions are specially intense between regions of the posterior part of the brain (Angular, Precuneus and PCC areas) and the hippocampal-thalamic pathway. It suggests that this hub could provoke an abnormal inhibitory control of negative episodic memories (Grecius et al. 2009) and overgeneral AM (X. Zhu et al. 2012; Cavanna & Trimble, 2006; Hassabis, Kumaran, and Maguire, 2007) in depressed people. This fact also seems to show a connection with depressive rumination (Catherine Crane et al. 2007).

The strong loss of variability in phase-coupling between interhemispheric areas in the DN (OPFC and DLPFC) is another alteration which has been shown in this chapter, and which seems to be relevant a priori in the characterization of MDD and may explain part of the clinical heterogeneity that this disorder presents. Previous studies have analyzed these areas as another important hub involved in depressive traits, precisely in the codification of negative emotional judgment and anxiety problems (Sheline et al. 2010; Simone Grimm et al. 2008; Joseph L. Price and Wayne C. Drevets 2009).

Finally, a decrease of the dispersion index of phase-coupling (IDP) is also observed among FPN areas in patients with MDD. This could produce an ineffective transmission of the information between the executive cortical network and intra/parietal regions, with the DMN (Aneta Brzezicka 2013). Besides, other studies suggest that this type of inflexibility in FC in MDD could be responsible for maladaptive control and problems in the control of cognitive faculties (Nico U. F. Dosenbach et al. 2007).

However, we observe that clinical depressive phenomenons such as the level of depression, length of the episode, total number of episodes and initial age of the first depressive episode can be partially explained by the combination of static and dynamic network descriptors on these components (networks, RSN) in resting-state condition.

In this sense, the results show that both the HDRS and the age of onset of depression can be partially predicted from network descriptors of the PFL and posterior DMN. In chapter 1, the existence of fluctuations in the OPFC and parietal regions was already observed, and it was correlated with the global synchronization signal. This suggests that the global synchronization patterns of depression could exist in components of the DMN and PFL. They might be caused by altered BOLD signals in

specific regions such as the mPFC, ACC, OPFC, Precuneus, Angular, PCC. Furthermore, previous studies have demonstrated the existence of a strong association between the HDRS and the level of rumination in patients with depression (Hoekseman Susan 2000). Consequently, it can also be assumed that these global patterns located in the posterior DMN and PFL could be reflected in some way in the severity level of the disorder, and thus could be used as prognostic markers for patients with MDD.

Moreover, patients suffering from major depression show structural changes in the functional connectivity of the right FPN which, together with efficiency problems in the functional connectivity found in the PF area on the one hand and the posterior part of the DMN on the other hand, seem to enable a partial explanation about the length of depression or the total number of depressive episodes, respectively. This suggests that the length of an episode in major depression could be a phenotype resulting from the static and dynamic anomalies found in functional connectivity between PF and FPN regions. Michael D. Grecius et al (2007) observed in his study a certain positive correlation between the length and the signal in the ACC region. However, the total number of depressive episodes could be explained by the alterations found in regions of the posterior part of DMN and FPN. All this leads us to the idea that an unbalanced information-processing in the FPN might trigger difficulties in breaking of depressive rumination (Donaldson, Lam and Mathews, 2007; Burwell and Shirk, 2007; Joormann, 2006). In this sense, Ernst H. W. Koster et al. (review, 2010) suggested programs to improve attentional control as a protective effect in at-risk patients.

Finally, the results also indicate that the length of depression may be correlated with the level of anxiety of the patient or with negative emotional judgment traits where the serotonin transporter (SERT) would possibly be involved (Ramin V. Parsey et al. 2006). However, the total number of depressive episodes in patients could be more connected with an accumulation of impairment of memory performance (Philip Gorwood et al. 2008). The selection of negative autobiographical memories could be due to problems of inability to inhibit the attention towards negative episodic past events (review Cristiano A. Köhler et al. 2015: C. Lemogne et al. 2006; G. G. Lloyd and W. A. Lishman et al. 1975). These inhibitory problems could be caused by hyperconnectivity between the posterior hub (PCC, Precunues, Angular cortices) and the Hippocampal-Thalamic pathway.

In previous studies, the SERT has been associated to genetic factors, increasing the risk of developing depression under stress (Caspi et al. in 2003). Besides, it might be

directly linked to a possible decrease of volume in the ACC region (Pezawas et al. 2005). In this sense, regions such as the amygdala, ACC, insula, hippocampus, dorsal raphe nuclei and mPFC have shown alterations in the metabolic activity of serotonin (Parsey RV et al. 2006; Wayne C. Drevets et al. 2009). Likewise, previous studies have demonstrated that structural alterations in the ACC, PFC or amygdala found in depression under stress might have some relation with a fall in the metabolic activity of serotonin (Joseph L. Price and Wayne C. Drevets, 2009), triggering dysfunctions among the limbic structures (Drevets et al. 2006) and problems in emotional expression and anxiety.

This suggests that these regions- the prefrontal and limbic parts (PFL)- could be especially sensitive to changes in the expression level of SERT. This could happen for a need of endogenous metabolism, which could trigger changes in the supply of serotonin within a stressful environment in individuals with genetic predisposition, provoking dysfunctions in connectivity between these regions and other brain systems. That is why these areas could play a certain role in the etiology of depression.

However, considering depression as a multifactorial mental disorder, to explain the incipient psychopathological mechanisms it would be necessary to clarify the relation between environmental and genetic factors on these regions. In other words, the influence of the environment and genes over alterations in particular areas would have to be analyzed.

As we commented before, the oingoing spontaneous fluctuations found in resting-state might unmask an intrinsic functional architecture reflecting an evolutionarily conserved aspect of brain organization. In studies performed on macaques, these fluctuations showed characteristics similar to those found in human beings (Vincent JL et al. 2007). Moreover, the fluctuations present patterns that would form complex organizations or networks which are likely to describe underlying structural connectivity (review Gustavo Deco, Viktor K. Jirsa and Anthony R. Mcintosh 2011). The basis of the working assumption we made in chapters 3 and 4 consists of considering that the BOLD signal with rs-fMRI techniques could embed both specific genetic traits and environment. It could be differentiated in order to design descriptors that could help to evaluate the influence of these factors in alterations in particular brain regions of patients with MDD.

More specifically in chapter 3, we explored the analytic components of the amygdalar resting-state activity due to its close relation with the SERT. However, in

chapter 4, we focus on cerebellar regions, as they can also constitute a key mechanism for psypopathology, specially with regards to depression liability and anxiety vulnerability. It also seems to be connected to large brain regions for its homeostatic regulation. For this second part of the study, we used a sample of 48 twins (24 monozygotic pairs) informative for depressive psychopathology (6 concordant, 8 discordant and 10 healthy control pairs). In order to extract these components from the rs-fMRI signal, we design descriptors that can evaluate not only the conventional signal but also other analytic components of this rs-fMRI activity.

The results concerning the amygdala show that both genes and environment would modify different patterns in the amygdala, and this would create problems of connectivity, increasing thus the risk of developing depression. Besides, we can see that analytic components and the amplitude envelope from band-pass time series (Hilber transform) elicit better the genetic relation between amygdala connectivity and depression. However, the findings from the study on the cerebellum indicate that some environmental factors in some regions of the vermis and crus may lead to depression. It could be observed analyzing the amplitude envelope of rs-fMRI oscillations. Non-genetic factors are thought to be a possible explanation of the strong influence of the environment on depressive liability (Sullivan et al. 2000). Furthermore, it has very recently been demonstrated that early stressful experiences could modify the cerebellar functionality (Blanco et al. 2015).

*CONCLUSION*

The main interest in this study was to gain insight into the ongoing fluctuations that might be exclusive in patients with depression by means of the BOLD signal in resting state. Some of them might unmask underlying structural anomalies which trigger depressive behaviors.

In the first part of this study, we have focused on discovering those altered depressive features in patients that could be susceptible of being considered as putative clinical markers for prognosis by using descriptors built from the brain activity at rest.

Assuming that both environment and genetic factors are key in the genesis of the depression, we explored more precisely the amygdala for its close relation with the serotonin transporter (SERT or 5-HTT), and cerebellum regions for their connection to large areas of the brain (for their homeostatic regulation) and relation with social anxiety, depression liability and anxiety vulnerability, using identical twins rs-fMRI data. The second part of this work thus focused on assessing the influence of genes and environment on analytic components of the rs-fMRI activity into these areas, in relation to depression risk. The main contributions of this study can be summarized as follows:

1. *The global synchronization and temporal stability were significantly increased in the group of patients with MDD.*

2. *Static and dynamic descriptors unmask anomalies in the Default Mode Network (DMN), specially in its posterior part: the PreFrontal-Limbic network (PFL) and FrontoParietal network (FPN) in patients with MDD.*

3. *The group suffering from MDD showed a significant increase in the overall average functional connectivity (static FC, hyperconnectivity), however a decrease of variability in phase-coupling among regions (dynamic FC) within the DMN was observed.*

4. *A general loss of variability in phase-coupling in connectivity exists among regions of the DMN, PFC and FP networks in the group of patients.*

5. *Static network descriptors of the PFL and right FP, and dynamic network descriptors of posterior DMN can be used to characterize MDD.*

6. *There is a possible disconnection between the anterior and posterior part of brain. It is specially noted in the DMN. The SFGdor, mPFC, ACC and ORB areas on the one hand, and the PCC, Precuneus and Angular on the other hand could be relevant pivote regions of the disconnection in MDD.*

7. *The alterations found in the posterior part of DMN might trigger episodic negative memories in patients.*

8. *The severity level of depression (HDRS) is strongly associated with local deficiencies in the functional connectivity among regions of the PFL such as the Orbitofrontal Cortex (OFC), Dorsolateral Prefrontal Cortex (DLPFC) and Anterior Cingulate Cortex (ACC) regions, as well as with global problems of efficiency on dynamic aspects of the activity in the posterior DMN area.*

9. *Both the length and total number of depressive episodes of patients seem to be related mainly with alterations in the functional connectivity between FP regions.*

10. *Both phase-coupling problems in the BOLD signal and possible underlying structural alterations seem to coexist within the DMN, PFL and FPN in patients with MDD. These might trigger depressive traits such as: maladaptive, high level of rumination, brooding, overgeneral autobiographical or episodic memories, negative emotional judgment and anxiety problems.*

11. *We hypothesize that the inflexibility in phase-coupling found in these RSNs might be connected somehow with the idea of a gradual process of hypogyrification, specially of the DMN, which might be directly proportional to the length of depression or its severity level (HDRS).*

12. *Both genes and the environment modify different patterns of the amygdala resting-state connectivity to increase depression risk.*

13. *The genetic relationship between amygdalar connectivity and depression may be better elicited by examining analytic components obtained from rs-fMRI BOLD signals.*

14. *Non-genetic factors leading to depression alter the cerebellar synchronization.*

15. *The alterations in depression, within cerebellar regions such as the crus and vermis that are lead by environmental factors may be observed using the amplitude envelop of low-frequency rs-fMRI BOLD oscillations. This suggests that the activity at rest in these regions could be associated with environmental liability.*

*LINES FOR FUTURE WORKS*

On the one hand, despite rs-fMRI can provide new insights on the functional architecture of the brain and the studies to date are promising- specially regarding prognosis and personalized monitoring of mental disorders for prevention and efficient treatment- it is still necessary to advance to use it during a clinic routine.

As we commented in the introduction, the functional connectivity matrix obtained from the BOLD signal with rs-fMRI techniques does not only show correlations between regions that have a direct structural connectivity (Michael D. Grecius et al. 2009), but also reveals certain correlations due to false positives or simply represents indirect connectivity by the synchronization of information among third regions which might cooperate in the same task execution (Jessica S. Damoiseaux and Michale D. Grecius 2009). Besides, correlations could exist because of the noise in rs-fMRI, or hemodynamic or vascular artifacts (Honey et al. 2009; Skudlarski et al. 2008).

On the other hand, as explained at the time, the data obtained from techniques such as diffusion tensor imaging (DTI) also show obvious limitations to identify tracts in regions of bilateral basal ganglia circuits- they are currently based on animal models (A. Di Martino et al. 2008: Selemon and Goldman-Rakic 1985; Cavada and Goldman-Rakic 1991; Middleton and Strick 1994; Ferry et al. 2000; Haber et al. 2000, 2006; Middleton and Strick 2002). For instance, although a connection between the cingulate cortex and the ventral striatum was observed in primates, this connection could not be found in human beings (Kunishio and Haber 1994; Haber et al. 2006). Besides, the DTI fiber tract reconstruction is quite complex among regions localized on the frontal lobe or interhemispheric areas (A. Di Martino et al. 2008). So that, this constitutes a problem when searching markers or abnormalities in a disease like MDD, where the basal ganglia circuit can be relevant. This could produce a number of inconsistencies among studies.

Thus, the idea is that the EC (*see background*) could be used for the analysis and finding of possible abnormalities in circuitries in patients with MDD which could help to clarify neurophysiological factors of the disorder.

This methodology is being actually applied in studies on patients with Bipolar (BP) and Obsessive Compulsive Disorder (OCD). In concrete, in the OCD study, a comparative study is carried out between a group of patients (64 subjects) and a group of controls (25 subjects), using the EC matrices with the idea of finding potential abnormalities in the circuitry in patients with OCD. These matrices, EC, should present

less problems in the basal ganglia and angular-lateral regions, among the posterior and anterior areas of the DMN, and the prefrontal lobe regarding the SC matrices extracted from DTI data (A. Di Martino et al. 2008). For many years, the dysfunctional cortical-striato-thalamic-cortical circuit has been pointed out as the main cause of OCD pathophysiology (Federica Piras et al. Review 2013: Graybiel and Rauch 2000; Menzies et al. 2008; Saxena and Rauch 2000).

Concretely, a putative altered circuit has been found from EC matrices in patients, where it seems that the basal ganglia tracts gain weight showing problems in the fibers which go from the putamen-thalamus to the cortical regions via both the parieto-occipital and prefrontal side. This structural connectivity alteration in patients with OCD is not present in the original DTI. This suggests a priori that the EC results could be used to complement deficiencies found in the structural connectivity of the SC matrix, and which could exist in this case between regions of the reward system, RS.

Finally, descriptors of the EC have been also extracted improving the models of SC. It has to be noted that conventional descriptors obtained through rs-fMRI data did not improve the DTI model.

In sum, the EC matrices might be used to analyze the tracts in the brain in those regions where the DTI data present limitations. In concrete, the posterior, together with the anterior part of the brain, via the nuclei striato showed to be disconnected in OCD. Likewise, it was possible to create a bimodal model to classify the subjects between groups by using the nodal descriptors associated to regions such as left putamen and left cuneus from SC matrix, and left superior temporal pole from EC matrix. We consider that this approximation could be used on the DMN or PFL in depression for a better understanding of the role of these networks in the disorder.

# Altered resting-state whole-brain functional brain networks of neonates with intrauterine growth restriction

Dafnis Batalle [a, 1], Emma Muñoz-Moreno [a], Cristian Tornador [b], Nuria Bargallo [c,d], Gustavo Deco [b,e], Elisenda Eixarch [a,f,g], Eduard Gratacos [a,f,g]

*Under review in Cortex*

**Affiliations:**

a) Fetal and Perinatal Medicine Research Group, Institut d'Investigacions Biomediques August Pi i Sunyer (IDIBAPS), Barcelona, Spain

b) Center for Brain and Cognition, Computational Neuroscience Group, Department of Information and Communication Technologies, Universitat Pompeu Fabra, Barcelona, Spain

c) Centre de Diagnòstic per la Imatge Clínic (CDIC), Hospital Clínic, Barcelona, Spain

d) Clinical Imaging Research, Institut d'Investigacions Biomediques August Pi i Sunyer (IDIBAPS), Barcelona, Spain

e) Institució Catalana de la Recerca i Estudis Avançats (ICREA), Universitat Pompeu Fabra, Barcelona, Spain

f) Maternal-Fetal Medicine Department, ICGON, Hospital Clínic, Universitat de Barcelona, Barcelona, Spain

g) Centro de Investigación Biomédica en Red de Enfermedades Raras (CIBERER), Barcelona, Spain


**Corresponding author:**

[1] Dafnis Batalle

Fetal and Perinatal Medicine Research Group, Hospital Clínic – IDIBAPS

Sabino de Arana 1, Helios III, 08028 Barcelona, Spain

dbatalle@clinic.ub.es

*Advisor report on the contribution of the Ph.D. candidate to the article.*

Prof. Dr. Gustavo Deco associate professor at the Universitat Pompeu Fabra of Barcelona, and supervisor of the present doctoral thesis by Cristian Tornador Antolin, hereby certifies that the participation of the Ph.D. candidate in the article "Altered resting-state whole-brain functional brain networks of neonates with intrauterine growth restriction" included the following tasks:

- Participation in study design
- MRI data pre- and post- processing.
- Part of statistical analysis.
- Critical revision

Batalle D, Muñoz-Moreno E, Tornador C, Bargallo N, Deco G, Eixarch E, Gratacos E.
Altered resting-state whole-brain functional networks of neonates with intrauterine growth
restriction. Cortex. 2016 Apr; 77: 119-31. doi: 10.1016/j.cortex.2016.01.012.

Smith SM, Jenkinson M, Woolrich MW, Beckmann CF, Behrens TE, Johansen-Berg H, Bannister PR, De Luca M, Drobnjak I, Flitney DE, Niazy RK, Saunders J, Vickers J, Zhang Y, De Stefano N, Brady JM, Matthews PM. Advances in functional and structural MR image analysis and implementation as FSL. Neuroimage. 2004;23 Suppl 1:S208-19.

Smirnakis SM, Brewer AA, Schmid MC, Tolias AS, Schüz A, Augath M, Inhoffen W, Wandell BA, Logothetis NK.Lack of long-term cortical reorganization after macaque retinal lesions. Nature. 2005 May 19;435(7040):300-7.

Ogawa S, Tank DW, Menon R, Ellermann JM, Kim SG, Merkle H, Ugurbil K.Intrinsic signal changes accompanying sensory stimulation: functional brain mapping with magnetic resonance imaging.Proc Natl Acad Sci U S A. 1992 Jul 1;89(13):5951-5.

Hoge RD, Atkinson J, Gill B, Crelier GR, Marrett S, Pike GB.Investigation of BOLD signal dependence on cerebral blood flow and oxygen consumption: the deoxyhemoglobin dilution model.Magn Reson Med. 1999 Nov;42(5):849-63.

Wicker B, Ruby P, Royet JP, Fonlupt P (2003) A relation between rest and the self in the brain?. Brain Res Brain Res Rev, 43 (2):224-30.

Beckmann CF, DeLuca M, Devlin JT, Smith SM (2005) Investigations into resting-state connectivity using independent component analysis. Philos Trans R Soc Lond B Biol Sci, 360:1001-1013.

De Luca M., Beckmann C. F., De Stefano N., Matthews P. M., Smith S. M. (2006) fMRI resting state networks define distinct modes of long-distance interactions in the human brain. Neuroimage 29, 1359–136710.1016/j.neuroimage.2005.08.035

Biswal B, Yetkin FZ, Haughton VM, Hyde JS (1995) Functional connectivity in the motor cortex of resting human brain using echo-planar MRI. Magn Reson Med, (34):537-541.

Lowe M. J., Mock B. J., Sorenson J. A. (1998). Functional connectivity in single and multislice echoplanar imaging using resting-state fluctuations. Neuroimage 7, 119–13210.1006/nimg.1997.0315

Damoiseaux J. S., Rombouts S. A., Barkhof F., Scheltens P., Stam C. J., Smith S. M., Beckmann C. F. (2006) Consistent resting-state networks across healthy subjects. Proc. Natl. Acad. Sci. U.S.A. 103,13848–1385310.1073/pnas.0601417103

Raichle M. E., MacLeod A. M., Snyder A. Z., Powers W. J., Gusnard D. A., Shulman G. L. (2001) A default mode of brain function. Proc. Natl. Acad. Sci. U.S.A. 98, 676–68210.1073/pnas.98.2.676

Fox M. D., Raichle M. E. (2007) Spontaneous fluctuations in brain activity observed with functional magnetic resonance imaging. Nat. Rev. Neurosci, 8, 700–71110.1038/nrn2201

Shulman G. L., Fiez J. A., Corbetta M., Buckner R. L., Miezin F. M., Raichle M. E., Petersen S. E. (1997) Common blood flow changes across visual tasks: II. Decreases in cerebral cortex. J. Cogn. Neurosci. 9, 648–66310.1162/jocn.1997.9.5.648

S.M. Smith, P.T. Fox, K.L. Miller, D.C. Glahn, P.M. Fox, C.E. Mackay, N. Filippini, K.E. Watkins, R. Toro, A.R. Laird, and C.F. Beckmann (2009) Correspondence of the brain's functional architecture during activation and rest. Proc Natl Acad Sci USA (PNAS), 106 (31):13040-13045

Larson-Prior L. J., Zempel J. M., Nolan T. S., Prior F. W., Snyder A. Z., Raichle M. E. (2009). Cortical network functional connectivity in the descent to sleep. Proc. Natl. Acad. Sci. U.S.A. 106, 4489–449410.1073/pnas.0900924106

Horovitz S. G., Braun A. R., Carr W. S., Picchioni D., Balkin T. J., Fukunaga M., Duyn J. H. (2009). Decoupling of the brain's default mode network during deep sleep. Proc. Natl. Acad. Sci. U.S.A. 106, 11376–1138110.1073/pnas.0901435106

Greicius MD, Kiviniemi V, Tervonen O, Vainionpää V, Alahuhta S, Reiss AL, Menon V.Persistent default-mode network connectivity during light sedation.Hum Brain Mapp. 2008 Jul;29(7):839-47. doi: 10.1002/hbm.20537.

Fox MD, Corbetta M, Snyder AZ, Vincent JL, Raichle ME.Spontaneous neuronal activity distinguishes human dorsal and ventral attention systems. Proc Natl Acad Sci U S A. 2006 Jun 27;103(26):10046-51. Epub 2006 Jun 20.

Rissman J, Gazzaley A, D'Esposito M. Measuring functional connectivity during distinct stages of a cognitive task.Neuroimage. 2004 Oct;23(2):752-63.

Martuzzi R, Ramani R, Qiu M, Rajeevan N, Constable RT.Functional connectivity and alterations in baseline brain state in humans.Neuroimage. 2010 Jan 1;49(1):823-34. doi: 10.1016/j.neuroimage.2009.07.028. Epub 2009 Jul 22.

Peltier SJ, Kerssens C, Hamann SB, Sebel PS, Byas-Smith M, Hu X.Functional connectivity changes with concentration of sevoflurane anesthesia.Neuroreport. 2005 Feb 28;16(3):285-8.

Pawela CP. Biswal BB. Cho YR. Kao DS. Li R. Jones SR. Schulte ML. Matloub HS. Hudetz AG. Hyde JS. Resting-state functional connectivity of the rat brain. Magn Reson Med. 2008;59:1021–1029.

Majeed W. Magnuson M. Keilholz SD. Spatiotemporal Dynamics of Low Frequency Fluctuations in BOLD fMRI of the Rat. J Magn Reson Imag. 2009;30:384–393.

Vincent JL, Patel GH, Fox MD, Snyder AZ, Baker JT, Van Essen DC, Zempel JM, Snyder LH, Corbetta M, Raichle ME (2007) Intrinsic functional architecture in the anaesthetized monkey brain. Nature, 447 (7140):83-6.

Fox MD, Greicius M.Clinical applications of resting state functional connectivity.Front Syst Neurosci. 2010 Jun 17;4:19. doi: 10.3389/fnsys.2010.00019. ECollection 2010.

Abramowitz JS1, Jacoby RJ.Obsessive-compulsive and related disorders: a critical review of the new diagnostic class.Annu Rev Clin Psychol. 2015;11:165-86. doi: 10.1146/annurev-clinpsy-032813-153713. Epub 2015 Jan 2.

Maldjian JA.Functional connectivity MR imaging: fact or artifact?.AJNR Am J Neuroradiol. 2001 Feb;22(2):239-40.

Greicius MD, Supekar K, Menon V, Dougherty RF (2009) Resting-state functional connectivity reflects structural connectivity in the default mode network. Cereb Cortex, 19 (1):72-8. doi: 10.1093/cercor/bhn059.

Damoiseaux JS, Greicius MD. Greater than the sum of its parts: a review of studies combining structural connectivity and resting-state functional connectivity. Brain Struct Funct. 2009 Oct;213(6):525-33. doi: 10.1007/s00429-009-0208-6. Epub 2009 Jun 30

Honey CJ, Sporns O, Cammoun L, Gigandet X, Thiran JP, Meuli R, Hagmann P. Predicting human resting-state functional connectivity from structural connectivity. Proc Natl Acad Sci U S A. 2009 Feb 10; 106(6):2035-40.

Cordes D, Haughton VM, Arfanakis K, Carew JD, Turski PA, Moritz CH, Quigley MA, Meyerand ME. Frequencies contributing to functional connectivity in the cerebral cortex in "resting-state" data. AJNR Am J Neuroradiol. 2001 Aug; 22(7):1326-33.

Lee MH, Smyser CD, Shimony JS.Resting-state fMRI: a review of methods and clinical applications.AJNR Am J Neuroradiol. 2013 Oct;34(10):1866-72. doi: 10.3174/ajnr.A3263. Epub 2012 Aug 30.

Birn RM, Diamond JB, Smith MA, Bandettini PA. Separating respiratory-variation-related fluctuations from neuronal-activity-related fluctuations in fMRI.Neuroimage. 2006 Jul 15; 31(4):1536-48.

Shmueli K, van Gelderen P, de Zwart JA, Horovitz SG, Fukunaga M, Jansma JM, Duyn JH. Low-frequency fluctuations in the cardiac rate as a source of variance in the resting-state fMRI BOLD signal. Neuroimage. 2007 Nov 1; 38(2):306-20.

Hampson M, Peterson BS, Skudlarski P, Gatenby JC, Gore JC (2002) Detection of functional connectivity using temporal correlations in MR images. Hum Brain Mapp, 15:247-262.

Seeley WW, Menon V, Schatzberg AF, Keller J, Glover GH, Kenna H, Reiss AL, Greicius MD (2007) Dissociable intrinsic connectivity networks for salience processing and executive control. J Neurosci, 27:2349–2356.

Greicius MD, Krasnow B, Reiss AL, Menon V (2003) Functional connectivity in the resting brain: a network analysis of the default mode hypothesis. Proc Natl Acad Sci U S A, 100:253–258.

De Luca M., Beckmann C. F., De Stefano N., Matthews P. M., Smith S. M. (2006) fMRI resting state networks define distinct modes of long-distance interactions in the human brain. Neuroimage 29, 1359–136710.1016/j.neuroimage.2005.08.035

David M. Cole, Stephen M. Smith, Christian F. Beckmann (2010) Advances and Pitfalls in the Analysis and Interpretation of Resting-State FMRI Data. Front Syst Neurosci, 4: 8. doi: 10.3389/fnsys.2010.00008.

Saini S., DeStefano N., Smith S., Guidi L., Amato M. P., Federico A., Matthews P. M. (2004). Altered cerebellar functional connectivity mediates potential adaptive plasticity in patients with multiple sclerosis. J. Neurol. Neurosurg. Psychiatr. 75, 840–84610.1136/jnnp.2003.016782

Lewis C. M., Baldassarre A., Committeri G., Romani G. L., Corbetta M. (2009). Learning sculpts the spontaneous activity of the resting human brain. Proc. Natl. Acad. Sci. U.S.A. 106, 17558–1756310.1073/pnas.0902455106

Deco G, Jirsa VK, McIntosh AR (2011) Emerging concepts for the dynamical organization of resting-state activity in the brain. Nat Rev Neurosci, 12 (1):43-56. doi: 10.1038/nrn2961.

Schölvinck ML, Rees G.Attentional influences on the dynamics of motion-induced blindness.J Vis. 2009 Jan 29;9(1):38.1-9. doi: 10.1167/9.1.38.

Bianciardi M, Fukunaga M, Van Gelderen P, Horovitz SG, De Zwart JA, Duyn JH (2009) Modulation of spontaneous fMRI activity in human visual cortex by behavioral state. Neuroimage 45:160-168.

Eckert MA, et al. A cross-modal system linking primary auditory and visual cortices: Evidence from intrinsic fMRI connectivity analysis. Hum Brain Mapp. 2008;29:848–857

Cordes D, et al. Mapping functionally related regions of brain with functional connectivity MR imaging. AJNR Am J Neuroradiol. 2000;21:1636–1644.

Xiong J, Parsons LM, Gao JH, Fox PT. Interregional connectivity to primary motor cortex revealed using MRI resting state images. Hum Brain Mapp. 1999;8:151–156.

Zhang D, et al. Intrinsic functional relations between human cerebral cortex and thalamus. J Neurophysiol. 2008;100:1740–1748.

O'Reilly JX, Beckmann CF, Tomassini V, Ramnani N, Johansen-Berg H. Distinct and overlapping functional zones in the cerebellum defined by resting state functional connectivity. Cereb Cortex. 2010;20:953–965.

Di Martino A, et al. Functional connectivity of human striatum: A resting state fMRI study. Cereb Cortex. 2008;18:2735–2747.

S.M. Smith, P.T. Fox, K.L. Miller, D.C. Glahn, P.M. Fox, C.E. Mackay, N. Filippini, K.E. Watkins, R. Toro, A.R. Laird, and C.F. Beckmann. Correspondence of the brain's functional architecture during activation and rest. Proc Natl Acad Sci USA (PNAS), 106(31):13040-13045, 2009.

A.R. Laird, P.M. Fox, S.B. Eickhoff, J.A. Turner, K.L. Ray, D.R. McKay, D.C. Glahn, C.F. Beckmann, S.M. Smith, and P.T. Fox. Behavioral interpretations of intrinsic connectivity networks. Journal of Cognitive Neuroscience, 2011.

Sheline YI, Barch DM, Price JL, Rundle MM, Vaishnavi SN, Snyder AZ, Mintun MA, Wang S, Coalson RS, Raichle ME (2009) The default mode network and self-referential processes in depression. Proc Natl Acad Sci USA., 106 (6):1942-7. doi: 10.1073/pnas.0812686106.

Raichle ME, MacLeod AM, Snyder AZ, Powers WJ, Gusnard DA, Shulman GL.A default mode of brain function.Proc Natl Acad Sci U S A. 2001 Jan 16;98(2):676-82.

Raichle ME, Snyder AZ.A default mode of brain function: a brief history of an evolving idea. Neuroimage. 2007 Oct 1;37(4):1083-90; discussion 1097-9. Epub 2007 Mar 6

Buckner RL, Carroll DC.Self-projection and the brain.Trends Cogn Sci. 2007 Feb;11(2):49-57. Epub 2006 Dec 22.

Assaf Y, Pasternak O.Diffusion tensor imaging (DTI)-based white matter mapping in brain research: a review.J Mol Neurosci. 2008;34(1):51-61.

Le Bihan D, Mangin JF, Poupon C, Clark CA, Pappata S, Molko N, Chabriat H.Diffusion tensor imaging: concepts and applications.J Magn Reson Imaging. 2001 Apr;13(4):534-46.

Le Bihan D.Looking into the functional architecture of the brain with diffusion MRI.Nat Rev Neurosci. 2003 Jun;4(6):469-80.

Diffusion-weighted MR imaging of acute stroke: correlation with T2-weighted and magnetic susceptibility-enhanced MR imaging in cats. Moseley ME1, Kucharczyk J, Mintorovitch J, Cohen Y, Kurhanewicz J, Derugin N, Asgari H, Norman D. AJNR Am J Neuroradiol. 1990 May;11(3):423-9

Le Bihan D, Breton E, Lallemand D, Grenier P, Cabanis E, Laval-Jeantet M.MR imaging of intravoxel incoherent motions: application to diffusion and perfusion in neurologic disorders.Radiology. 1986 Nov;161(2):401-7.

Warach S, Li W, Ronthal M, Edelman RR.Acute cerebral ischemia: evaluation with dynamic contrast-enhanced MR imaging and MR angiography.Radiology. 1992 Jan;182(1):41-7.

Kunishio K, Haber SN.Primate cingulostriatal projection: limbic striatal versus sensorimotor striatal input.J Comp Neurol. 1994 Dec 15;350(3):337-56.

Mori S, Zhang J. Principles of diffusion tensor imaging and its applications to basic neuroscience research.Neuron. 2006 Sep 7; 51(5):527-39.

Peled S, Friman O, Jolesz F, Westin CF. Geometrically constrained two-tensor model for crossing tracts in DWI. Magn Reson Imaging. 2006 Nov; 24(9):1263-70.

Deco G, McIntosh AR, Shen K, Hutchison RM, Menon RS, Everling S, Hagmann P, Jirsa VK.Identification of optimal structural connectivity using functional connectivity and neural modeling.J Neurosci. 2014 Jun 4;34(23):7910-6. doi: 10.1523/JNEUROSCI.4423-13.2014.

Brookes MJ, Woolrich M, Luckhoo H, Price D, Hale JR, Stephenson MC, Barnes GR, Smith SM, Morris PG (2011) Investigating the electrophysiological basis of resting state networks using magnetoencephalography. Proc Natl Acad Sci U S A 108:16783–16788

Mantini D, Perrucci MG, Del Gratta C, Romani GL, Corbetta M (2007) Electrophysiological signatures of resting state networks in the human brain. Proc Natl Acad Sci U S A 104:13170–13175

Honey CJ, Sporns O, Cammoun L, Gigandet X, Thiran JP, Meuli R, Hagmann P (2009) Predicting human resting-state functional connectivity from structural connectivity. Proc Natl Acad Sci U S A 106:2035–2040.

Ghosh A, Rho Y, McIntosh AR, Kötter R, Jirsa VK (2008) Noise during rest enables the exploration of the brain's dynamic repertoire. PLoS Comput Biol 4:e1000196.

Deco G, Jirsa VK (2012) Ongoing cortical activity at rest: criticality, multistability, and ghost attractors. J Neurosci 32:3366–3375

Buxton RB, Frank LR (1997) A model for the coupling between cerebral blood flow and oxygen metabolism during neural stimulation. J Cereb Blood Flow Metab 17:64–72

Mandeville JB, Marota JJ, Ayata C, Zaharchuk G, Moskowitz MA, Rosen BR, Weisskoff RM (1999) Evidence of a cerebrovascular postarteriole windkessel with delayed compliance. J Cereb Blood Flow Metabol 19:679–689.

Ritter P, Schirner M, McIntosh AR, Jirsa VK (2013) The virtual brain integrates computational modeling and multimodal neuroimaging. Brain Connect 3:121–145

Sanz Leon P, Knock SA, Woodman MM, Domide L, Mersmann J, McIntosh AR, Jirsa V (2013) The Virtual Brain: a simulator of primate brain network dynamics. Front Neuroinform 7:10.

Beckmann CF, Smith SM. Neuroimage. Tensorial extensions of independent component analysis for multisubject FMRI analysis.2005 Mar; 25(1):294-311.

Calhoun VD, Adali T, McGinty V, Pekar JJ, Watson T, Pearlson GD. fMRI Activation In A Visual-Perception Task: Network Of Areas Detected Using The General Linear Model And Independent Component Analysis. NeuroImage.2001;14(5):1080–1088.

Calhoun VD, Adali T, Pearlson GD, Pekar JJ. A method for making group inferences from functional MRI data using independent component analysis. Hum. Brain Map. 2001;14(3):140–151.

Calhoun VD, Adali T, Pearlson GD, Pekar JJ. Spatial and temporal independent component analysis of functional MRI data containing a pair of task-related waveforms. Hum. Brain Map. 2001:13(1):43–53.

Calhoun VD, Pekar JJ, McGinty VB, Adali T, Watson TD, Pearlson GD. Different activation dynamics in multiple neural systems during simulated driving. Hum.Brain Map. 2002;16(3):158–167.

Calhoun VD, Adali T, Pekar JJ. A method for testing conjunctive and subtractive hypotheses on group fMRI data using independent component analysis. Mag. Res.Imag. 2004;22(9):1181–1191.

Calhoun VD, Pekar JJ, Pearlson GD. Alcohol intoxication effects on simulated driving: exploring alcohol-dose effects on brain activation using functional MRI. Neuropsychopharmacology. 2004;29:2097–2107.

Schmithorst VJ, Holland SK. Comparison of three methods for generating group statistical inferences from independent component analysis of functional magnetic resonance imaging data. J. Magn. Reson. Imaging. 2004;19(3):365–368.

Rubinov M, Sporns O (2010) Complex network measures of brain connectivity: Uses and interpretations. NeuroImage 52:1059-69.

WHO (2001) The world health report. http://www.who.int; Chap 2,4

Wayne C. Drevets, Joseph L. Price, Maura L. Furey (2008) Brain structural and functional abnormalities in mood disorders: implications for neurocircuitry models of depression. Brain Struct Funct, 213 (1-2): 93–118. doi: 10.1007/s00429-008-0189-x

Ferrari, Alize J., Fiona J. Charlson, Rosana E. Norman, Scott B. Patten, Greg Freedman, Christopher J.L. Murray, Theo Vos, and Harvey A. Whiteford (2013) Burden of Depressive Disorders by Country, Sex, Age, and Year: Findings from the Global Burden of Disease Study 2010. PLoS Med, 10 (11): e1001547. doi:10.1371/journal.pmed.1001547.

Grimm S, Ernst J, Boesiger P, Schuepbach D, Hell D, Boeker H, Northoff G (2009) Increased self-focus in major depressive disorder is related to neural abnormalities in subcortical-cortical midline structures. Hum Brain Mapp, 30 (8):2617-27. doi: 10.1002/hbm.20693.

Grunebaum MF, Keilp J, Li S, Ellis SP, Burke AK, Oquendo MA, Mann JJ (2005): Symptom components of standard depression scales and past suicidal behavior. J Affect Disord 87:73–82.

Ingram RE (1990): Self-focused attention in clinical disorders: Review and a conceptual model. Psychol Bull 107:156–176.

Northoff G (2007): Psychopathology and pathophysiology of the self in depression Neuropsychiatric hypothesis. J Affect Disord 104:1–14.

Rimes KA, Watkins E (2005): The effects of self-focused rumination on global negative self-judgements in depression. Behav Res Ther 43:1673–1681.

Treynor E (2003): Rumination reconsidered: A psychometric analysis. Cogn Ther Res 27:247–259.

Caspi A, Sugden K, Moffitt TE, Taylor A, Craig IW, Harrington H, McClay J, Mill J, Martin J, Braithwaite A, Poulton R (2003) Influence of life stress on depression: moderation by a polymorphism in the 5-HTT gene. Science. 301 (5631):386-9.

Price JL, Drevets WC (2010) Neurocircuitry of mood disorders. Neuropsychopharmacology, 35 (1):192-216. doi: 10.1038/npp.2009.104.

Parsey RV, Olvet DM, Oquendo MA, Huang YY, Ogden RT, Mann JJ (2006) Higher 5-HT(1A) receptor binding potential during a major depressive episode predicts poor treatment response: preliminary data from a naturalistic study. Neuropsychopharmacology. 31:1745–9.

Pezawas L, Meyer-Lindenberg A, Drabant EM, Verchinski BA, Munoz KE, Kolachana BS, Egan MF, Mattay VS, Hariri AR, Weinberger DR (2005) 5-HTTLPR polymorphism impacts human cingulate-amygdala interactions: a genetic susceptibility mechanism for depression. Nat Neurosci. 8 (6):828-34.

Dichter GS, Gibbs D, Smoski MJ. A systematic review of relations between resting-state functional-MRI and treatment response in major depressive disorder.J Affect Disord. 2014 Sep 26;172C:8-17. doi: 10.1016/j.jad.2014.09.028.

Wittchen HU1, Jacobi F, Rehm J, Gustavsson A, Svensson M, Jönsson B, Olesen J, Allgulander C, Alonso J, Faravelli C, Fratiglioni L, Jennum P, Lieb R, Maercker A, van Os J, Preisig M, Salvador-Carulla L, Simon R, Steinhausen HC. The size and burden of mental disorders and other disorders of the brain in Europe 2010. Eur Neuropsychopharmacol. 2011 Sep;21(9):655-79. doi: 10.1016/j.euroneuro.2011.07.018.

Frank E1, Kupfer DJ, Wagner EF, McEachran AB, Cornes C.Efficacy of interpersonal psychotherapy as a maintenance treatment of recurrent depression. Contributing factors. Arch Gen Psychiatry. 1991 Dec;48(12):1053-9.

Frank E, Kupfer DJ, Wagner EF, McEachran AB, Cornes C.Efficacy of interpersonal psychotherapy as a maintenance treatment of recurrent depression. Contributing factors.Arch Gen Psychiatry. 1991 Dec;48(12):1053-9.

Duman RS, Li N, Liu RJ, Duric V, Aghajanian G.Signaling pathways underlying the rapid antidepressant actions of ketamine.Neuropharmacology. 2012 Jan;62(1):35-41. doi: 10.1016/j.neuropharm.2011.08.044. Epub 2011 Sep 2.

Berman MG, Peltier S, Nee DE, Kross E, Deldin PJ, Jonides J. Soc Cogn (2011) Depression, rumination and the default network. Affect Neurosci. 6 (5):548-55. doi: 10.1093/scan/nsq080.

Berman, Marc G., Bratislav Misic, Martin Buschkuehl, Ethan Kross, Patricia J. Deldin, Scott Peltier, Nathan W. Churchill, et al. 2014. "Does Resting-State Connectivity Reflect Depressive Rumination? A Tale of Two Analyses." NeuroImage 103 (December): 267–79. doi:10.1016/j.neuroimage.2014.09.027

Anand, Amit, Yu Li, Yang Wang, Jingwei Wu, Sujuan Gao, Lubna Bukhari, Vincent P. Mathews, Andrew Kalnin, and Mark J. Lowe. 2005. "Activity and Connectivity of Brain Mood Regulating Circuit in Depression: A Functional Magnetic Resonance Study." Biological Psychiatry 57 (10): 1079–88. doi:10.1016/j.biopsych.2005.02.021

Guo, Wen-bin, Xue-li Sun, Ling Liu, Qiang Xu, Ren-rong Wu, Zhe-ning Liu, Chang-lian Tan, Hua-fu Chen, and Jing-Ping Zhao. 2011. "Disrupted Regional Homogeneity in Treatment-Resistant Depression: A Resting-State fMRI Study." Progress in Neuro-Psychopharmacology and Biological Psychiatry 35 (5): 1297–1302. doi:10.1016/j.pnpbp.2011.02.006.

Wang, Li, Ke Li, Qing-E Zhang, Ya-Wei Zeng, Zhen Jin, Wen-Ji Dai, Yun-Ai Su, et al. 2013. "Interhemispheric Functional Connectivity and Its Relationships with Clinical Characteristics in Major Depressive Disorder: A Resting State fMRI Study." PLoS ONE 8 (3): e60191. doi:10.1371/journal.pone.0060191.

Sheline, Y.I., Price, J.L., Yan, Z., Mintun, M.A. (2010) Resting-state functional MRI in depression unmasks increased connectivity between networks via the dorsal nexus. Proceedings of the National Academy of Sciences of the United States of America, 107:11020-5.

Zhou Y, Yu C, Zheng H, Liu Y, Song M, Qin W, Li K, Jiang T (2010) Increased neural resources recruitment in the intrinsic organization in major depression. J Affect Disord. 121 (3):220-30. doi: 10.1016/j.jad.2009.05.029.

Zhu X, Wang X, Xiao J, Liao J, Zhong M, Wang W, Yao S (2012) Evidence of a dissociation pattern in resting-state default mode network connectivity in first-episode, treatment-naive major depression patients. Biol Psychiatry, 71 (7):611-7. doi: 10.1016/j.biopsych.2011.10.035.

Chang C, Glover GH (2010) Time-frequency dynamics of resting-state brain connectivity measured with fMRI. Neuroimage, 50 (1):81-98. doi: 10.1016/j.neuroimage.2009.12.011.

Yang, Genevieve J., John D. Murray, Grega Repovs, Michael W. Cole, Aleksandar Savic, Matthew F. Glasser, Christopher Pittenger, et al. 2014. "Altered Global Brain Signal in Schizophrenia." Proceedings of the National Academy of Sciences of the United States of America 111 (20): 7438–43. doi:10.1073/pnas.1405289111.

Nixon NL, Liddle PF, Nixon E, Worwood G, Liotti M, Palaniyappan L (2014) Biological vulnerability to depression: linked structural and functional brain network findings. Br J Psychiatry, 204:283-9. doi: 10.1192/bjp.bp.113.129965.

Cavanna AE, Trimble MR (2006) The precuneus: a review of its functional anatomy and behavioural correlates. Brain. 129 (Pt 3):564-83.

Hassabis D, Kumaran D, Maguire EA (2007) Using imagination to understand the neural basis of episodic memory. J Neurosci. 27 (52):14365-74.

Crane C, Barnhofer T, Mark J, Williams G. (2007) Cue self-relevance affects autobiographical memory specificity in individuals with a history of major depression. Memory, 15 (3):312-23.

Dosenbach NU, Fair DA, Miezin FM, Cohen AL, Wenger KK, Dosenbach RA, Fox MD, Snyder AZ, Vincent JL, Raichle ME, Schlaggar BL, Petersen SE (2007) Distinct brain networks for adaptive and stable task control in humans. Proc Natl Acad Sci U S A. 2007 Jun 26;104(26):11073-8.

Köhler CA, Carvalho AF, Alves GS, McIntyre RS, Hyphantis TN, Cammarota M (2015) Autobiographical Memory Disturbances in Depression: A Novel Therapeutic Target?. Neural Plast. 2015;2015:759139. doi: 10.1155/2015/759139.

Lemogne C., Piolino P., Jouvent R., Allilaire J.-F., Fossati P (2006) Episodic autobiographical memory in depression: a review. L'Encéphale. 32 (5, part 1):781–788. doi: 10.1016/s0013-7006(06)76231-5.

Nolen-Hoeksema S (2000) The role of rumination in depressive disorders and mixed anxiety/depressive symptoms. J Abnorm Psychol. 109 (3):504-11.

Joormann, J. (2006). The relation of rumination and inhibition: Evidence from a negative priming task.Cognitive Therapy and Research,30, 149−160.

Gorwood P, Corruble E, Falissard B, Goodwin GM (2008) Toxic effects of depression on brain function: impairment of delayed recall and the cumulative length of depressive disorder in a large sample of depressed outpatients. Am J Psychiatry. 165 (6):731-9. doi: 10.1176/appi.ajp.2008.07040574.

Aneta Brzezicka (2013) Integrative deficits in depression and in negative mood states as a result of fronto-parietal network dysfunctions. Review Acta Neurobiol Exp 2013, (73) : 313-325

Michael D. Greicius, MPH, Benjamin H. Flores, Vinod Menon, Gary H. Glover, Hugh B. Solvason, Heather Kenna, MA, Allan L. Reiss, and Alan F. Schatzberg (2007)

Resting-State Functional Connectivity in Major Depression: Abnormally Increased Contributions from Subgenual Cingulate Cortex and Thalamus. Biol Psychiatry, 62 (5): 429–437.

Koster EH, De Lissnyder E, Derakshan N, De Raedt R (2011) Understanding depressive rumination from a cognitive science perspective: the impaired disengagement hypothesis. Clin Psychol Rev. 31 (1):138-45. doi: 10.1016/j.cpr.2010.08.005.

Donaldson C, Lam D, Mathews A, (2007) Attention and rumination in major depression. Behaviour Research and Therapy,45, 2664−2678.

Buckner, R. L., & Carroll, D. C. (2007). Self-projection and the brain. Trends in Cognitive Science,11,49−57.

Lloyd G. G., Lishman W. A (1975) Effect of depression on the speed of recall of pleasant and unpleasant experiences. Psychological Medicine. 5 (2):173–180. doi: 10.1017/s0033291700056440

Blanco, L., Nydegger, L.A., Camarillo, G., Trinidad, D.R., Schramm, E., Ames, S.L. (2015) Neurological changes in brain structure and functions among individuals with a history of childhood sexual abuse: A review. Neuroscience and biobehavioral reviews, 57:63-69.

Sullivan, P.F., Neale, M.C., Kendler, K.S. (2000) Genetic epidemiology of major depression: review and meta-analysis. The American journal of psychiatry, 157:1552-62.

Finger S. Paul Broca (1824–1880) *Journal of Neurology*. 2004;251(6):769–770

Papez JW. A proposed mechanism of emotion. *Archives of Neurology and Psychiatry*. 1937;38:725–743.

James W. What is an emotion? *Mind*. 1884;9:188–205.

Kluver H, Bucy PC. "Psychic blindness" and other symptoms following bilateral temporal lobectomy. *American Journal of Physiology*. 1937;119:254–284.

MacLean PD. Psychosomatic disease and the visceral brain; recent developments bearing on the Papez theory of emotion. *Psychosomatic Medicine*. 1949;11(6):338–353.

Nauta WJ.Neural associations of the amygdaloid complex in the monkey.Brain. 1962 Sep;85:505-20.

Krettek JE, Price JL.The cortical projections of the mediodorsal nucleus and adjacent thalamic nuclei in the rat.J Comp Neurol. 1977 Jan 15; 171(2):157-91.

Krettek JE, Price JL.Projections from the amygdaloid complex and adjacent olfactory structures to the entorhinal cortex and to the subiculum in the rat and cat. J Comp Neurol. 1977 Apr 15; 172(4):723-52.

Russchen FT, Bakst I, Amaral DG, Price JL.The amygdalostriatal projections in the monkey. An anterograde tracing study. Brain Res. 1985 Mar 11; 329(1-2):241-57.

Buckwalter JA, Schumann CM, Van Hoesen GW. Evidence for direct projections from the basal nucleus of the amygdala to retrosplenial cortex in the Macaque monkey. Exp Brain Res. 2008 Mar; 186(1):47-57.

Carmichael ST, Price JL. Limbic connections of the orbital and medial prefrontal cortex in macaque monkeys. J Comp Neurol. 1995 Dec 25; 363(4):615-641.

Kondo H, Saleem KS, Price JL. Differential connections of the perirhinal and parahippocampal cortex with the orbital and medial prefrontal networks in macaque monkeys. J Comp Neurol. 2005 Dec 26; 493(4):479-509.

Price JL, Amaral DG.An autoradiographic study of the projections of the central nucleus of the monkey amygdala. J Neurosci. 1981 Nov; 1(11):1242-59

Likhtik E, Pelletier JG, Paz R, Paré D. Prefrontal control of the amygdala. J Neurosci. 2005 Aug 10; 25(32):7429-37.

Bacon SJ, Headlam AJ, Gabbott PL, Smith AD. Amygdala input to medial prefrontal cortex (mPFC) in the rat: a light and electron microscope study. Brain Res. 1996 May 13; 720(1-2):211-9.

Jackson ME, Moghaddam B. Amygdala regulation of nucleus accumbens dopamine output is governed by the prefrontal cortex. J Neurosci. 2001 Jan 15; 21(2):676-81.

Ray JP, Price JL. The organization of projections from the mediodorsal nucleus of the thalamus to orbital and medial prefrontal cortex in macaque monkeys. J Comp Neurol. 1993 Nov 1; 337(1):1-31.

Petrides M, Pandya DN. Dorsolateral prefrontal cortex: comparative cytoarchitectonic analysis in the human and the macaque brain and corticocortical connection patterns. Eur J Neurosci. 1999 Mar; 11(3):1011-36.

Botteron KN, Raichle ME, Drevets WC, Heath AC, Todd RD. Volumetric reduction in left subgenual prefrontal cortex in early onset depression. Biol Psychiatry. 2002 Feb 15; 51(4):342-4.

Drevets WC, Price JL, Simpson JR Jr, Todd RD, Reich T, Vannier M, Raichle ME. Subgenual prefrontal cortex abnormalities in mood disorders. Nature. 1997 Apr 24; 386(6627):824-7.

Savitz J, Lucki I, Drevets WC. 5-HT(1A) receptor function in major depressive disorder.Prog Neurobiol. 2009 May;88(1):17-31. doi: 10.1016/j.pneurobio.2009.01.009. Epub 2009 Feb 7.

Adinoff B (2004). Neurobiologic processes in drug reward and addiction. Harv Rev Psychiatry 12: 305–320

de la Fuente-Fernandez R, Phillips AG, Zamburlini M, Sossi V, Calne DB, Ruth TJ et al (2002). Dopamine release in human ventral striatum and expectation of reward. Behav Brain Res 136: 359–363.

Klimek V, Schenck JE, Han H, Stockmeier CA, Ordway GA.Dopaminergic abnormalities in amygdaloid nuclei in major depression: a postmortem study.Biol Psychiatry. 2002 Oct 1;52(7):740-8.

Northoff G, Wiebking C, Feinberg T, Panksepp J. (2011) The 'resting-state hypothesis' of major depressive disorder a translational subcortical-cortical framework for a system disorder. Neurosci Biobehav Rev, 35 (9):1929-45. doi: 10.1016/j.neubiorev.2010.12.007.

Rao SM, Mayer AR, Harrington DL (2001) The evolution of brain activation during temporal processing. Nat Neurosci. 4 (3):317-23.

Gross M, Nakamura L, Pascual-Leone A, Fregni F. (2007) Has repetitive transcranial magnetic stimulation (rTMS) treatment for depression improved? A systematic review and meta-analysis comparing the recent vs. the earlier rTMS studies. Acta Psychiatrica Scandinavica, 116 (3):165–173.

Bench CJ, Friston KJ, Brown RG, Scott LC, Frackowiak RSJ, Dolan RJ (1992) The Anatomy of Melancholia - Focal Abnormalities of Cerebral Blood-Flow in Major Depression. Psychological Medicine, 22 (3):607–615.Mayberg HS, Lozano AM, Voon V, McNeely HE, Seminowicz D, Hamani C, et al. (2005) Deep brain stimulation for treatment-resistant depression. Neuron, 45 (5):651–660

Pizzagalli DA, Holmes AJ, Dillon DG, Goetz EL, Birk JL, Bogdan R, et al. (2009) Reduced Caudate and Nucleus Accumbens Response to Rewards in Unmedicated Individuals With Major Depressive Disorder. American Journal of Psychiatry, 166 (6):702–710.

Strigo IA, Simmons AN, Matthews SC, Craig AD, Paulus MP (2008) Association of Major Depressive Disorder With Altered Functional Brain Response During Anticipation and Processing of Heat Pain. Archives of General Psychiatry, 65 (11):1275–1284.

Seeley WW, Menon V, Schatzberg AF, Keller J, Glover GH, Kenna H, Reiss AL, Greicius MD (2007) Dissociable intrinsic connectivity networks for salience

processing and executive control. J Neurosci, 27:2349–2356.

Vythilingam M, Heim C, Newport J, Miller AH, Anderson E, Bronen R, Brummer M, Staib L, Vermetten E, Charney DS, Nemeroff CB, Bremner JD. Childhood trauma associated with smaller hippocampal volume in women with major depression.Am J Psychiatry. 2002 Dec; 159(12):2072-80.

Sheline YI, Gado MH, Kraemer HC. Untreated depression and hippocampal volume loss. Am J Psychiatry. 2003 Aug; 160(8):1516-8.

Gong, Qiyong, and Yong He. 2015. "Depression, Neuroimaging and Connectomics: A Selective Overview." Biological Psychiatry 77 (3): 223–35. doi:10.1016/j.biopsych.2014.08.009.

McCabe C, Mishor Z.Antidepressant medications reduce subcortical-cortical resting-state functional connectivity in healthy volunteers. Neuroimage. 2011 Aug 15;57(4):1317-23. doi: 10.1016/j.neuroimage.2011.05.051. Epub 2011 May 27.

Anand A1, Li Y, Wang Y, Wu J, Gao S, Bukhari L, Mathews VP, Kalnin A, Lowe MJ. Antidepressant effect on connectivity of the mood-regulating circuit: an FMRI study.Neuropsychopharmacology. 2005 Jul;30(7):1334-44.

Auer DP, Putz B, Kraft E, Lipinski B, Schill J, Holsboer F. Reduced glutamate in the anterior cingulate cortex in depression: an in vivo proton magnetic resonance spectroscopy study. Biol Psychiatry 47: 305-313

Karolewicz B, Maciag D, O'Dwyer G, Stockmeier CA, Feyissa AM, Rajkowska G.Reduced level of glutamic acid decarboxylase-67 kDa in the prefrontal cortex in major depression.Int J Neuropsychopharmacol. 2010 May;13(4):411-20. doi: 10.1017/S1461145709990587. Epub 2009 Sep 15

Rajkowska G, Miguel-Hidalgo JJ, Wei J, Dilley G, Pittman SD, Meltzer HY, et al. Morphometric evidence for neuronal and glial prefrontal cell pathology in major depression. Biol Psychiatry. 1999;45:1085–1098.

Cotter D, Mackay D, Chana G, Beasley C, Landau S, Everall IP. Reduced neuronal size and glial cell density in area 9 of the dorsolateral prefrontal cortex in subjects with major depressive disorder. Cereb Cortex. 2002 Apr; 12(4):386-94.

Cotter D, Hudson L, Landau S.Evidence for orbitofrontal pathology in bipolar disorder and major depression, but not in schizophrenia.Bipolar Disord. 2005 Aug; 7(4):358-69.

Swanson CJ, Bures M, Johnson MP, Linden AM, Monn JA, Schoepp DD. Metabotropic glutamate receptors as novel targets for anxiety and stress disorders. Nat Rev Drug Discov. 2005 Feb;4(2):131-44.

Bechtholt-Gompf AJ, Walther HV, Adams MA, Carlezon WA Jr, Ongür D, Cohen BM.Blockade of astrocytic glutamate uptake in rats induces signs of anhedonia and impaired spatial memory.Neuropsychopharmacology. 2010 Sep;35(10):2049-59. doi: 10.1038/npp.2010.74. Epub 2010 Jun 9.

Cortese BM1, Phan KL.The role of glutamate in anxiety and related disorders.CNS Spectr. 2005 Oct;10(10):820-30.

Tremblay LK, Naranjo CA, Graham SJ, Herrmann N, Mayberg HS, Hevenor S, Busto UE.Functional neuroanatomical substrates of altered reward processing in major depressive disorder revealed by a dopaminergic probe.Arch Gen Psychiatry. 2005 Nov;62(11):1228-36.

Brunswick DJ, Amsterdam JD, Mozley PD, Newberg A.Greater availability of brain dopamine transporters in major depression shown by [99m Tc]TRODAT-1 SPECT imaging.Am J Psychiatry. 2003 Oct;160(10):1836-41.

**List of publications during the *Thesis:***

**Neuroscience:**

**Córdova-Palomera A, <u>Tornador C</u>**, Falcón C, Bargalló N, Nenadic I, Deco G, Fañanás L (2015) Altered amygdalar resting-state connectivity in depression is explained by both genes and environment. Hum Brain Mapp. 36 (10):3761-76. doi: 10.1002/hbm.22876.

**Murat Demirtaş,** <u>Cristian Tornador</u>, Carles Falcón, Marina López-Solà, Rosa Hernández-Ribas, Jesús Pujol, José M. Menchón, Petra Ritter, Narcis Cardoner, Carles Soriano Mas, Gustavo Deco. Dynamic Functional Connectivity Reveals Altered Variability in Functional Connectivity Among Patients with Major Depressive Disorder. Hum Brain Mapp. *(under review).*

**Aldo Córdova-Palomera, <u>Cristian Tornador</u>** Carles Falcón, Nuria Bargalló, Igor Nenadic,Gustavo Deco, Lourdes Fañanás. Environmental factors inducing depression alter the cerebellar resting-state synchronization. Hum Brain Mapp. *(under review).*

**Dafnis Batalle**, Emma Muñoz-Moreno, <u>Cristian Tornador</u>, Nuria Bargallo, Gustavo Deco, Elisenda Eixarch, Eduard Gratacos. Altered resting-state whole-brain functional brain networks of neonates with intrauterine growth restriction. Cortex. **(under review).**

*In proceeding:*

Cristian Tornador, Murat Demirtaş, Dafnis Batalle, Carles Falcón, Marina López-Solà, Rosa Hernández-Ribas, Jesús Pujol, José M. Menchón, Petra Ritter, Narcis Cardoner, Carles Soriano Mas, Gustavo Deco. Altered resting state networks in Major Depression are explained by both static and dynamic aspects of the BOLD signal at rest

**Genetics:**

**Puente XS**, Pinyol M, Quesada V, Conde L, Ordóñez GR, Villamor N, Escaramis G, Jares P, Beà S, González-Díaz M, Bassaganyas L, Baumann T, Juan M, López-Guerra M, Colomer D, Tubío JM, López C, Navarro A, Tornador C, Aymerich M, Rozman M, Hernández JM, Puente DA, Freije JM, Velasco G, Gutiérrez-Fernández A, Costa D, Carrió A, Guijarro S, Enjuanes A, Hernández L, Yagüe J, Nicolás P, Romeo-Casabona CM, Himmelbauer H, Castillo E, Dohm JC, de Sanjosé S, Piris MA, de Alava E, San Miguel J, Royo R, Gelpí JL, Torrents D, Orozco M, Pisano DG, Valencia A, Guigó R, Bayés M, Heath S, Gut M, Klatt P, Marshall J, Raine K, Stebbings LA, Futreal PA, Stratton MR, Campbell PJ, Gut I, López-Guillermo A, Estivill X, Montserrat E, López-Otín C, Campo E (2011) Whole-genome sequencing identifies recurrent mutations in chronic lymphocytic leukaemia. Nature, 475 (7354):101-5. doi: 10.1038/nature10113

**Trujillano D**, Ramos MD, González J, Tornador C, Sotillo F, Escaramis G, Ossowski S, Armengol L, Casals T, Estivill X (2013) Next generation diagnostics of cystic fibrosis and CFTR-related disorders by targeted multiplex high-coverage resequencing of CFTR. J Med Genet. 2013 Jul;50(7):455-62. doi: 10.1136/jmedgenet-2013-101602.

**Trujillano D**, Perez B, González J, Tornador C, Navarrete R, Escaramis G, Ossowski S, Armengol L, Cornejo V, Desviat LR, Ugarte M, Estivill X. (2014) Accurate molecular diagnosis of phenylketonuria and tetrahydrobiopterin-deficient hyperphenylalaninemias using high-throughput targeted sequencing. Eur J Hum Genet. 22 (4):528-34. doi: 10.1038/ejhg.2013.175.

**Bassaganyas L**, Beà S, Escaramís G, Tornador C, Salaverria I, Zapata L, Drechsel O, Ferreira PG, Rodriguez-Santiago B, Tubio JM, Navarro A, Martín-García D, López C, Martínez-Trillos A, López-Guillermo A, Gut M, Ossowski S, López-Otín C, Campo E, Estivill X (2013). Sporadic and reversible chromothripsis in chronic lymphocytic leukemia revealed by longitudinal genomic analysis. Leukemia, (12):2376-9. doi: 10.1038/leu.2013.127

**Escaramís G, <u>Tornador C</u>, Bassaganyas L**, Rabionet R, Tubio JM, Martínez-Fundichely A, Cáceres M, Gut M, Ossowski S, Estivill X (2013) PeSV-Fisher: identification of somatic and non-somatic structural variants using next generation sequencing data. PLoS One, 8 (5):e63377. doi: 10.1371/journal.pone.0063377. Print 2013.

**Simonetti FL, <u>Tornador C</u>, Nabau-Moretó N**, Molina-Vila MA, Marino-Buslje C (2014) Kin-Driver: a database of driver mutations in protein kinases. Database (Oxford), bau104. doi: 10.1093/database/bau104.

**Tubio JM, Tojo M**, Bassaganyas L, Escaramis G, Sharakhov IV, Sharakhova MV, <u>Tornador C</u>, Unger MF, Naveira H, Costas J, Besansky NJ (2011). Evolutionary dynamics of the Ty3/gypsy LTR retrotransposons in the genome of Anopheles gambiae. PLoS One, 6 (1):e16328. doi: 10.1371/journal.pone.0016328.

**Molina-Vila MA, Nabau-Moretó N, <u>Tornador C</u>**, Sabnis AJ, Rosell R, Estivill X, Bivona TG, Marino-Buslje C (2014) Activating mutations cluster in the "molecular brake" regions of protein kinases and do not associate with conserved or catalytic residues. Hum Mutat. 35 (3):318-28. doi: 10.1002/humu.22493.

**Monika Gulia-Nuss**, Andrew Nuss, Jason Meyer, Daniel Sonenshine, Michael Roe, David Sattelle, Robert Waterhouse, José de la Fuente, Jose Ribeiro, Karine Megy, Jyothi Thimmapuram, Jason Miller, Brian Walenz, Sergey Koren, Jessica Hostetler, Mathangi Thiagarajan, Vinita Joardar, Linda Hannick, Shelby Bidwell, Martin Hammond, Ms. Sarah Young, Qiandong Zeng, Jenica Abrudan, Francisca Almeida, Nieves Ayllón, Miss Ketaki Bhide, Brooke Bissinger, Elena Bonzon-Kulichenko, Steven Buckingham, Daniel Caffrey, Melissa Caimano, Vincent Croset, Timothy Driscoll, Don Gilbert, Joseph Gillespie, Gloria Giraldo-Calderón, Jeffrey Grabowski, David Jiang, Sayed M. S. Khalil, Donghun Kim, Katherine Kocan, Juraj Koči, Richard Kuhn, Timothy Kurtti, Kristin Lees, Miss Emma Lang, Ryan Kennedy, Hyeogsun Kwon, Rushika Perera, Yumin Qi, Justin Radolf, Joyce Sakamoto

, Alejandro Sánchez-Gracia , Maiara Severo , Neal Silverman , Ladislav Šimo , Marta Tojo , <u>Cristian Tornador</u> , Janice Van Zee , Jesus Vazquez , Filipe Vieira , Margarita Villar , Adam Wespiser , Yunlong Yang , Jiwei Zhu , Peter Arensburger , Patricia Pietrantonio , Stephen Barker , Renfu Shao , Evgeny Zdobnov , Frank Hauser , Cornelis Grimmelikhuijzen , Yoonseong Park , Julio Rozas , Richard Benton , Joao Pedra , David Nelson , Maria Unger , Jose Tubio , Zhijian Tu , Hugh Robertson , Martin Shumway , Granger Sutton , Jennifer Wortman , Daniel Lawson , Stephen Wikel , Vishvanath Nene , Claire Fraser , Frank Collins , Bruce Birren , Karen Nelson , Elisabet Caler. Genomic insights into the Ixodes scapularis tick vector of Lyme disease. Nature Communications. (*under consideration*).